MECHANOTRANSDUCTION OF INTERSTITIAL FLOW MODULATES VASCULAR SMOOTH MUSCLE CELL AND FIBROBLAST MOTILITY AND PHENOTYPE IN 2-D AND 3-D

by

ZHONGDONG SHI

A dissertation submitted to the Graduate Faculty in Biomedical Engineering in partial fulfillment of the requirements for the degree of Doctor of Philosophy
The City University of New York

2010

This manuscript has been read and accepted for the Graduate Faculty in Engineering in satisfaction of the dissertation requirement for the degree of Doctor of Philosophy.

Dr. John M. Tarbell

June 10, 2010

Date

Chair of Examining Committee

Dr. Mumtaz K. Kassir

June 10, 2010

Date

Executive Officer

Dr. Maribel Vazquez

Dr. Sihong Wang

Dr. Sheldon Weinbaum

Dr. Herb B. Sun

Supervisory Committee

THE CITY UNIVERSITY OF NEW YORK

ABSTRACT

MECHANOTRANSDUCTION OF INTERSTITIAL FLOW MODULATES VASCULAR SMOOTH MUSCLE CELL AND FIBROBLAST MOTILITY AND PHENOTYPE IN 2-D AND 3-D

by

Zhong-Dong Shi

Advisor: Dr. John M. Tarbell

Vascular lesion formation often occurs in regions where the endothelium has been damaged and the transmural interstitial flow is elevated. Vascular smooth muscle cells (SMCs) and fibroblasts/myofibroblasts (FBs/MFBs) contribute to vascular repair or vascular lesion formation by migrating from the vessel media and adventitia into the site of the injury intima. During the damage period, vascular SMCs and FBs/MFBs are exposed to luminal blood flow (2-dimensional, 2-D) or elevated interstitial flow (3-D). Therefore, we hypothesize that the alterations of fluid flow during vascular injury modulate SMC and FB/MFB phenotype and motility, which may contribute to vascular remodeling and lesion formation.

To test this hypothesis, we first established a 3-D interstitial flow-cell migration system and then through a series of newly-designed experimental methods, we have generated following primary findings: 1) Interstitial flow can promote rat vascular SMC, FB, and MFB motility in collagen gels by upregulation of matrix metalloproteinase-13 (MMP-13) expression; 2) Flow-induced upregulation of MMP-13 is mediated by

activation of extracellular signal-regulated kinase 1/2 (ERK1/2) mitogen-activated protein kinase (MAPK) and the downstream transcription factor, activating protein-1 (AP-1), specifically c-Jun; 3) Furthermore, cell surface heparan sulfate proteoglycans (HSPGs) mediate focal adhesion kinase (FAK) activation which regulates the ERK signaling cascade; 4) We propose a conceptual mechanotransduction model wherein surface HSPGs, with the synergism of integrin-mediated cell-matrix adhesions, sense interstitial flow and activate the FAK and ERK pathway, leading to upregulation of MMP and cell motility in 3-D.

In a differentiation study, we have found that: 1) 2-D laminar flow shear stress reduces expression of SMC marker genes in both SMCs and MFBs: α-smooth muscle actin (α-SMA), smooth muscle protein 22 (SM22), SM myosin heavy chain (SM-MHC), smoothelin, and calponin; 2) 3-D interstitial flow suppresses expression of SM-MHC, smoothelin, and calponin, but enhances expression of α-SMA and SM22; 3) The effects of laminar flow and interstitial flow on SMC marker expression is dependent on HSPG-mediated ERK activation.

Taken together, we propose that mechanotransduction of fluid flow may be involved in vascular remodeling and lesion formation by affecting SMC, FB, and MFB phenotype and motility. This is the first study to describe a flow-induced mechanotransduction mechanism in 3-D. This study has implications in understanding the flow-related mechanobiology in vascular lesion formation, tumor cell invasion, and stem cell differentiation.

ACKNOWLEDGEMENTS

I would like to thank all the people who helped me made this dissertation possible. First, I would like to express the utmost thanks and gratitude to my research mentor, Distinguished Professor Dr. John M. Tarbell, for his tremendous amount academic guidance, support, and encouragement throughout my graduate study. I also highly appreciate Dr. Tarbell's invaluable help in writing supporting or recommendation letters whenever needed. I would like also to thank the members of my Ph.D. committee: Dr. Maribel Vazquez, Dr. Sihong Wang, Dr. Herb B. Sun, and Dr. Sheldon Weinbaum for their help, support, and understanding during my doctoral dissertation research.

I also would like to extend my thanks to my labmates: Drs. Xin-Ying Ji, Danielle E. Berardi, Jeffery S. Garanich, Limary M. Cancel, Veronica Lopez, and Eno E. Ebong; Mr. Henry Qazi, Rishi Mathura, and Ronny Amaya; Ms. Maria Nikmanesh, Giya Abraham, and Rocio Palomino. I completely enjoyed the time we spent together either in the lab, or in the restaurants, or on the sport courts and hope that our friendship and collaboration continue. Special thanks to BME department, Dr. Zhiyong Qiu, Carol and Pat. In addition, many thanks to my friends, especially, Dr. Yongzhong Hou for his great help in cell biology, and Drs. Xiang I. Gu and Yilin Wang for playing sport together.

Finally, I would like to give my deepest gratitude and appreciation to my father, Mingzhi Shi, for his unconditional love, support, guidance, and scarifice throughout my entire life. Many thanks to my grandfather Yutian Shi, my uncle Mingan Shi and my brothers Zhonghua Shi and Zhongjun Shi for their endless support during all these years, and also the most important person, my beloved wife Hui Wang, for her true love and unconditional support.

This dissertation is dedicated to my mother Yanju Li

and my grandmother Yineng Dou!

谨以此论文献给我的母亲李延菊和祖母亲窦以能!

TABLE OF CONTENTS

LIST OF FIGURES

LIST OF TABLES

Chapter 1

Introduction

1.1 Hypothesis and aims

Interstitial fluid flow is an important coupling factor between mechanical stress and signaling on cells that are embedded in a 3-D matrix. When the vessel wall is injured, the transmural interstitial flow is elevated immediately in the injury site due to the reduced resistance, and hence both mass transport conveyed by transmural convection and shear stress on medial smooth muscle cells (SMCs) and adventitial fibroblasts are augmented. When the intima is damaged, SMCs on the superficial layer are exposed to luminal blood flow. It has been shown that in 2-D shear stress affects vascular SMC and fibroblast migration, proliferation and differentiation. Combing these facts, we therefore **hypothesize** that during vascular injury, the alteration of transmural interstitial flow in the vessel wall can affect vascular SMC and fibroblast properties and functions, such as proliferation, differentiation, and migration. In response to changes of interstitial flow, SMCs and fibroblasts can rapidly switch their phenotypes from a more contractile or quiescent state to a more synthetic and proliferative state, and migrate into the wound areas in the intima, where these cells contribute to vascular repair, remodeling, or vascular lesion formation in atherosclerosis and neointimal hyperplasia. Therefore, in this dissertation, we will test our hypothesis by pursuing the following specific aims:

Specific aim 1: To establish a 3-D interstitial flow – cell migration system for studying the effects of interstitial flow on cell motility. Collagen I is used as 3-D ECM. Rat vascular SMCs and fibroblasts are suspended in collagen gels and loaded into the cell culture inserts (8 μm of pore size). After spreading out, cells are exposed to interstitial

flow with different intensities driven by different pressure drops. Then the cells in gels are incubated with PDGF-BB for a Boyden chamber chemotaxis assay. The number of migrated cells through the pores of culture inserts is counted. This system allows us to quantify cell migration and examine the changes in cellular and molecular biology.

Specific aim 2: To determine the effects of interstitial flow on cell motility and the underlying mechanism. Using the 3-D flow - migration system, we will determine the effects of flow on cell migration, either enhancing or supressing. Since rat collagenase (MMP-13) plays a major role in native collagen I digestion and gelatinase (MMP-2) is responsible for degrading denatured collagens, the potentital involvement of both MMP-13 and MMP-2 will be examined. The roles of some signaling molecules such as MAPK (ERK1/2 and p38) and transcription factors (c-Jun and c-Fos) will be investigated.

Specific aim 3: To elucidate the mechanotransduction mechanism of interstitial flow on cell motility. FAK is a well-known mechanosensitive kinase that mediates mechanical stimuli. Cell surface glycoclayx components such as heparan sulfate proteoglycans (HSPGs) are flow sensors in 2-D. Therefore, the potential mechanosensing roles of FAK and HSPGs will be determined.

Specific aim 4: To investigate the effects of fluid flow on SMC and myofibroblast phenotypic modulation in 2-D and 3-D. Using flow systems to recapitulate the environments of cells in 3-D and in 2-D, the effects of interstitial flow and laminar flow on SMC marker gene expression in both SMC and myofibroblast and the underlying mechanotransduction mechanism will be investigated.

1.2 Artery wall components and their function

The arterial wall represents a highly plastic three-dimensional (3-D) structure possessing a unique adaptive capacity to face alterations in blood pressure, flow, and shear stress taking place during development and in certain vascular diseases [152]. Arteries are usually composed of three layers: the tunica intima, tunica media, and tunica adventitia (Fig. 1-1). The intima consists of a layer of endothelial cells (ECs) lining the vessel lumen, as well as a subendothelial layer made up mostly of loose connective tissue. The internal elastic lamina (IEL) separates the intima from media. The media is composed mostly of circumferentially arranged smooth muscle cells (SMCs). The external elastic lamina (EEL) separates the media from the adventitia. Finally, the tunica adventitia is primarily composed of loose connective tissue made up of fibroblasts (FBs) and associated collagen fibers (Table 1-1).

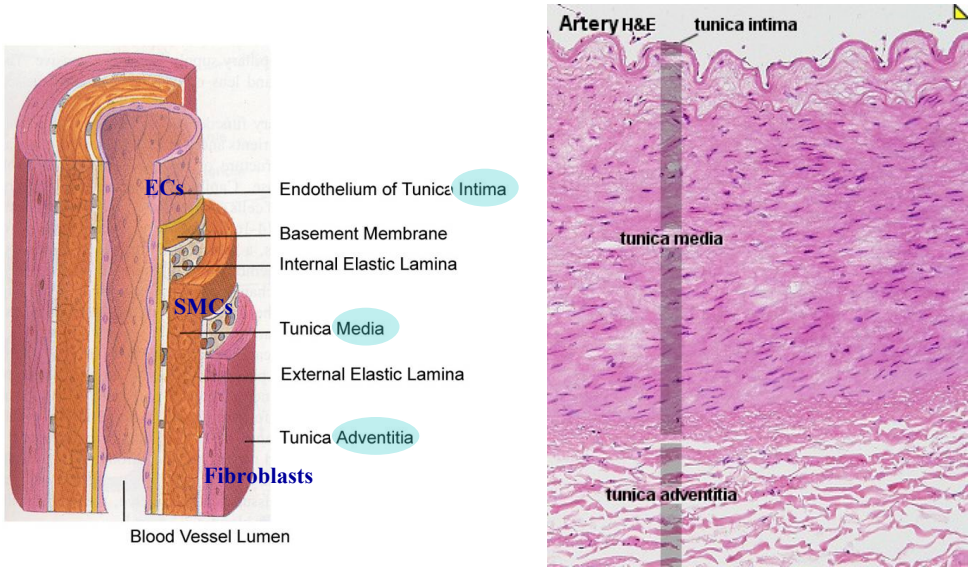

(A) Schematic artery wall (B) Elastic aorta layers

Figure 1-1. Arterial wall components.
(http://www.ucc.ie/bluehist/CorePages/Vascular/Vascular.htm)

This tissue compartmentalization inherently gives rise to structural-functional interfaces that allow for the maintenance of arterial wall homeostasis. Pathological stimuli can target all wall layers and interfaces simultaneously or only one layer/interface. The response to injury may be initially localized to a specific layer, and later it can invest other layers depending on time, severity of the lesion, responsiveness, and functional connectivity among the wall tissues. In response, a repair program is activated which eventually leads to vascular wall remodeling [152].

Table 1-1. Blood vessel wall components
(http://w3.ouhsc.edu/histology/Text%20Sections/Cardiovascular.html)

Tunica intima	Tunica media	Tunica adventitia
1. Endothelial cell lining 2. Subendothelial layer 3. Internal elastic lamina	1. Smooth muscle cells 2. Collagen fibers 3. Elastin lamellae 3. External elastic lamina	1. Mostly collagenous fibers 2. Elastic fibers 3. Fibroblasts and macrophages 4. Vasa vasorum

1.3 Neointima formation and atherosclerosis

Neointima formation (or intimal thickening, intimal hyperplasia), the accumulation of cells and new extracelluar matrix (ECM) within the inner vessel wall, is a physiological response to mechanical injury, increased wall stress, or chemical insult. If excessive, it can lead to the obstruction of blood flow and tissue ischemia [115]. Neointima formation is often induced in regions where the endothelium has been damaged by vascular procedures such as angioplasty or at the anastomoses of vascular grafts [99, 156]. An example of neointima formation is shown in Fig. 1-2. Atherosclerosis involves multiple processes including endothelial dysfunction, inflammation, vascular proliferation and matrix alteration. Vascular proliferation contributes to the pathobiology of atherosclerosis

and is linked to other cellular processes such as inflammation, apoptosis and matrix alterations. Cardiovascular risk factors alter the vascular endothelium, which may trigger a cascade of events, including the recruitment of leukocytes. Cytokines and growth factors are released by inflammatory cells and vascular cells, generating a highly mitogenic milieu. Vascular SMCs (VSMCs) migrate, proliferate and synthesize extracellular matrix (ECM) components on the luminal side of the vessel wall, forming the fibrous cap of the atherosclerotic lesion. Inflammatory mediators ultimately induce thinning of the fibrous cap by expression of proteases, rendering the plaque weak and susceptible to rupture and thrombus formation. In advanced disease, fibroblasts (FBs) and VSMCs with extracellular calcification give rise to fibrocalcific lesions [42]. See Fig. 1-3 for detail.

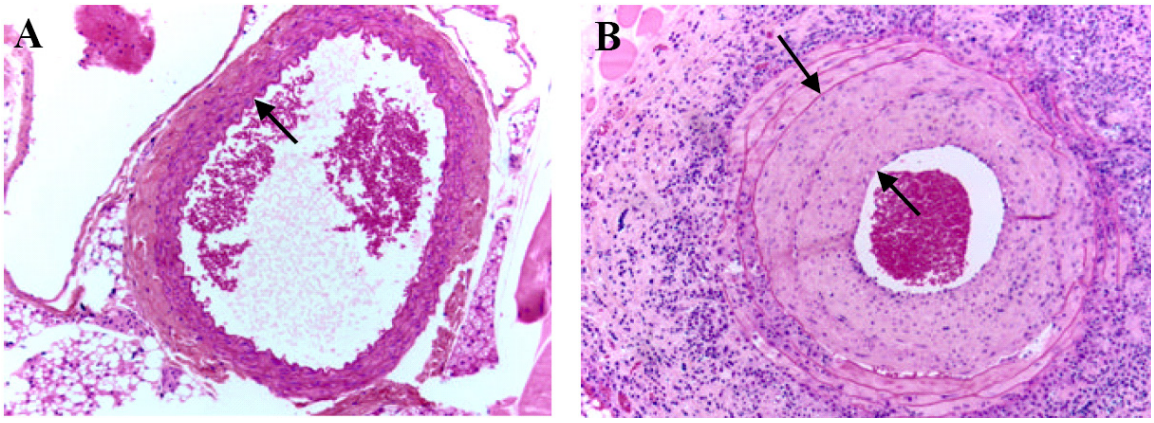

Figure 1-2. Neointima formation in the mouse abdominal aorta. A. H&E staining of abdominal aorta collected from uninfected IFN-γR-/- mouse 2 months after whole body irradiation. Arrow points to the intima. B. H&E staining of a large abdominal vessel collected from murine cytomegalovirus (MCMV) infected IFN-γR-/- mouse 4 months after infection and 2 months after whole body irradiation. Space between arrows indicates the thickness of the neointima [59].

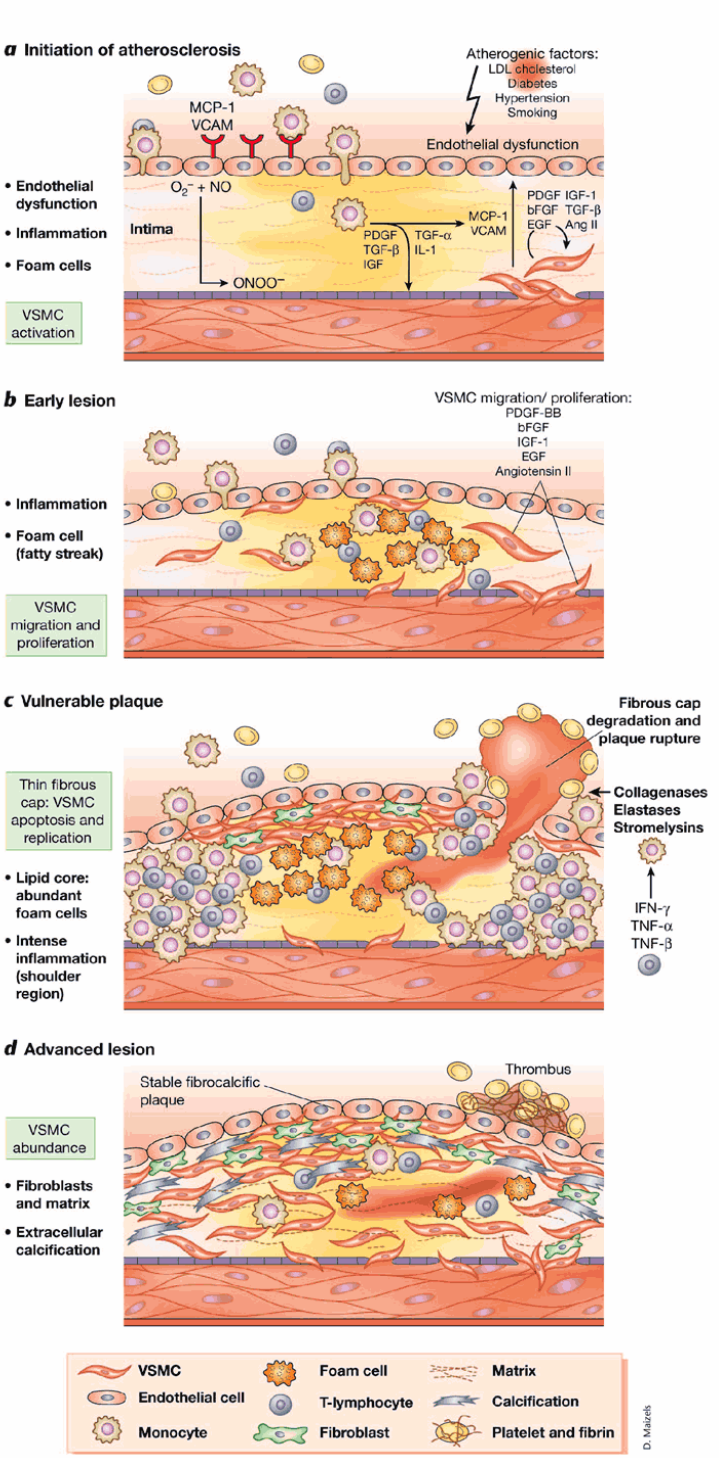

Figure 1-3. Development of atherosclerosis. LDL, low-density lipoprotein; MCP, monocyte chemoattractant protein; VCAM, vascular cell adhesion molecule; PDGF-BB, platelet-derived growth factor (BB, beta-chain homodimer); TNF, tumor necrosis factor; TGF, transforming growth factor; IL, interleukin 1; IGF, insulin-like growth factor; bFGF, basic fibroblast growth factor; Ang II, angiotensin II; EGF, epidermal growth factor; IFN, interferon [42].

1.4 Role of medial SMC and adventitial fibroblast in vascular remodeling and diseases

The vascular SMCs in animals and humans are highly specialized cells whose principal function is to regulate blood vessel tone, blood pressure, and blood flow distribution. SMCs within adult blood vessels have an extremely low proliferation rate, exhibit very low synthetic activity, and express a unique repertoire of contractile proteins, ion channels, and signaling molecules required for cell contractile function [124]. Unlike skeletal or cardiac muscle cells that are terminally differentiated, SMCs retain remarkable plasticity and can undergo rather profound and reversible changes in phenotype in response to changes in local environmental cues [124]. SMC phenotype is a continuum and the terms "contractile" and "synthetic" refer to relative positions along this continuum, indicating cell functions and marker expression that are associated with either a contractile or a synthetic function [178]. SMC plasticity plays an important role in vascular development, repair, and remodeling. During vascular development, SMCs display high plasticity and play a key role in morphogenesis of the blood vessel by exhibiting high rates of proliferation, migration, and production of ECM components such as collagen, elastin, and proteoglycans that make up a major portion of the vessel wall while at the same time acquiring contractile capabilities [125]. In response to injury, SMCs dramatically increase proliferation rate, motility, and synthetic capacity and play a critical role in vascular repair [125]. However, on the other hand, due to the high degree of plasticity, SMCs may be led to adverse phenotypic switching and migration under abnormal environmental conditions that can contribute to development and progression of vascular diseases such as atherosclerosis and hypertension and cancer [125].

Vascular SMCs have received a great deal of attention for their role in vascular disease, while adventitial fibroblasts have not been as well characterized as SMC because of their remote origin in the outer adventitial layer of the blood vessel, which has historically been considered a supporting tissue [152]. Recent in vivo work, however, has shown that, in addition to SMCs, adventitial fibroblasts (FBs) and their activated counterpart myofibroblasts (MFBs), contribute to neointima formation following vascular injury [87, 147, 158, 163, 174]. Adventitial MFBs appear to be capable of migrating from the adventitia to the media or even to the intima and contribute to the thickening of the neointima, which has been observed in response to endothelial injury [163, 174].

One of the most consistent findings in experimental models of systemic vascular injury and hypertension is early and often dramatic adventitial remodeling [152, 179]. Early evidence of adventitial cell activation and phenotypic change has been reported following balloon injury to the vessel wall [132, 174]. A more recent experiment using animal models of hypercholesterolemia and hypertension has also demonstrated that adventitial remodeling precedes intimal and medial remodeling [62]. Studies also have shown that under conditions of elevated blood pressure, the adventitia becomes the predominant wall component due to its pronounced stiffening behavior [155, 173]. Thus the adventitia has been suggested to be the most appropriate arterial layer for "sensing" hypertensive states [102, 155]. A rapidly emerging concept is that the activation of adventitial FBs plays a key role in regulating vascular function and structure from the "outside-in" [179, 209]. The adventitial FBs display an important partnership with the medial SMCs in terms of phenotypic conversion, proliferation, apoptotic, and migratory properties, and contribute to neointima formation and vascular remodeling [152].

1.5 Characteristics of vascular SMC, fibroblast, and myofibroblast and their involvement in vascular diseases

The vascular fibroblast, myofibroblast, and SMC can be distinguished according to their expression of SMC markers, as shown in Tables 1-2 and 1-3, and Figs. 1-4 and 1-5. Fibroblasts do not express either α-SM actin (α-SMA) or SM myosins; myofibroblasts express α-SMA but not SM myosins; SMCs express both α-SMA and SM myosins. Only differentiated (mature) SMCs express smoothelin. α-SMA expression, stress fiber formation, and robust collagen secretion are the distinguishing features of myofibroblasts [192]. Adventitial fibroblasts can differentiate into myofibroblasts and even SMCs by mechanical tension or treatment with TGF-β1 (Fig. 1-6) [144, 152, 193]. In response to injury, medial SMCs de-differentiate into immature SMCs which migrate into the intima; and quiescent adventitial fibroblasts can be activated and converted into myofibroblasts and then migrate into the intima through the media (Fig. 1-7) [152], where these cells contribute to vascular lesion formation.

Table 1-2. SMC marker expression in fibroblast, myofibroblast and SMC

	α-SM actin	SM Myosins	Smoothelin
Fibroblast	-	-	-
Myofibroblast	+	-	-
Immature SMC	+	$SM1^+$, $SM2^-$	-
Differentiated SMC	+	$SM1^+$, $SM2^+$	+

SM1: smooth muscle-type 1 MHC isoforms; SM2: smooth muscle-type 2 MHC isoforms.

Table 1-3. Comparison of cell characteristics in vivo

	Contractility	Proliferation	Synthesis	Migration
Fibroblast	Low	Low	Low	Low
Myofibroblast	High	High	High	High
Immature SMC	Low	High	High	High
Differentiated SMC	High	Low	Low	Low

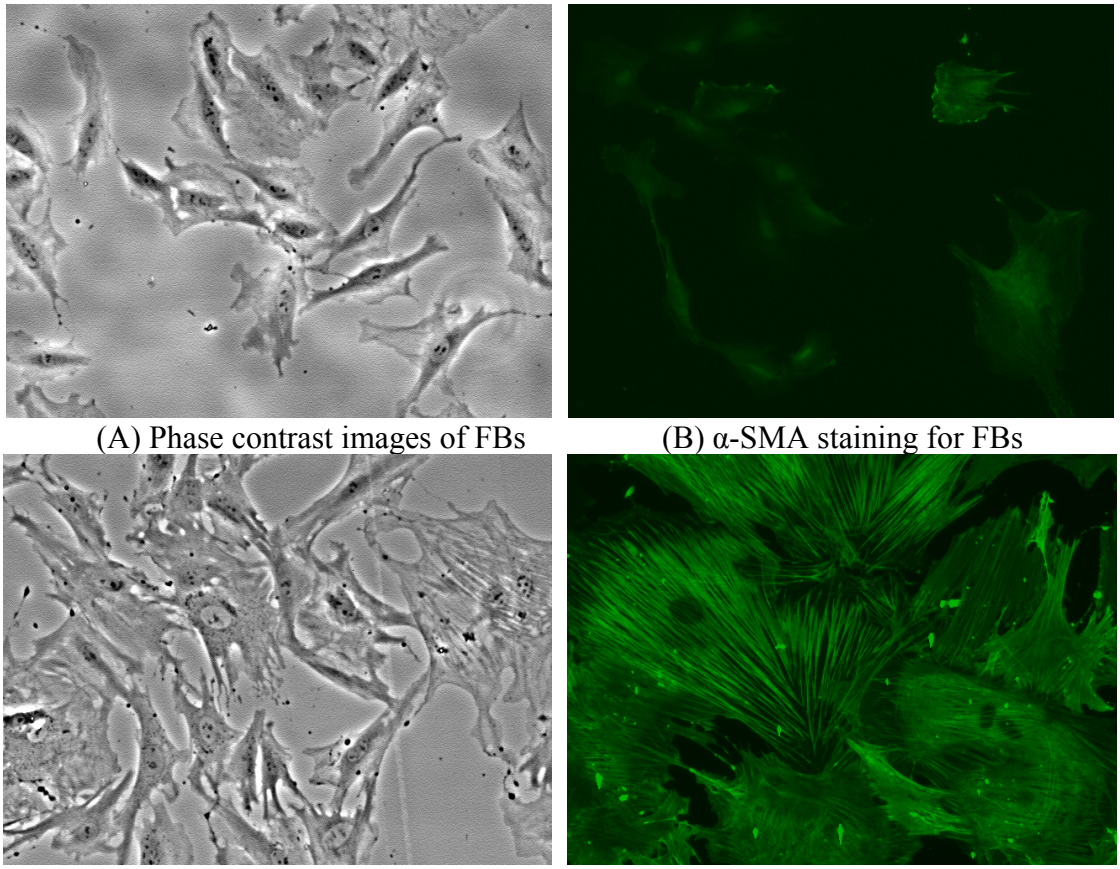

Figure 1-4. Morphology and α-SMA staining to characterize FBs and MFBs (personal unpublished data)**.**

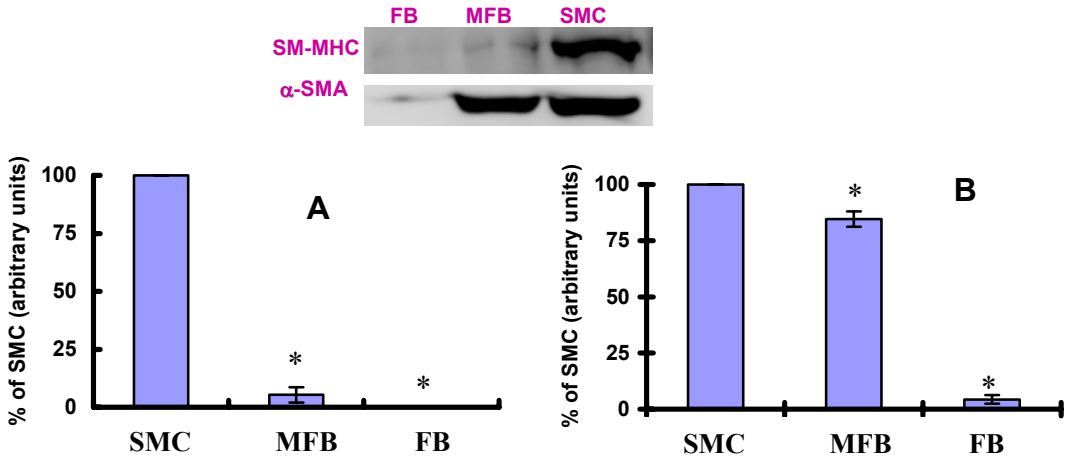

Figure 1-5. Western blotting to characterize FB, MFB and SMC. Top, Western blot gel bands; A, SM-MHC; B, α-SMA. Data are presented as means ± SEM. *P < 0.05 compared to the normalized SMC corresponding protein content. From [50].

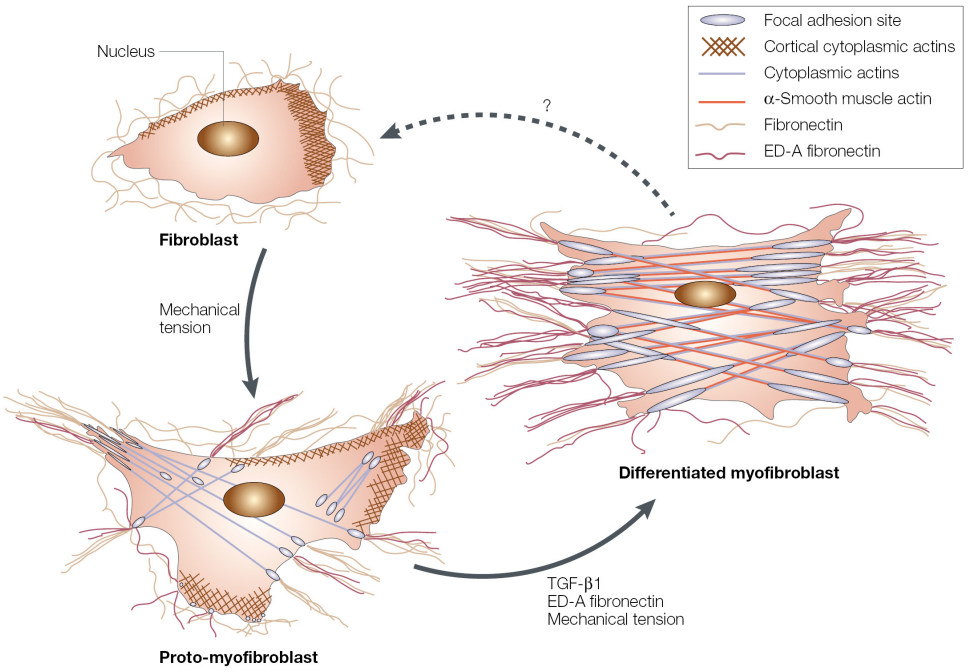

Figure 1-6. The two-stage model of myofibroblast differentiation [193].

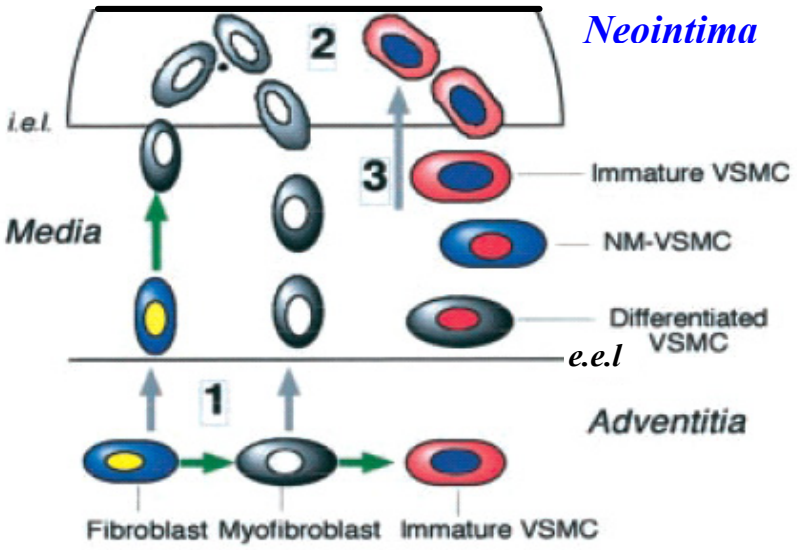

Figure 1-7. A model for cell contribution to neointima formation in response to injury. Gray arrows: direction of cell migration; green arrows: cell phenotypic transitions. 1, Adventitial fibroblasts can be converted into myofibroblasts in adventitia or in media. 2, Fibroblasts/myofibroblasts are characterized by an overt migratory ability toward the subendothelial space. 3, Neointima can also be formed with the contribution of vascular SMCs. i.e.l: internal elastic lamina; e.e.l.: external elastic lamina; NM: non-muscle [152].

1.6 Matrix metalloproteinases and their role in SMC and fibroblast migration

The major components of the interstitial matrix of the media and adventitia are collagen I and III, produced by vascular SMCs and fibroblasts [136, 140]. ECM-cell interactions affect the physical coupling of cells via the regulation of cell-surface adhesion molecules and may also regulate, via a positive feedback loop, the deposition of ECM [21]. Thus, under normal conditions, there must be a homeostatic relationship between resident cells and this collagen matrix to maintain SMCs and fibroblasts in a quiescent state. Activation of SMCs and fibroblasts leads to alterations in the production and relative composition of matrix components, which in turn ultimately contributes to further changes in cell growth, behavior, and phenotype switching.

Matrix metalloproteinases (MMPs) are a family of zinc enzymes responsible for degradation of ECM components, including basement membrane collagen, interstitial collagen, fibronectin, and various proteoglycans (see Table 1-4). MMPs are key mediators of the normal ECM remodeling that takes place during development, tissue morphogenesis, and repair. In addition, MMPs have been implicated in the untoward ECM degradation that occurs in various diseases. MMPs are conventionally classified as “collagenases”, “gelatinases”, “stromelysins”, “membrane type MMPs (MT-MMPs)” and “other MMPs” based on substrate specificity [80]. All MMPs possess an N-terminal signal sequence or “pre” domain, a propeptide “pro” domain that is removed during activation, and a conserved catalytic domain. With the exception of matrilysin, all MMPs contain a hemopexin-like domain which is connected to the catalytic domain by a hinge

domain (Fig.1-8). The initial step of ECM degradation involves active collagenases, especially MMP-1, -8, -13, and -18, which digest intact collagens followed by further digestion by gelatinases, mainly MMP-2 and MMP-9 [72]. Excessive or inappropriate expression of MMPs may contribute to the pathogenesis of tissue-destructive processes in a wide variety of diseases. MMPs in the blood vessel wall are produced by a number of cells, including endothelial cells (ECs), SMCs, fibroblasts and macrophages. Endogenous tissue inhibitors of metalloproteinases (TIMPs) reduce excessive proteolytic ECM degradation by MMPs. The balance between MMPs and TIMPs plays a major role in vascular remodeling and diseases [137].

Table 1-4. The MMP family (Adapted from Calbiochem)

The Matrix Metalloproteinase (MMP) Family

Enzyme	E.C. No.	Pseudonyms	Mol. Wt. (Latent/Active)	Collagen Substrates	Additional Substrates
MMP-1	3.4.24.7	Collagenase-1, Fibroblast Collagenase, Interstitial Collagenase, Tissue Collagenase	55,000/45,000	I, II, III, VII, VIII, X	Aggrecan, Gelatin, MMP-2, MMP-9
MMP-2	3.4.24.24	72 kDa Gelatinase, 72 kDa Gelatinase/Type IV Collagenase, Gelatinase A, TBE-1	72,000/66,000	I, II, III, IV, V, VII, X, XI	Aggrecan, Elastin, Fibronectin, Gelatin, Laminin, MMP-9, MMP-13
MMP-3	3.4.24.17	Procollagenase, PTR1 protein, SL-1, Stromelysin-1, Transin-1	57,000/45,000	II, III, IV, IX, X, XI	Aggrecan, Elastin, Fibronectin, Gelatin, Laminin, MMP-7, MMP-8, MMP-13
MMP-7	3.4.24.33	Matrilysin, Matrin, PUMP-1 Protease, Uterine Metalloproteinase	28,000/19,000	IV, X	Aggrecan, Elastin, Fibronectin, Gelatin, Laminin, MMP-1, MMP-2, MMP-9
MMP-8	3.4.24.34	Collagenase–2, Neutrophil Collagenase, PMNL Collagenase	75,000/58,000	I, II, III, V, VII, VIII, X	Aggrecan, Elastin, Fibronectin, Gelatin, Laminin
MMP-9	3.4.24.25	92 kDa Gelatinase, 92 kDa Gelatinase/Type IV Collagenase, Gelatinase B	92,000/86,000	IV, V, VII, X, XIV	Aggrecan, Elastin, Fibronectin, Gelatin
MMP-10	3.4.24.22	SL-2, Stromelysin-2, Transin-2	57,000/44,000	III, IV, V	Aggrecan, Elastin, Fibronectin, Gelatin, Laminin, MMP-1, MMP-8
MMP-11		SL-3, Stromelysin-3, ST-3	51,000/44,000		Aggrecan, Fibronectin, Laminin
MMP-12	3.4.24.65	HME, Macrophage Metalloelastase MME	54,000/45,000 and 22,000	IV	Elastin, Fibronectin, Gelatin, Laminin
MMP-13		Collagenase-3	60,000/48,000	I, II, III, IV	Aggrecan, Gelatin
MMP-18		*Xenopus* Collagenase-4, xCol4	70,000/53,000		
MMP-19		RASI-1	54,000/45,000	IV	Fibronectin, Aggrecan, COMP, Laminin, Gelatin
MMP-20		Enamelysin	54,000/22,000		Aggrecan, Amelogenin, COMP
MMP-23		CA-MMP			
MMP-26		Matrilysin-2, Endometase	28,000/19,000	IV	Gelatin, Fibronectin
MMP-28		Epilysin			
MT1-MMP		MMP-14, Membrane-Type Metalloproteinase-14	66,000/56,000	I, II, III	Aggrecan, Elastin, Fibronectin, Gelatin, Laminin, MMP-2, MMP-13
MT2-MMP		MMP-15, Membrane-Type Metalloproteinase-15	72,000/60,000		Fibronectin, Gelatin, Laminin, MMP-2
MT3-MMP		MMP-16, Membrane-Type Metalloproteinase-16	64,000/52,000		MMP-2
MT4-MMP		MMP-17, Membrane-Type Metalloproteinase-17	57,000/53,000		Fibrin, Gelatin
MT5-MMP		MMP-24	–/62,000		
MT6-MMP		MMP-25, Leukolysin		IV	Gelatin, Fibronectin, Laminin-I

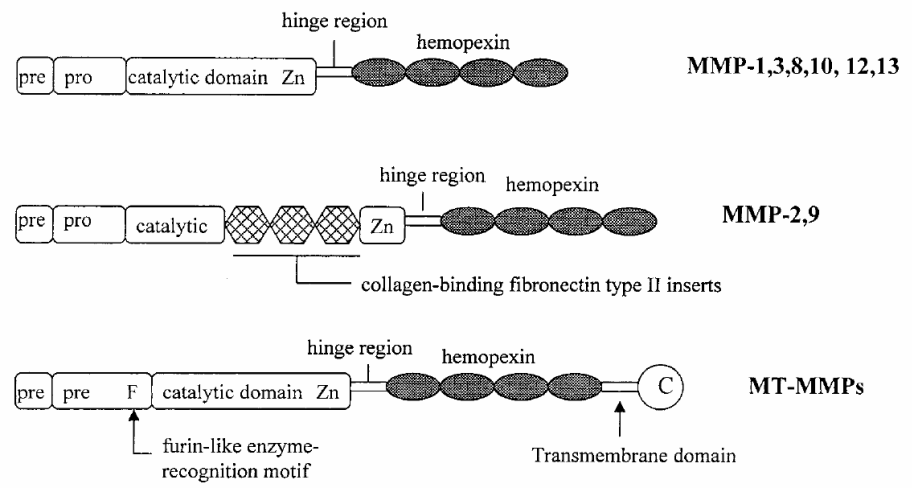

Figure 1-8. Domain structure of the MMPs. Pre: signal sequence, Pro: propeptide with a free-zinc-ligating thiol group, Zn: zinc-binding site [80].

MMP-1 (interstitial collagenase, pro-/active: 55/45 kDa) cleaves native triple helical collagen I at a specific site three-fourths of the way from the N-terminus, releasing ¼ and ¾ length collagen fragments. MMP-2 (gelatinase-A, type IV collagenase, pro-/active: 72/66 kDa) mainly digests denatured collagens (gelatins) and collagen fragments. MMP-2 is thought to be unable to cleave the native interstitial collagens. However, MMP-2 is capable of cleaving native type IV and V collagens [3]. Increased MMP expression and activity were associated with development of neointimal arterial lesions and SMC migration after arterial balloon injury in animal models [13, 214]. Upregulated expression of MMPs may also be necessary for fibroblasts to move through the adventitial matrix into the media and even into intima [164]. Previous work has shown that pig coronary adventitial fibroblasts secrete significantly greater levels of MMPs than SMC. Even more strikingly, the level of TIMPs expression is more than 10-fold less in fibroblasts. Fibroblasts may hence have a greater propensity to generate MMP activity, which could give them an advantage over SMC when migrating into areas of vascular injury [164].

Human interstitial collagenase is referred to as MMP-1. In rodents, however, MMP-1 is developmentally silenced and not present, and its collagenolytic function is mainly performed by MMP-13 [54]. MMP-13 (pro-/active: 60/48 kDa) is the major interstitial collagenase in rats and mice to digest collagens. Due to confusion in MMP nomenclature, rat interstitial collagenase (genebank locus: M60616) should be recognized as rat MMP-13, not MMP-1 as many other articles and ours have designated [8, 166, 167].

The controlled degradation of ECM components helps cells migrate. MMPs can contribute to cell migration in several ways: 1) they can clear a path through the ECM; 2) they can expose cryptic sites on the cleaved proteins that promote cell binding, cell migration, or both; 3) they can promote cell detachment so that a cell can move onward, or 4) they can release extracellular signal proteins that stimulate cell migration [5].

Remodeling of ECM and non-matrix substrates by MMPs could influence vascular SMC migration in many ways [116]. Cells in the media or adventitia would need to break physical barriers between basement membrane (BM) components and cell surface integrins. For vascular SMC to move, several signal transduction pathways must be activated to reorganize the cytoskeleton and to form reversible contacts with existing or newly expressed cell surface and ECM components. Signaling pathways originating from growth factor receptors, cadherins and integrins appear to be very important [1, 22, 114]. ECM-integrin interactions, in particular, promote activation of focal adhesion kinase (FAK) and focal adhesion formation (Fig.1-9). Cellular adhesion on native collagen I is mediated by $\alpha_2\beta_1$ and $\alpha_1\beta_1$ integrins and on proteolytically cleaved, denatured collagen can also be mediated by $\alpha_v\beta_3$ integrins [107, 210]. Loss of contact with BM components, type IV collagen and laminin, are likely to be responsible at least in part for the profound

changes in gene expression that occur in VSMC during neointima formation. Hence, MMPs by degrading BMs can indirectly facilitate a host of new ECM-integrin interactions leading to activation of FAK and increased migration (Fig.1-9). Cleavage of ECM proteins may also reveal cryptic integrin binding sites. For example, PDGF stimulated vascular SMC migrate more rapidly on collagen I that has been cleavaged into 1/4, 3/4 length fragments than on intact collagen I [181]. Moreover, SMC adhesion and migration on cleaved collagen is mediated by newly induced $\alpha_v\beta_3$ integrins, while migration on native collagen I is mediated by constitutive $\alpha_2\beta_1$ integrins (Fig.1-9) [116].

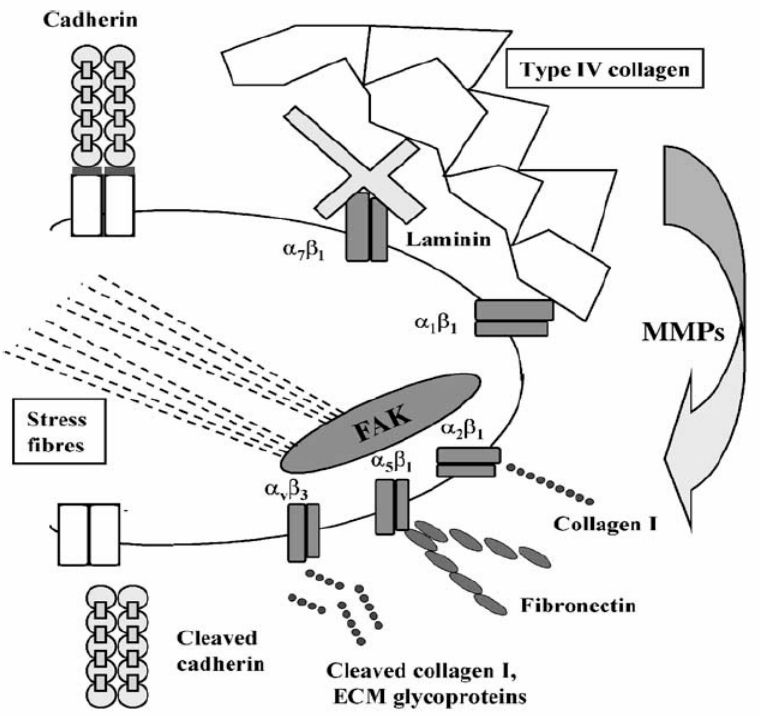

Figure 1-9. MMP influences on vascular SMC migration. MMPs can remodel basement membrane components, including laminin and collagen IV and free cells to migrate. Loss of basement membranes promotes SMC phenotypic modulation. This leads to synthesis, amongst other things, of new integrin subunits and new matrix components that include glycoprotein ligands for these integrins. MMPs also fragment existing membrane components such as collagen I and this can create new integrin-binding sites. By acting through integrins and FAK, ECM components influence intracellular pathways that regulate the cytoskeletal changes necessary for motion. MMPs could shed cadherins and could thereby relieve constraints on movement caused by adherens junctions [116].

1.7 Hemodynamic forces on vascular SMC and fibroblast

Modeling studies have shown that: 1) interstitial flow driven by the transmural pressure gradient imposes fluid shear stresses on SMCs, 2) the SMC layer adjacent to the porous internal elastic lamina (IEL) is exposed to shear stresses an order of magnitude greater than underlying SMC layers, which is around 0.1 to 1 dyn/cm^2, and 3) the underlying SMCs far away from IEL are exposed to much lower shear stress [183-185, 201] (see Fig.1-10). Although, to our knowledge, there have been no studies conducted to estimate the magnitude of shear stress that adventitial fibroblasts are subjected to in an artery, we hypothesize that the interstitial flow shear stress on fibroblasts would be less than that on SMC, since the permeability of "loose" adventitia is greater than the "dense" media. When the IEL is damaged, SMCs may also be exposed to luminal blood fluid shear stress.

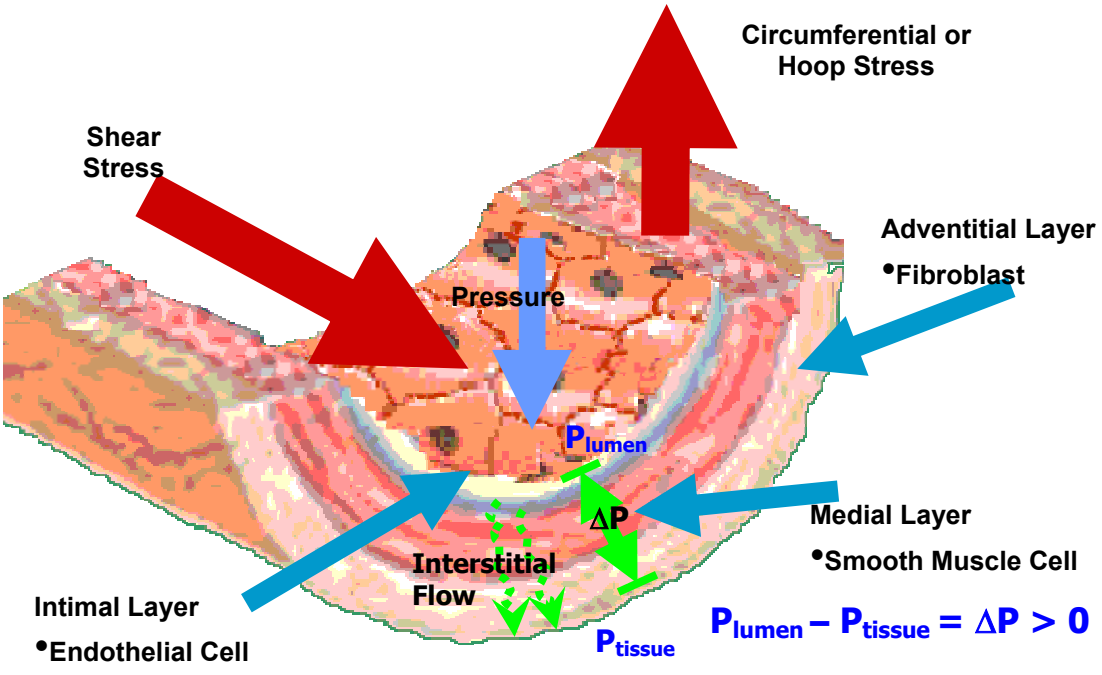

Figure 1-10. Hemodynamic forces acting on artery wall. The transmural pressure differentitial ΔP drives transmural interstitial flow across the arterial wall.

Interstitial flow on SMCs and fibroblasts as well as transmural mass transport conveyed by hydraulic conductance will be elevated after endothelial denudation following angioplasty or other injury [56, 104, 186] (Fig.1-11). For example, when the endothelium is denuded in rabbit aortas, both hydraulic conductance (Lp) and Darcy permeability (Kp) are increased 2.5-fold [10], which can lead to a 60% increase in shear stress. Endothelial denudation in rat aortas induces a 75% increase in hydraulic conductivity [171], which can result in a 30% increase in shear stress. (see equations (1) and (2) for estimation of shear stress). In the hypertensive condition, not only is the vessel wall stress higher than normal, but the interstitial flow is elevated due to elevated blood pressure. Shortly after injury (within minutes, less than one hour), a fibrin clot will form at the injury site, which reduces the elevated interstitial flow. The interstitial flow is still higher than that in the uninjured blood vessel because the permeability of blood clot (10^{-10} cm^2) is much higher than aortic intima and media (10^{-14} cm^2, see Table 1-5) [39, 86]. However, the fibrin clot would largely block the elevated cytokine convection to vascular SMCs and fibroblasts. Transmural interstitial flow decreases during wound healing.

The Darcy permeability (Kp) of a porous media is defined by

$$Kp = \mu(Jv/A)/(\Delta P/L) \qquad (1),$$

and Wang and Tarbell [204] developed a theory for the interstitial flow induced shear stress (τ) on cells that can be expressed approximately as

$$\tau \approx \mu(Jv/A)/\sqrt{Kp} = (\Delta P/L)\sqrt{Kp} \qquad (2).$$

In equations (1) and (2), μ is the viscosity of the fluid flow, Jv is the volumetric flow rate, A is the cross section area, ΔP is the pressure drop across the porous media, and L is the thickness of the porous media.

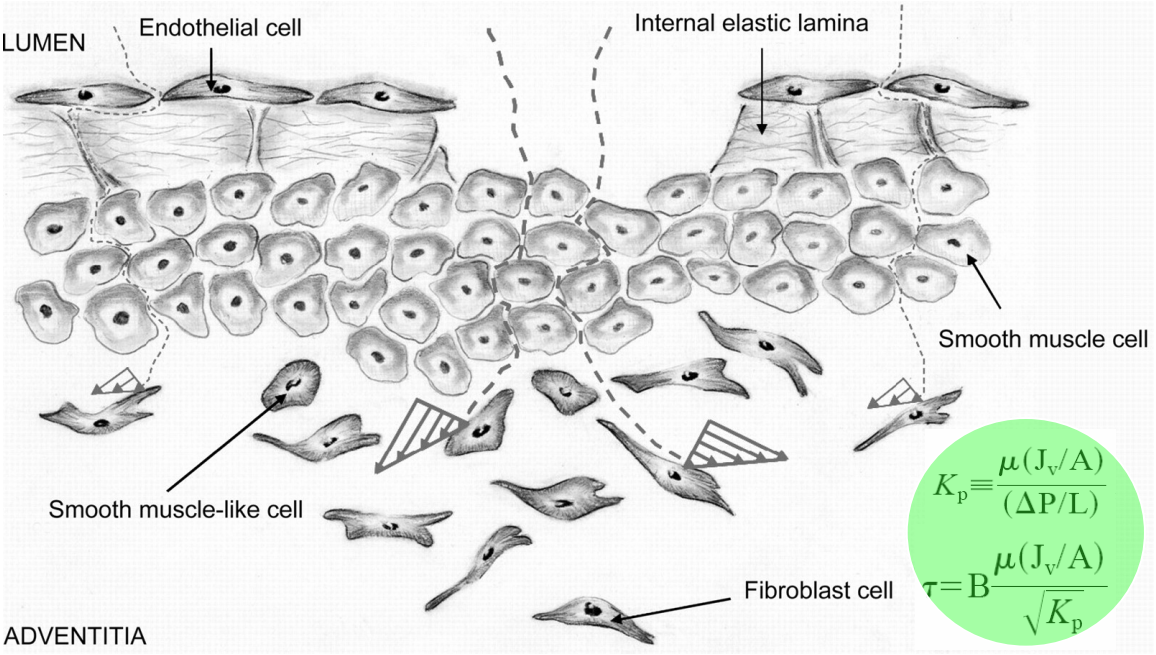

Figure 1-11. Interstitial flow increases after vascular injury. Darcy permeability and interstitial flow-induced shear stress can be estimated using the equations in the figure [50].

Table 1-5. Selected permeabilities of some tissues and collagen gels

Tissue/material	K_p (cm^2)
Collagen gel (2.5-45 mg/ml)	10^{-8}-10^{-12} cm^2 [118, 138, 204]
Aortic media and intima	0.3-1.5x10^{-14} [86]
Adventitia	**? >10^{-14}**
Blood clot (unretracted/retracted)	10^{-8}-10^{-10} [39]

Several previous studies have demonstrated that mechanical stimuli affect vascular SMC and fibroblast migration. Li *et al.* (2002) [89] provided evidence that adventitial fibroblasts respond to mechanical stretch. Their work provides a possible mechanism for the activation of fibroblast migration from adventitia into neointima. SMCs have displayed reduced migratory activity in response to elevated blood flow in a balloon catheter injury model in vivo [76] and have also demonstrated inhibition of 2-D migration

in response to fluid shear stress (12 dyn/cm^2) in vitro [127]. Garanich et al. (2005) [51] applied shear stress (~15 dyn/cm^2) using a rotating shear apparatus directly on the surfaces of SMCs which were cultured on a thin layer of Matrigel. They found that the migration of SMC was suppressed via nitric oxide-mediated downregulation of MMP-2 activity. Furthermore, Garanich et al. (2007) [50] revealed that shear stress could also inhibit myofibroblast migration and promote fibroblast migration using the same experimental methods.

Fluid shear stress also affects vascular SMC proliferation and differentiation. In some 2-D studies, fluid shear stress has reduced cell proliferation [180, 196] and induced apoptosis [46]. Other 2-D studies, however, have shown that fluid shear stress can reduce expression of SMC marker genes [9, 202] and promote SMC proliferation [9, 57]. The controversy of different effects of shear stress on SMC proliferation probably is due to the level of shear stress and the patterns of shear stress that were applied to cells, and also the species and phenotypic state of SMCs that were used.

Taking these in vitro 2-D studies together, it is clear that fluid flow shear stress has a significant impact on vascular SMC and fibroblast/myofibroblast proliferation, migration, and differentiation at least in vitro in 2-D. It is now well known that a 3-D cell culture system can better recapitulate the in vivo microenvironment [32]. However, to date, there have been no studies to investigate whether fluid flow affects vascular SMC and fibroblast proliferation, differentiation, and migration in 3-D environment.

The thesis that follows will address the questioins raised above. In chapter 2, we investigate the effects of interstitial flow on vascular fibroblast, myofibroblast, and smooth muscle cell motility in 3-D collagen I gels and the potential role of MMPs. In

chapter 3, we consider the involvement of signaling molecules including MAPK (ERK1/2 and p38) and transcription factor AP-1 (c-Jun and c-Fos) in MMP expression and cell motility when cells are exposed to interstitial flow in 3-D. Chapter 4 is devoted to exploring the roles of FAK and cell surface HSPGs in the mechanotransduction of interstitial flow; and chapter 5 examines the effects of both laminar flow (2-D) and interstitial flow (3-D) on modulation of SMC marker gene expression and the underlying mechanotransduction mechanism. The thesis closes with a chapter summarizing the whole work and discussing clinical implications and future research directions.

Chapter 2

Interstitial Flow Promotes Rat Vascular Fibroblast, Myofibroblast, and Smooth Muscle Cell Motility in 3-D Collagen I via Upregulation of MMP-13

2.1 Abstract

Neointima formation often occurs in regions where the endothelium has been damaged and the transmural interstitial flow is elevated. Vascular smooth muscle cells (SMC) and fibroblasts/myofibroblasts (FB/MFB) contribute to intimal thickening by migrating from the media and adventitia into the site of injury. In this study, for the first time, the direct effects of interstitial flow on SMC and FB/MFB migration were investigated in an in vitro 3-dimensional (3-D) system. Collagen I gels were used to mimic 3-D extracellular matrix (ECM) for rat aortic SMC and FB/MFB. Exposure to interstitial flow-induced by 1 cmH_2O pressure differential (shear stress ~0.05 dyn/cm^2, flow velocity ~0.5 μm/s, and Darcy permeability ~10^{-11} cm^2) substantially enhanced cell motility. Matrix metalloproteinase (MMP) inhibitor (GM 6001) abolished flow-induced migration augmentation, which suggested that enhanced motility was MMP-dependent. Upregulation of rat interstitial collagenase (MMP-13) played a critical role for flow-enhanced motility, which was further confirmed by silencing MMP-13 gene expression. Longer exposures to higher flows suppressed the number of migrated cells, although MMP-13 gene expression remained high. This suppression was a result of both flow-induced tissue inhibitor of metalloproteinase-1 (TIMP-1) upregulation and increased apoptotic and necrotic cell death. Interstitial flow did not affect MMP-2 gene expression or activity in the collagen I gel for any cell type. Our findings shed light on the mechanism by which vascular SMC and FB/MFB contribute to intimal thickening in regions of vascular injury where interstitial flow is elevated.

Keywords: interstitial flow; migration; matrix metalloproteinase; neointima formation

2.2 Introduction

Neointima formation is often induced in regions where the endothelium has been damaged by mechanical injury, increased wall stress (as in hypertension), or chemical insult [68, 99, 101, 115, 157]. The migration of smooth muscle cells (SMC) from the media to the intima and their subsequent proliferation and new extracellular matrix (ECM) secretion are well recognized characteristics of neointima formation [99, 115]. In addition to medial SMC, adventitial fibroblasts (FB) and their activated counterpart, myofibroblasts (MFB) are also capable of migrating from the adventitia to the media and even to the intima where they contribute to the thickening of the neointima in response to endothelial injury [152, 158, 163, 174].

It has been shown that matrix metalloproteinases (MMPs) are involved in intimal lesion formation. MMPs are a family of zinc-dependent enzymes responsible for degradation of ECM. Human interstitial collagenase is referred to as MMP-1. In the rodents, however, MMP-1 is developmentally silenced and not present. The collagenolytic function of MMP-1 is mainly performed by MMP-13 (e.g., rat interstitial collagenase, or collagenase-3) [54]. MMP-13 (pro-/active: 60/48 kDa) is the major interstitial collagenase in rats and mice to digest collagens. Due to confusion in MMP nomenclature, rat interstitial collagenase (genebank locus: M60616) should be recognized as rat MMP-13, not MMP-1 as many other articles and ours have designated [8, 166, 167]. The ECM degradation initially involves active collagenases (especially MMP-1, -8, and -13) which digest intact collagens, and then gelatinases (mainly MMP-2 and MMP-9) for further digesting collagen fragments and gelatins [72]. The excessive proteolytic ECM

degradation by MMPs can be reduced by endogenous tissue inhibitors of metalloproteinases (TIMPs). The balance between MMPs and TIMPs plays a major role in vascular remodeling and diseases [137]. Increased MMP expression and activity are associated with neointimal lesion development and SMC migration after arterial balloon injury [13, 214]. Upregulated MMP matrix-degrading activity may also be necessary for FB to move through the adventitial matrix into the media and intima [164]. MMP expression and SMC migration were promoted at vein-to-graft anastomoses in hemodialysis grafts, leading to intimal thickening and stenosis [105]. However, the mechanisms by which SMC and FB "sense" vascular injury and then contribute to neointima formation still remain unclear.

Interstitial flow, the movement of fluid through the ECM, is present in all tissues [198]. It is an important coupling factor between mechanical stress and signaling in the 3-D matrix [56]. Modeling studies have shown that transmural interstitial flow (driven by transmural pressure) passes through the oriented SMC layers to the adventitia and imposes shear stresses on SMC that are of the order of 0.1 to 1 dyn/cm^2, depending on the location of the cells in the media [184, 185, 201]. Shear stress on FB would be expected to be lower than on SMC since the permeability of "loose" adventitia is higher than that of "dense" media. In the case of vascular injury or hypertension, interstitial flow and flow-induced shear stress on SMC and FB will be elevated [104, 184, 186]. For example, when the endothelium is denuded, the hydraulic conductance is increased 2.5-fold [10] in rabbit aortas and 1.75-fold [171] in rat aortas, which leads to 2.5-fold and 1.75-fold increases in shear stress, respectively (see equation (2) for shear stress estimation). Previous studies have demonstrated that shear stress on cell monolayers (2-D) affects

vascular SMC and FB migration in vitro [50, 51]. Changes in shear stress in venous grafts also may cause SMC migration and intimal thickening [105]. However, there has been no assessment of whether interstitial flow directly affects vascular SMC and FB/MFB migration in 3-D.

Vascular SMC and FB/MFB reside in a 3-D ECM which is mostly collagen I. The migration of SMC and FB/MFB initially occurs in collagen I; cells then penetrate the external/internal elastic lamina (EEL/IEL) and basement membrane as they move into the intima. To model the in vivo environment more faithfully, therefore, we use 3-D collagen I as the ECM to investigate the direct effects of interstitial flow on the motilities of vascular SMC and FB/MFB. We show that interstitial flow can promote SMC and FB/MFB migration rates in 3-D collagen I gels and this enhanced motility is controlled by upregulation of MMP-13, not MMP-2.

2.3 Methods

2.3.1 3-D gel preparation. Rat aortic SMC, adventitial FB and MFB were obtained as previously described [50, 51]. Cells (passage 3-5) were first suspended in rat tail collagen I (BD Science) gels (cell density: 2.5×10^5 cells/ml; final gel concentration: 4 mg/ml). Then 200 μl of gel was loaded into each 12-well cell culture insert with 8 μm pore size membrane (BD Science) whose edge had been precoated with 50 μl of 4 mg/ml of cell-free collagen without serum to prevent the gel from later contracting and detaching during cell spreading (Fig. 2-1*A*). 1 ml of growth medium (DMEM containing 10% FBS

and 1% P/S) was added to each well, and the gels were continuously incubated for 24 hours to allow cell spreading.

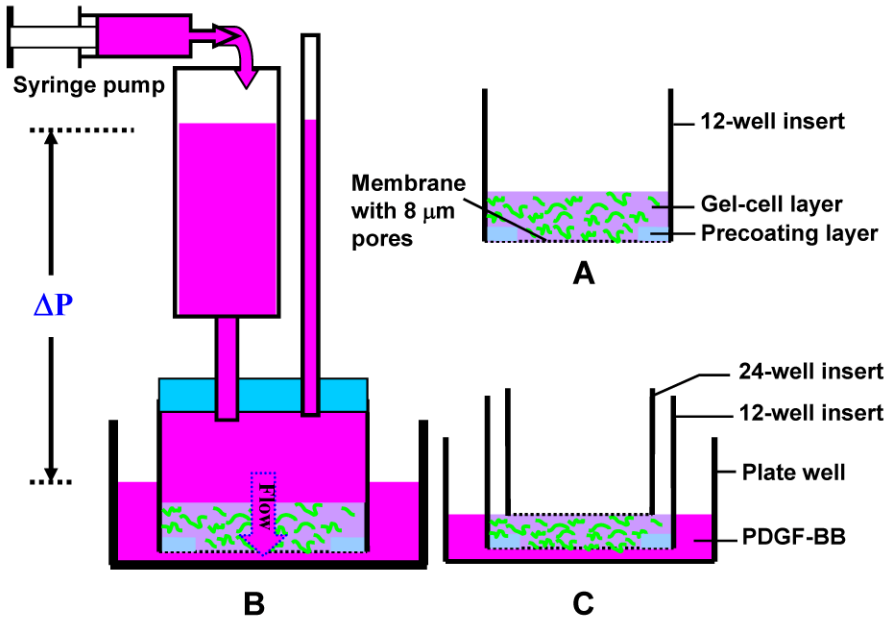

Figure 2-1. Schematic of the 3-D interstitial flow and cell migration system. A: 200 μl of cell/gel mixture was loaded into a 12-well insert with a 50 μl cell-free collagen precoating layer along the edge. Gel concentration was 4 mg/ml and cell density was 2.5×10^5 cells/ml. B: The gel was exposed to interstitial flow driven by a pressure drop. C: After exposure to flow, to check cell motility, the gel was pre-compacted with a 24-well insert on top and then incubated with 20 ng/ml of PDGF-BB to initiate migration.

2.3.2 Interstitial flow experiment and cell migration assay. Gels were subjected to interstitial flow driven by 1, 3, or 10 cmH_2O pressure drop for 1, 3, or 6 h (Fig. 2-1*B*). The flow medium was the same as the growth medium. Other gels not exposed to flow served as no flow controls. Immediately after the flow exposure period, the undersides of insert membranes were swabbed by wet and sterile cotton tipped applicators to remove any cells which had already migrated to the undersides. In this way, all inserts indicated zero cell migration at the start of the migration period.

Because the compaction of gels due to different flow rates could affect cell migration rates, all gels were pre-compacted to a defined state just before the migration phase of the experiment. To accomplish the pre-compaction, a 24-well format insert was placed on the top of each gel (Fig. 2-1*C*) and compressed to a fixed depth by placing the lid over the 12-well plate. Then by confocal microscopy we did not see any change in cell distribution between flow treated gels and controls, which suggests that cells did not migrate in the gels during 6 h of flow period (data not shown). Thus to check the effect of flow on cell motility, we added 1 ml of 20 ng/ml PDGF-BB (Sigma) to each plate well to initiate migration to the bottom of the insert membrane. This way we were able to count migrated cells easily as a modified Boyden chamber. After 48 hours of chemotactic incubation, cells that had migrated to the undersides of insert membranes were stained with Diff-Quik (Dade Behring Inc), and 5 fields (100X) (1 center, 4 edges) were randomly picked for counting. We observed that there was no difference in cell migration whether pre-compacting gel right before flow or after flow; however, the level of compaction significantly affected cell migration. Preliminary experiments with 4 mg/ml collagen gels showed that compaction reduced cell migration by ~ 30% (data not shown).

2.3.3 MMP activity inhibition experiments. A potent, broad-spectrum MMP inhibitor, GM 6001 (Calbiochem), and its structural analog, GM 6001-NC, as a negative control were used in some experiments to block MMP activity. 1 ml of 10 μM GM 6001 or GM 6001-NC were mixed with 1 ml of 20 ng/ml PDGF-BB and then added to some plate wells at the start of the migration period.

2.3.4 MMP activity assay. The MMP-2 activity in the conditioned media of control, 1 h flow, and 6 h flow treated gels were determined using the SensoLyte™ 520 MMP-2 Assay Kit from AnaSpec Co. (San Jose, CA). Briefly, the conditioned media was collected from the companion plate well after the 48 h migration period. To measure MMP activity, the conditioned media was concentrated to the same fold by an YM-10 Microcon centrifugal filter device (Millipore). In the MMP-2 assay, 50 µl either with or without 1 mM APMA treated medium was added to each microplate well, followed by adding MMP-2 substrate 5-FAM/QXL^{TM}520 FRET peptide. The fluorescence intensity representing the MMP-2 activity was measured at 490/520 nm wavelength.

2.3.5 Collagen/gelatin zymography and reverse collagen zymography. Collagen and gelatin zymography was used to reinforce MMP activity assay data. The collagen and gelatin proteolytic activities of MMPs in the conditioned media of control, 1 h flow, and 6 h flow treated gels were assessed by collagen or gelatin substrate zymography as previously described [55]. Electrophoresis was carried out using a Mini-PROTEAN 3 Cell system (Bio-Rad). 20 µl of conditioned media was mixed in non-reducing 5X sample buffer containing SDS, glycerol, and bromophenol blue (without 2-mercaptoethanol) and subjected to electrophoresis on 10% polyacrylamide SDS gels (1.5 mm thick) containing 0.5 mg/ml of calf skin collagen type I (C9791, Sigma) or 1 mg/ml of porcine skin gelatin (G2500, Sigma). After electrophoresis, the polyacrylamide gels were washed 3 times (20 min each) in 2.5% Triton X-100 for 1 h to remove all traces of SDS. Gels were rinsed in distilled water for 5 min and finally incubated at 37 °C in developing buffer containing 100 mM Tris-HCl, 5 mM $CaCl_2$, 0.005% Brij-35, 0.001%

NaN_3, pH 8.0 for 20 h. Gels were stained with 0.25% Coomassie brilliant blue G-250 in 50% methanol, 10% acetic acid solution and destained with 40% methanol, 10% acetic acid solution. MMP level was identified as clear zones of lysis against a blue background. Finally the gels were incubated in 5% methanol, 7.5% acetic acid. To check TIMP-1 levels, 40 μl of conditioned media each well was subjected to reverse zymography which was performed as previously described [176]. Reverse collagen zymography was very similar to collagen zymography except that the polyacrylamide SDS gels were not only incorporated with calf skin collagen I, but also contained day-4 rat aortic fibroblast conditioned medium. The level of TIMP-1 was identified by the blue bands. To quantify MMP levels, the images were acquired using ChemiDoc XRS (Bio-Rad) and processed using Quantity One software (Bio-Rad).

2.3.6 Releasing cells from collagen gels. To collect cells from collagen gels, gels were detached from cell culture inserts and transferred into centrifuge tubes. Each gel was then incubated with 100 μl of 0.2% of collagenase I (Worthington Biochemical) in complete growth media at 37^{o} C for about 1 h with gentle agitation. Once collagen gels were completely digested, the media with collagenase was removed by centrifugation. Cell pellets were then washed once with ice-cold PBS and collected.

2.3.7 Reverse transcription-polymerase chain reaction (RT-PCR). RT-PCR assays were performed to assess relative mRNA levels. Briefly, cells were lysed and reverse transcription was performed following the procedures for the "Cells-to-cDNA^{TM} II" kit (Ambion). PCR reactions were performed using designed primers and Multiplex PCR

Master Mix (New England Biolabs). A 383-bp rat MMP-13 product was amplified using the sense primer 5'-GAC CTC ATG TTC ATC TTT AG-3' and the antisense primer 5'-CAC CAC AAT AAG GAA TTC GT-3' (Genebank accession no. M60616). A 200-bp rat MMP-2 product was amplified using the sense primer 5'-GAT GGA TAC CCA TTT GAC GG-3' and the antisense primer 5'-CTG CTG TAT TCC CGA CCA TT-3' (Genebank accession no. NM_031054). A 203-bp TIMP-1 product was amplified using the sense primer 5'- GTG TTT CCC TGT TCA GCC AT-3' and the antisense primer 5'-GTT CAG GCT TCA GCT TTT GC-3' (Genebank accession no. NM_053819). A 232-bp GAPDH product was amplified using the sense primer 5'-TCT TCA CCA CCA TGG AGA A-3' and the antisense primer 5'-ACT GTG GTC ATG AGC CCT T-3' (Genebank accession no. NM_017008). PCR amplification was conducted using the following protocol: predenaturation at 95 ºC for 5 minutes, then either 40 cycles (for MMP-13) or 30 cycles (for all other genes) of denaturation at 94 ºC for 35 seconds, annealing at 52 ºC for 35 seconds, and extension at 72 ºC for 35 seconds, followed by a final extension at 72 ºC for 10 min. The amplified mRNA products were separated by electrophoresis in 2.5% agarose gels and photographed under UV light in the presence of ethidium bromide. The products were confirmed not only by DNA loading marker, but also by sequencing.

2.3.8 Hairpin siRNA plasmid construction. The hairpin siRNA oligonucleotides (MMP-13 sense, 5'-GATCC **GTGAACAAGCTTCAGGTAA** *TTCAAGAGA* **TTACCTGAAGCTTGTTCAC** AGA-3'; MMP-13 antisense, 5'-AGCTTCT **GTGAACAAGCTTCAGGTAA** *TCTCTTGAA* **TTACCTGAAGCTTGTTCAC** G-3')

contained a region specific to bases 1501 to 1519 of MMP-13 mRNA (bold underlined), a hairpin loop region (italic), and 5' and 3' linker sequences for subcloning into the BamHI and HindIII sites of the pSilencer 4.1 CMV-neo vectors (Ambion). After cloning, the plasmid was then confirmed by both BamHI and HindIII digestion and sequencing. The vector that had no siRNA insert was used as a vector sham control.

2.3.9 MMP-13 shRNA transfection. MMP-13 shRNA plasmid was transfected into rat aortic SMC and MFB (both at passage 4) using Lipofectamine^{TM} (Invitrogen), following manufacturer's instruction. Cells were then split once. After reaching 80% confluence, a fraction of the cells was used to verify MMP-13 gene knowdown by RT-PCR, and other cells were directly suspended into collagen gels for flow-migration experiments. After flow experiments, both RT-PCR and collagen zymography were performed to check MMP-13 gene knockdown and activity reduction.

2.3.10 Cell apoptosis and viability assay. After 48 h of chemotatic incubation, cells in flow treated collagen gels were stained using the Vybrant™ apoptosis assay kit #2 (Invitrogen). Live cells in different gels with the same flow treatment were stained with Calcein AM (Invitrogen) to check viability. Both assays were carried out according to the supplier's instructions. Images were taken under an inverted fluorescent microscope by focusing on the layer of cells right above the cell culture insert membrane.

2.3.11 Cell apoptosis induction and wound healing assay. Rat aortic MFB and SMC were grown in small dishes until 80% confluency. Then the growth media was replaced

by tissue necrosis factor (TNF)-α (20 ng/ml) and cycloheximide (CHX) (3 μg/ml) (Sigma) in complete growth media for 2.5 h to induce apoptosis. Wounds in monolayer cells were scratched using a small pipette tip. TNF-α/CHX then was replaced by PDGF-BB (20 ng/ml) in DMEM for cell migration for 24 h.

2.3.12 Confocal Microscopy. Cell distribution was observed by confocal microscopy. After certain flow experiments and the 48 h incubation with PDGF-BB, cells in the collagen gel were stained with Calcein AM (Molecular Probes) and scanned by a confocal laser scanning microscope (Leica TCS SP2 AOBS) with a 10X lens. Fluorescence intensity was quantified as an indicator of cell distribution.

2.3.13 Data Analysis. Results are presented as mean ± SEM. Data sets were analyzed for statistical significance using a Student's t-test with a two-tailed distribution, and $P < 0.05$ was considered statistically significant. For comparison of more than two groups, we used one-way ANOVA followed by the t-test with Bonferroni correction, and $P < 0.05/N$ (N stands for number of comparisons) was considered statistically significant.

2.4 Results

2.4.1 Flow velocity, Darcy permeability (Kp) and shear stress (τ) estimation

The Darcy permeability (Kp) of the gel/cell layer is defined by

$Kp = \mu(Jv/A)/(\Delta P/L)$ (1),

and Wang and Tarbell [204] developed a theory for the interstitial flow induced shear stress (τ) on cells that can be expressed approximately as

$\tau \approx \mu(Jv/A)/\sqrt{Kp} = (\Delta P/L)\sqrt{Kp}$ (2).

In equations (1) and (2), μ is the viscosity of the flow medium, Jv is the volumetric flow rate, A is the cross section area of the gel, ΔP is the pressure drop across the gel, and L is the thickness of the gel. Interstitial flows driven by 1, 3, and 10 cmH_2O pressure drops induced shear stresses on cells in collagen gels of 0.05, 0.10, and 0.36 dyn/cm^2, respectively. The Darcy permeability (Kp) was on the order of 10^{-11} cm^2, and the interstitial flow velocity was in the range of 0.5-2.4 μm/s. Gel compaction also occurred as the gel thickness decreased with increasing flow. The Darcy permeability, flow velocity, and shear stress for the experimental conditions are summarized in Table 2-1.

Table 2-1. Flow velocity, Darcy permeability and shear stress estimation

Pressure drop, ΔP (cmH_2O)	Thickness, L (mm)	Flow rate, Jv (μl/min)	Velocity, V (μm/s)	Permeability, Kp ($cm^2 \times 10^{-11}$)	Shear stress, τ (dyn/cm^2)
10	1.5 ± 0.2	13.0 ± 1.1	2.4 ± 0.4	2.6 ± 0.5	0.36 ± 0.04
3	1.8 ± 0.2	4.4 ± 0.4	0.7 ± 0.2	3.0 ± 0.4	0.10 ± 0.02
1	2.1 ± 0.2	3.5 ± 0.5	0.5 ± 0.2	5.6 ± 1.1	0.05 ± 0.01

Data are mean ± SEM (n=4). (A=0.9 cm^2, μ=0.8 cP at 37°C). The gel thickness before flow was about 2.4 mm. The values given in Table 2-1 for gel thickness were measured after the flow period but before pre-compaction. After pre-compaction, the gel thickness was about 1.4 mm for all samples.

2.4.2 Validation of 3-D interstitial flow - cell migration system

Fig. 2-2 shows that both fibroblasts and myofibroblasts can migrate from the collagen gel through 8 μm pores to the undersides of filter membranes. Without PDGF-BB in serum free DMEM medium, cells were barely seen on filter membranes, while the migration through membrane pores was dramatically promoted in the present of PDGF-BB. These results suggest that PDGF-BB is capable of attract these cell to migrate.

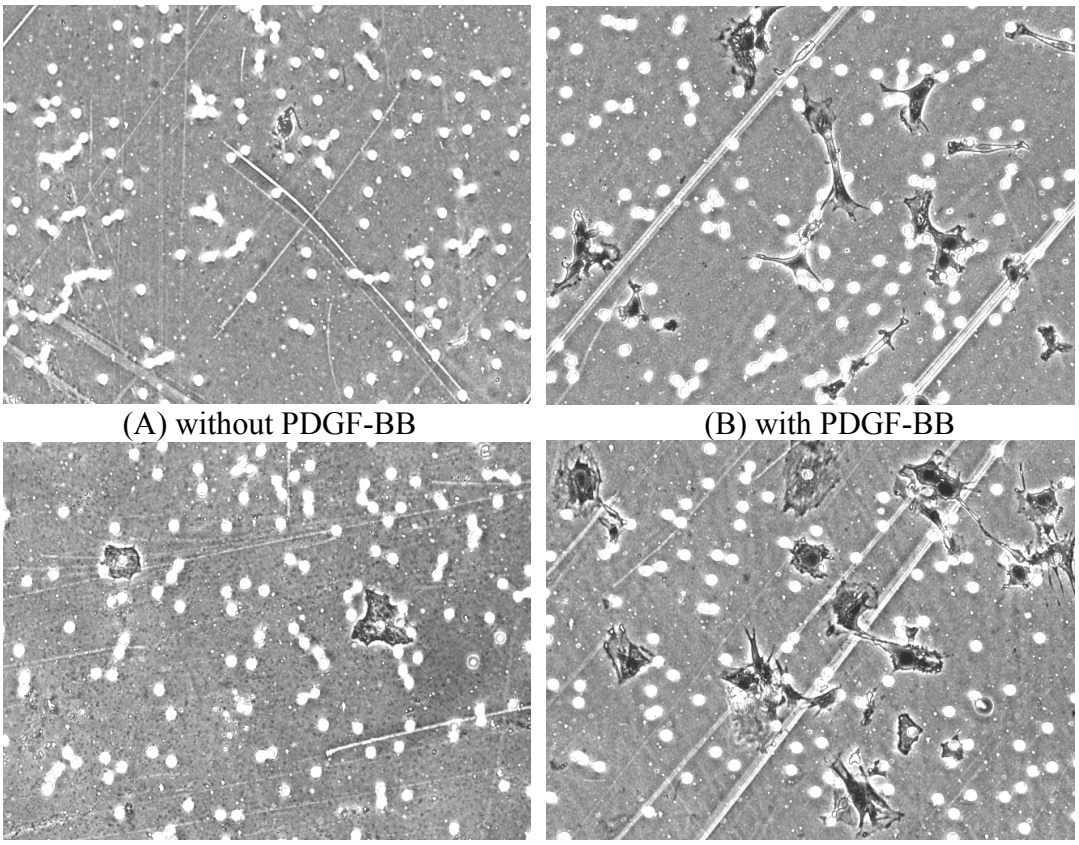

(A) without PDGF-BB (B) with PDGF-BB

(C) without PDGF-BB (D) with PDGF-BB

Figure 2-2. PDGF-BB induces vascular cell migration in the collagen gel. The PDGF-BB induced fibroblasts (A and B) and myofibroblasts (C and D) migration from collagen gels to the undersides of cell culture insert filter membranes through 8 μm pores. Cells ($1x10^6$ cells/ml) were mixed with collagen I (1 mg/ml) and incubated with DMEM containing 10% FBS in cell culture plates for 12 hours, then the growth medium was replaced with 100 ng/ml of PDGF-BB in serum free DMEM medium and incubated for 12 hours. The cells were stained with Diff-Quik. Phase contrast images were taken by a Roper Scientific Cascade 650 camera with a 10X lens on a Nikon Eclipse TE2000-E inverted microscope.

The effect of flow on cell motility in collagen gels was visualized using a confocal microscope. The motility can be inferred from the cell spatial distribution and more concisely from the intensity profile of fluorescently labeled cells (see Fig. 2-3 *A*, *B*, *C* and *D*). This observation suggests that interstitial flow does affect cell motility in 3-D gels.

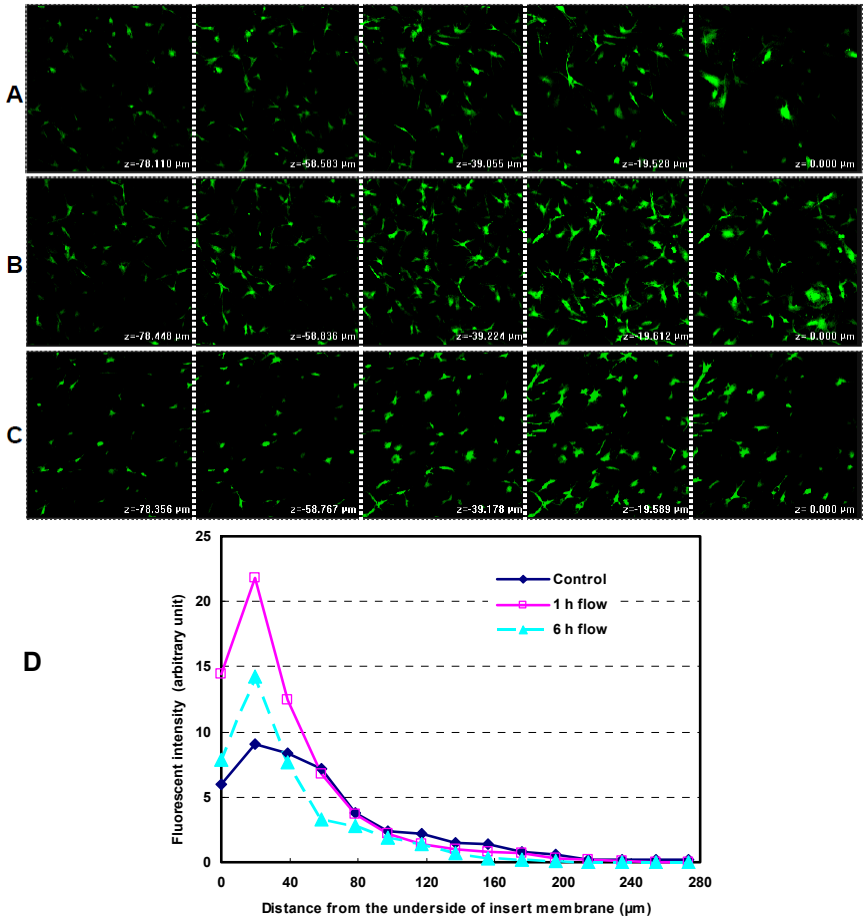

Figure 2-3. Effect of interstitial flow on cell distribution in collagen gels. Panels A, B and C are representative confocal images of cell (MFB) distributions in collagen gels after 48 h of migration to PDGF-BB. Cells in 3-D collagen gels were exposed to up to 6 h of flow (10 cmH_2O pressure drop) followed by 48 h of migration to 20 ng/ml PDGF-BB as chemoattractant. A, Cells in no flow control. B, 1 h flow treated gel. C, 6 h flow treated gel. Images in Panels A, B and C are XY scans in the Z-direction from the underside of the insert membrane (Z = 0 μm) up to Z = 80 μm depth in gels with 20 μm steps. Cells were stained with Calcein AM (green). D, Representative fluorescence intensity profile of cells in collagen gels. Intensities were measured from confocal images from the underside of the insert membrane (Z = 0 μm) up to Z = 280 μm depth in gels with 20 μm steps.

Then migrated cells through the pores to the undersides of insert membranes were visualized and counted. As indicated in Figs. 2-4, the number of migrated fibroblasts and myofibroblasts were significantly elevated after exposure to 1 hour of flow driven by a 3.3 cmH_2O (0.1 dyn/cm^2) pressure drop. However, for 6 hours, there were no statistically significant changes in migratory activity compared to no-flow controls for both cell types. This observation is consistent with confocal microscopy results, suggesting that our 3-D interstitial flow – cell migration system is able to detect effects of flow on cell motility.

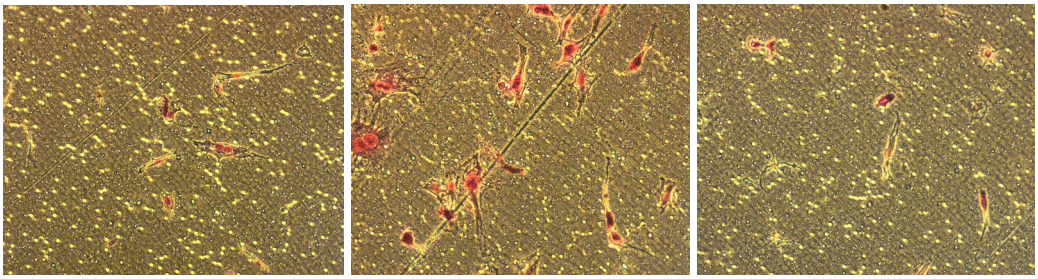

(A) No flow control (B) 1 h flow treated (C) 6 h flow treated

(D) No flow control (E) 1 h flow treated (F) 6 h flow treated

Figure 2-4. Interstitial flow affects cell migration. Migrated vascular fibroblasts (A, B and C) and myofibroblasts (D, E and F) to undersides of filter membranes with 48 h chemotactic incubation with 20 ng/ml PDGF-BB after treated with interstitial flow with 3.3 cmH_2O pressure differential. The images were taken by Olympus DP11-N camera under 10X lens of Nikon Eclipse TE2000-E inverted microscope.

2.4.3 Interstitial flow affects cell motility in collagen gels

The migration rates of MFB, FB and SMC (Fig. 2-5) were significantly elevated after exposure to 1-6 h of 1 cmH_2O flow compared to no flow controls. 1 h of 3 cmH_2O and 10 cmH_2O flow also promoted MFB and FB motility, but did not affect SMC. However, 6 h of 10 cmH_2O flow suppressed migration for all three types of cells. Overall, the migration

rates were higher in lower flow cases compared to corresponding time points in higher flow cases. The trends of migration rates in response to flow were very similar for FB and MFB. The difference between SMC and FB/MFB was that there was no enhancement of SMC migration in any of the 3 and 10 cmH_2O flow cases.

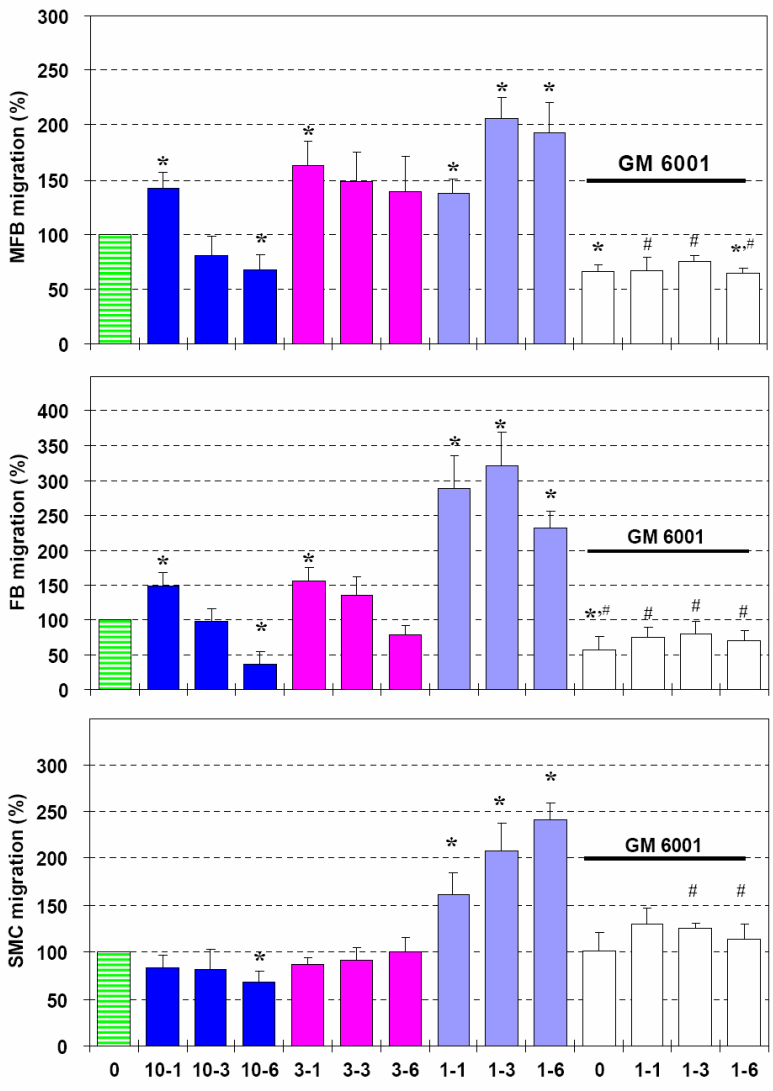

Figure 2-5. Effects of interstitial flow and MMP inhibitor (GM 6001) on vascular MFB, FB, and SMC motility in 3-D collagen gels. Cells in 3-D collagen gels were exposed to up to 6 h of flow driven by 10, 3, or 1 cmH_2O pressure drop and then incubated with 1 ml of 20 ng/ml PDGF-BB to examine cell migration. In the cases of MMP inhibition, GM 6001 (1 ml of 10 μM) was added together with PDGF-BB. In X-axis, "0" stands for "no-flow control", and "x1-x2" stands for "flow intensity (cmH_2O) – exposure time (hours)". Data are mean ± SEM (n = 4-19). *, $P < 0.05$ vs. no flow control; #, $P < 0.015$ vs. their corresponding flow cases without GM 6001 treatment.

2.4.4 MMP inhibitor abolishes interstitial flow-induced migration

A broad spectrum MMP inhibitor (GM 6001) was used to investigate the potential role of MMPs in interstitial flow-enhanced vascular FB, MFB and SMC motility. GM 6001 had very similar inhibitory effects on both FB and MFB migration (Fig. 2-5): it attenuated migration in no flow control gels to 70-80% and completely abolished elevated migration in 1 cmH_2O flow treated gels. Surprisingly, GM 6001 had no effect on SMC migration in no-flow control gels, but 1 cmH_2O flow-enhanced migration was attenuated nearly to control levels by GM 6001.

2.4.5 Interstitial flow affects MMP-13 and TIMP-1 protein levels, but not MMP-2

Collagen zymography was used to measure MMP-13 levels (Fig. 2-6). After exposure to flow, active MMP-13 levels for MFB were markedly increased. In SMC, active MMP-13 levels were only increased in lower flow cases and no significant changes were observed in the higher flow (10 cmH_2O) cases. These data are consistent with cell migration data (Fig. 2-5). The only exceptions are for the 3 and 10 cmH_2O flow cases at 6 h in MFB, where collagen zymography showed enhanced MMP-13 activity. Since collagen zymography detected all active MMP-13, not only free active MMP-13 but also MMP-13 in MMP-13/TIMP complexes which were dissociated in zymography [176]. To examine whether high flow induced more TIMP expression, reverse collagen zymography was performed, which clearly showed that longer exposure to higher flow induced more TIMP-1 expression in both MFB and SMC (Fig. 2-6). By gelatin zymography, we observed, surprisingly, that for both SMC and MFB, the active MMP-2 levels displayed

no significant changes in response to flow at any time point (Fig. 2-6). AnaSpec MMP-2 activity assays confirmed this finding (data not shown).

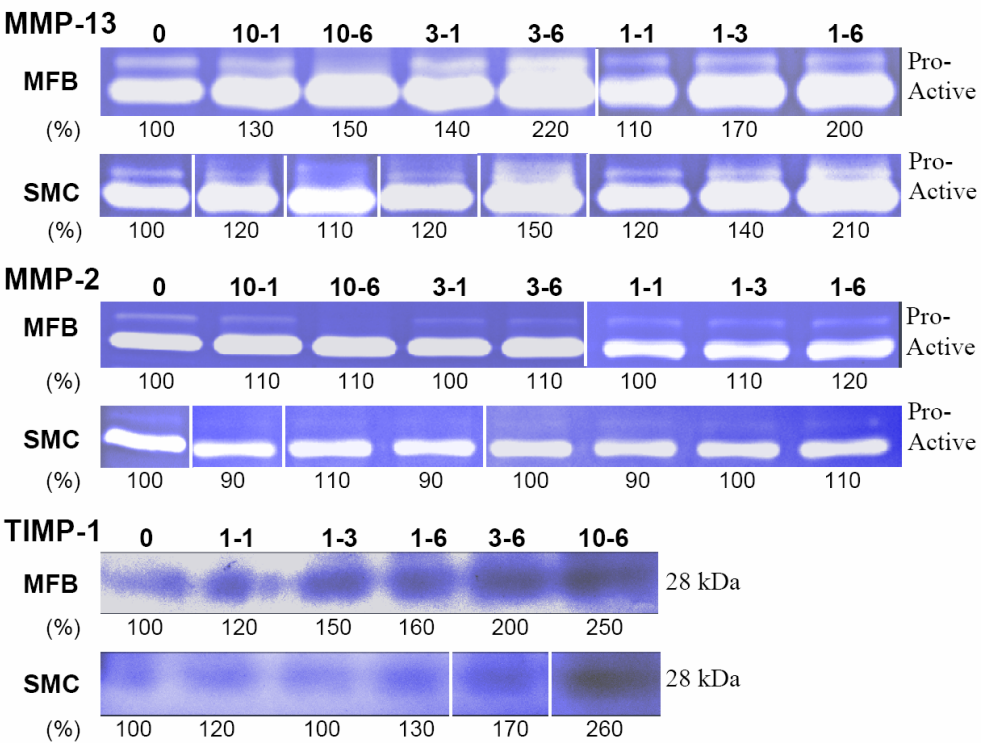

Figure 2-6. Collagen and gelatin zymography for MMP-13 and MMP-2, and reverse collagen zymography for TIMP-1. For MMP-13 and MMP-2, an identical volume (20 μl) of conditioned medium was loaded into each well. The first bands in the zymograms are the pro-MMPs and second bands are the active MMPs. For reverse collagen zymography, 40 μl of conditioned medium was loaded into each well. In the panels, "0" stands for "no-flow control", and "x1-x2" stands for "flow intensity (cmH_2O) – exposure time (hours)".

2.4.6 Interstitial flow upregulates gene expression of MMP-13 and TIMP-1 but not MMP-2

Interstitial flow significantly promoted MMP-13 gene expression for both MFB and SMC (Fig. 2-7). Overall, the longer the exposure, the higher the MMP-13 expression; and the higher the flow, the greater the expression. There was no detectable MMP-13 gene expression in SMC for the no-flow control case. By comparison, SMC expressed less

MMP-13 than MFB. The MMP-2 gene expression was much higher than MMP-13 expression in controls, but there was no change in any flow case compared to controls for either SMC or MFB. TIMP-1 gene expression was also significantly upregulated in MFB by longer exposure to higher intensity of flow and slightly upregulated in SMC.

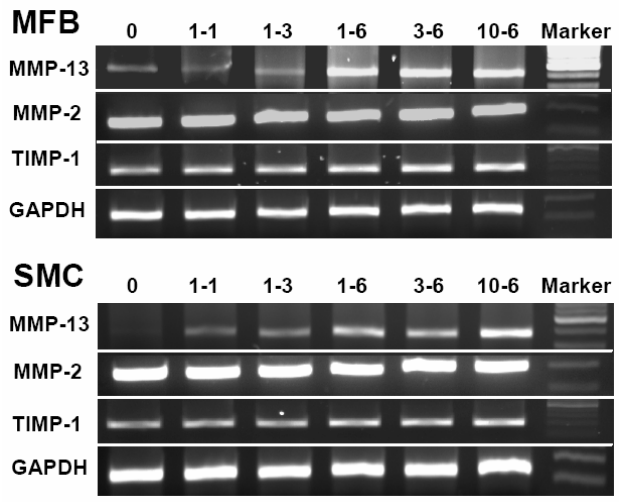

Figure 2-7. Interstitial flow up-regulates MMP-13 and TIMP-1 gene expression, but not MMP-2. Rat vascular MFB and SMC were released from collagen gels by collagenase I right after flow. Reverse transcription polymerase chain reaction (RT-PCR) was conducted to detect rat MMP-13, MMP-2 and TIMP-1 mRNA expression with GAPDH as a reference gene. The exposure times for taking images were different for different genes. In the panels, "0" stands for "no flow control", and "x1-x2" stands for "flow intensity (cmH_2O) – exposure time (hours)".

2.4.7 Silencing MMP-13 expression eliminates flow-enhanced cell motility

To further verify that MMP-13 was required for flow-induced migration, we silenced MMP-13 expression by small hairpin RNA (shRNA). As shown in Fig. 2-8, MMP-13 shRNA completely abolished the flow-enhanced migration for both MFB and SMC, while there was no effect on control cases. MMP-13 RNA interference data were highly consistent with the general MMP inhibitor (GM 6001) results (Fig. 2-5). MMP-1 gene expression knockdown and activity reduction were confirmed by RT-PCR and collagen zymography.

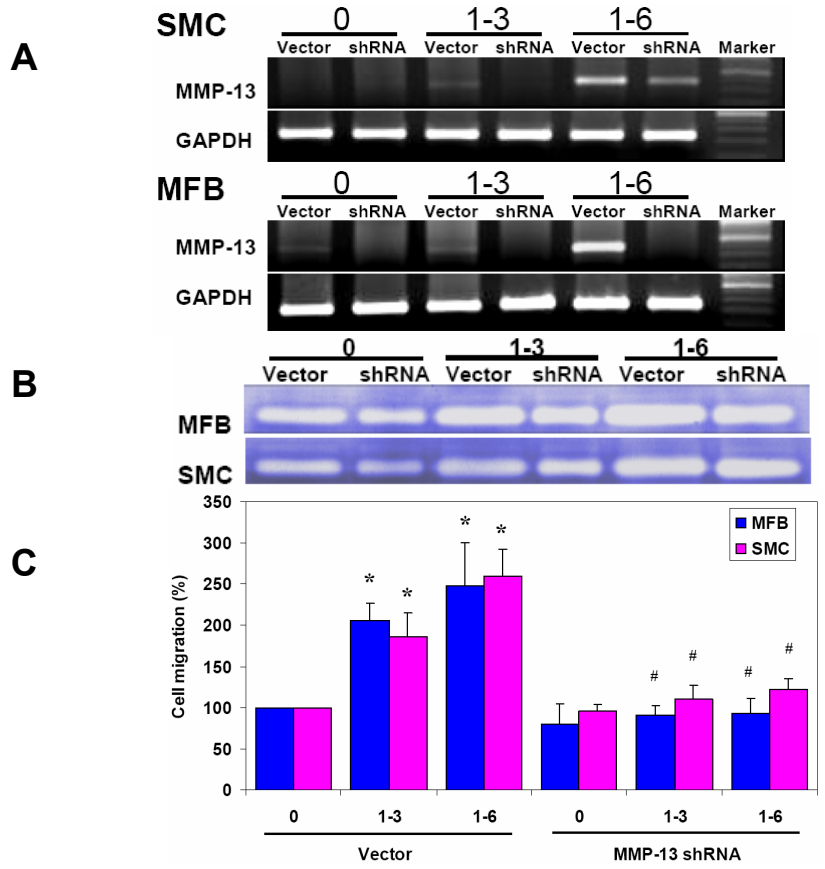

Figure 2-8. MMP-13 shRNA abolishes flow-enhanced cell migration. A: RT-PCR was used to confirm MMP-13 gene silencing. B: Collagen zymography was used to check MMP-13 activity reduction. C: Cell migration data. In the panels, "0" stands for "no flow control", and "x1-x2" stands for "flow intensity (cmH_2O) – exposure time (hours)". Data are mean ± SEM (n=3-4). *, $P < 0.05$ vs. no-flow control. #, $P < 0.008$ vs. their corresponding flow cases with vector transfection.

2.4.8 High intensity interstitial flow induces cell apoptosis in 3-D collagen

Longer exposure to higher intensity flow induced SMC and MFB apoptosis and necrosis (Fig. 2-9). 6 h of 10 cmH_2O flow induced apoptosis in many more cells compared to 3 h of 1 cmH_2O flow. In addition, many more dead cells and fewer normal live cells were observed due to longer exposure to higher intensity of flow. A wound healing assay showed that cells in the dish containing more apoptotic MFB-induced by TNF-α/CHX displayed much lower motility than the dish that had not been induced (Fig. 2-10). Similar phenomena were also observed for SMC (data not shown).

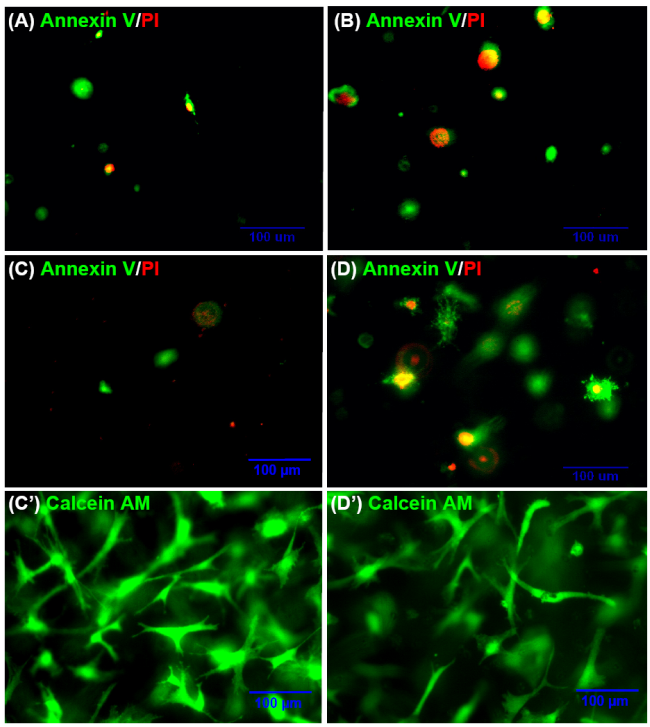

Figure 2-9. Longer exposure to higher flow induces cell apoptosis and necrosis. Cells in collagen were exposed to 1 cmH_2O flow for 3 h (A, C, and C') and 10 cmH_2O flow for 6 h (B, D, and D') and then incubated for 48 h with PDGF-BB. A and B are SMC; C, C', D, and D' are MFB. Cells were stained either by Vybrant™ apoptosis assay kit #2 or by Calcein AM. Images were taken by focusing on the layer of cells right above the cell culture insert membrane. In A, B, C, and D, apoptotic cells were stained with Alexa Fluor® 488 annexin V in green, dead (necrotic) cells were stained with propidium iodide (PI) in red. In C' and D', live cells in gels were stained with Calcein AM in green.

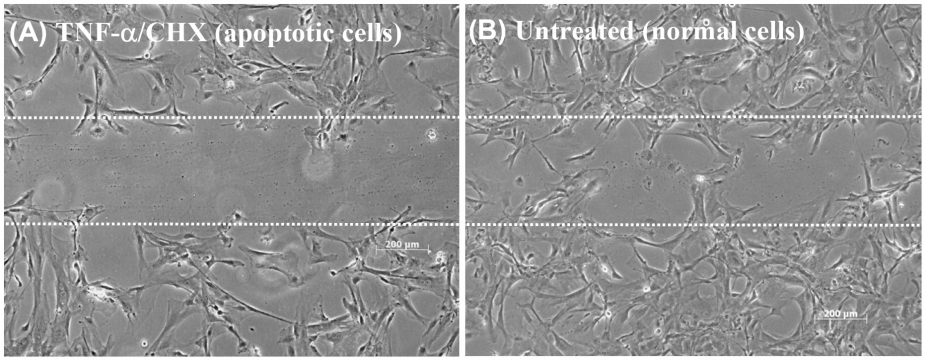

Figure 2-10. Apoptosis impairs cell motility. In the wound healing assay, a monolayer of cells in a dish was treated with tissue necrosis factor (TNF)-α (20 ng/ml) and cycloheximide (CHX) (3 μg/ml) (A) or without (B) for 2.5 h to induce apoptosis, followed by wound scratching shown as the space between two broken white lines; media then was replaced by DMEM with PDGF-BB (20 ng/ml) for cell migration for 24 h. Representative cell type was MFB.

2.5 Discussion

This was the first study to investigate the influence of interstitial flow on the migration of vascular wall cells (FB, MFB, and SMC) in a 3-D model and to determine the underlying mechanisms. The primary finding is that interstitial flow can promote vascular FB/MFB and SMC motility via upregulation of rat interstitial collagenase (MMP-13). By separating the migration period from the flow period, the effects of flow on motility could not be interpreted as resulting from the convection of chemoattractant or other molecules produced by the suspended cells. We also eliminated the effect of gel compaction due to flow, because gel compaction affects gel fiber density and thus gel permeability and stiffness, which in turn affect cell migration rates [91, 212]. It is also clear in Fig. 2-1*B* that the direction of interstitial flow corresponds to the direction of cell migration. However, one cannot argue that there was a direct mechanical enhancement of migration in the direction of flow (drag of flow on the suspended cells) during the initial 1-6 h flow period, because cell distributions in the gels, determined by confocal microscopy, were not different for no flow controls and gels exposed to flows (data not shown).

The permeability of the collagen gel is very important as it controls mass transport to cells by diffusion and convection and shear stress on cells. The permeability depends strongly on the gel concentration. In the present study, the Darcy permeability (Kp) of 4 mg/ml collagen gels was on the order of 10^{-11} cm^2, which is two to three orders higher than in the layers of the rabbit aortic wall (10^{-14} cm^2) [86]. However, our Kp is consistent with literature data: 10^{-8}-10^{-12} cm^2 for 2.5-45 mg/ml collagen gels [118, 138, 204]. The interstitial flow velocity in our experiments was in the range of 0.5-2.4 μm/s, which is

substantially higher than the interstitial flow velocity in the normal aorta (0.01-0.1 μm/s) [190, 201]. But the estimated shear stresses on suspended cells in our experiments (0.05-0.36 dyn/cm^2) are in the expected range for the aorta based on equations (1) and (2). In addition, the porous membrane of the culture inserts with 8 μm pore size (area fraction of the pores is 0.03) mimics the EEL/IEL, whose fenestral pore area fraction is 0.001-0.036 [185]. The pore size of an un-compacted 2.5 mg/ml collagen gel was observed by electron microscopy to be no more than 1 μm which is much smaller than the cell diameter (around 10 μm) [204]. The gel pore size in the present study that used compacted 4 mg/ml collagen gels should be somewhat smaller but of the same order of magnitude. Cells would not be able to crawl through pores of such small dimensions and must use enzymes (MMPs) to create accessible pathways through the matrix.

The basic phenomena of flow vs. migration displayed in Fig. 2-5 suggests that the lower levels of interstitial flow (1 cmH_2O differential pressure) enhance motility of all cell types studied (FB, MFB, and SMC) while the higher levels of interstitial flow (10 cmH_2O differential pressure) at longer exposure times (6 hours) suppress migration rate of all cell types. The roles of MMPs, TIMPs, and apoptosis in mediating these diverse phenomena have been investigated and all are discussed below.

In an earlier study using a 2-D flow system, we observed that much higher shear stress (~10 dyn/cm^2) enhanced FB migration, but inhibited MFB and SMC migration in Matrigel [50, 51]. Differences in shear stress level, matrix material (collagen vs. Matrigel) and system dimension (2-D vs. 3-D) undoubtedly contributed to these differences. In the more physiological 3-D system, cells exhibit matrix adhesions all over their surface, thus the interstitial flow not only acts directly on the cell surface, but also affects the matrix

structure, cell-matrix adhesion and tethering that could result in amplified mechanosignaling [91, 133, 182].

Vascular SMC, FB, and MFB migration and MMP secretion are typical features of neointima formation after endothelial injury [13, 152]. The proteolytic effects of MMPs play an important role in vascular remodeling and cellular migration [48], and there is abundant evidence of MMP upregulation in animal models of neointima formation [115]. Levels of MMP-1 and other MMPs are increased after femoral artery injury in mice [94], and MMP-1 upregulation occurs in injured monolayers of vascular SMC [70]. In the present study, a broad spectrum MMP inhibitor (GM 6001) completely abolished flow-promoted cell motility (Fig. 2-5), suggesting that MMPs play a major role in flow-enhanced cell motility in collagen matrices. We further investigated whether rat interstitial collagenase (MMP-13) and/or MMP-2 play a specific role in flow-enhanced migration rate. We found that the flow induced MMP-13 protein and gene expression and the trends in MMP-13 activity showed good agreement with the trends in cell migratory activity; however, there was no effect of flow on MMP-2 at either the gene or protein level (Figs. 2-6 and 2-7). Using MMP-13 shRNA we further confirmed the critical role of MMP-13 in flow-regulated migration rate (Fig. 2-8). MMP-13 shRNA almost completely abolished flow-induced migration. In addition, knockdown of MMP-13 did not affect membrane-type MMP-1 (MT-MMP-1; MMP-14) gene expression (data not shown). Combining the migration data with the MMP inhibitor, MMP-13 shRNA, and MMP-13 activity data (Figs. 2-5 and 2-8), we also noted that migration in no flow controls was partly MMP-dependent for FB/MFB and totally independent of MMP for SMC.

We have shown that upregulation of MMP-13 but not MMP-2 by interstitial flow substantially promoted vascular FB, MFB, and SMC migration in collagen I matrices. Consistent with this observation, it has also been reported that human interstitial collagenase (MMP-1) is essential for hepatocyte growth factor mediated human corneal epithelial cell migration on collagen I [33]. However, other studies have shown that MMP-2 plays an important role in vascular SMC and FB migration both in vivo and in vitro. Changes in MMP-2 activity affect SMC and FB migration which contribute to neointima formation [13, 116, 164, 214]. 2-D shear stress suppresses SMC migration in Matrigel via downregulation of MMP-2 activity [51, 127]. Upregulation of MMP-1 and -2 are responsible for chlorotyrosine-induced human aortic SMC migration [111]. Other recent studies reported that fluid shear stress modulated endothelial cell invasion into 3-D collagen matrices through MMP-2 activation and that collagen I but not Matrigel matrices form an MMP-dependent barrier to ovarian cancer cell penetration [71, 177]. However, it has been shown that MMP-2 activation is delayed in rat and mouse studies [115]. In vivo, the accumulation of new ECM into the extravascular space of the damage site could alter the properties of the matrix that cells migrate within, which might affect MMP expression and activation. Therefore, in our 6 h flow experiments MMP-2 might also have been delayed. All of these findings indicate that MMP activation is dependent on many factors including substrate materials, cell types, and the nature and duration of stimuli.

TIMPs play a crucial role in maintaining vascular wall homeostasis [105, 137, 164]. In addition to MMP-13, TIMP-1 gene and protein expression were also elevated by higher flow and longer exposure (Figs. 2-6 and 2-7). The TIMP-1 response may have

been the cell's attempt to eliminate excessive MMP formation in order to strike a balance. The elevated TIMP-1 expression by higher flow certainly could partially reduce MMP-13 activity, which in turn would reduce the cell migration rates.

We also observed that at the highest flow rate and longest exposure time, migration rates were suppressed for all cell types (Fig. 2-5). This was most likely related to both the elevation of TIMP-1 expression and the appearance of apoptotic and necrotic cells under these conditions (Fig. 2-9). The apoptotic cell populations displayed a reduced migration rate as expected (Fig. 2-10). The more apoptotic and necrotic cells induced by higher flow together could significantly reduce cell migration rates. It has been shown that enhanced SMC apoptosis and reduced migration are likely involved in inhibition of neointima formation by a Rho-kinase inhibitor [169]. Vascular SMC apoptosis is one characteristic of vascular remodeling that occurs in atherosclerosis, hypertension, and restenosis following angioplasty [100, 160]. Apoptosis of SMC often occurs rapidly right after vascular injury [134]. It has been reported that fluid shear stress can induce tumor cell cycle arrest and vascular SMC apoptosis in 2-D in vitro and that changes in wall tension can also cause SMC apoptosis in vivo [23, 46, 159]. Apoptosis also can be induced in the ECM with a low stiffness [77], and the collagen matrix stiffness can be reduced when MMP expression is overabundant. However, in the present study, the largest number of apoptotic cells appeared in the longest exposure to highest flow case, while the MMP-13 activity was at a lower level. These data suggest that cell apoptosis was mainly induced by interstitial flow, not reduced matrix stiffness.

The precise physiological relevance of the results of the present study can only be hypothesized at the present time. One plausible scenario that incorporates the basic

findings on interstitial flow and migration (Fig. 2-5) is that after vessel injury the intima is exposed to elevated concentrations of chemoattractant originating in blood elements that initiate cell migration to the intima. Elevated interstitial flow increases shear stress on all cells in the wall, but it induces a lower shear stress on cells like FB and MFB that are embedded in the loose connective tissue of the adventitia (with higher Kp than the medial connective tissue) than on the SMC in the media (recall equation (2)). Migration of these adventitial cells is therefore elevated early by the enhanced interstitial flow while the SMC migration is suppressed. As injury healing proceeds, the interstitial flow shear stresses are reduced and a period in which the SMC migration is enhanced and the FB/MFB migration is reduced ensues. The net result is enhanced migration of all cell types by interstitial flow during some phase of the injury healing process.

Taken together, our results indicate that interstitial flow may be one of the direct links between vessel injury and vascular FB and SMC migration. Interstitial flow can promote vascular cell motility by stimulating rat collagenase MMP-13 expression and activation (see Fig. 2-11 for a schematic model), while if the flow is too high, it might suppress cell motility by inducing cell apoptosis. However, to determine exactly how the vascular cells "sense" interstitial flow and then promote MMP-13 expression requires additional investigation. That longer exposure to higher interstitial flow induces cell apoptosis and necrosis also needs to be further clarified. Certainly, neointima formation from vascular injury in vivo is very complicated, involving not only elevated flow, but inflammatory cells and other factors. However, using a 3-D collagen I gel system as a model of physiological interstitial flow, we, for the first time, have been able to observe significant influences of interstitial flow on cell migration. Our results suggest a possible mechanism

whereby vessel injury enhances interstitial flow that activates medial SMC and adventitial FB and thus further contributes to neointima formation.

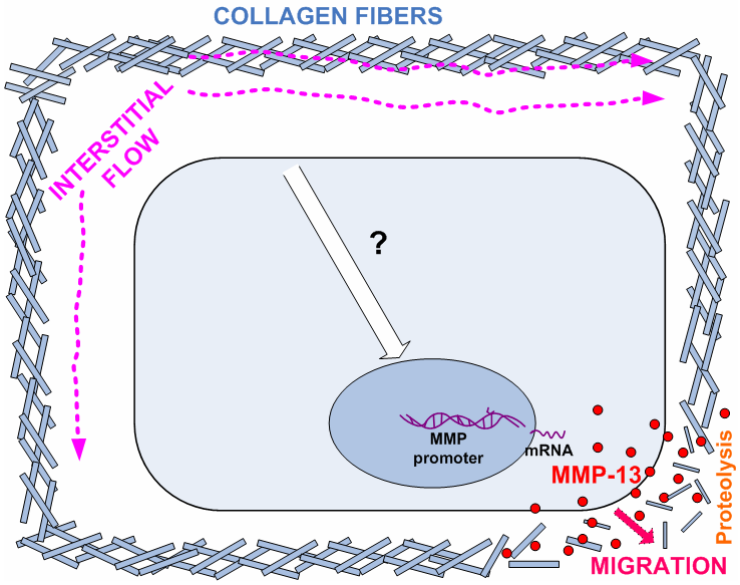

Figure 2-11. A schematic model to show that interstitial flow promotes MMP-13 expression and cell motility. Interstitial flow induces rat interstitial collagenase (MMP-13) expression, and upregulated MMP-13 digests collagen fibers and promotes cell migration. However, how cells "sense" interstitial flow and then trigger MMP expression still remain unclear.

Acknowledgements

We thank Dr. Herb Sun and Jeff Garanich for valuable discussions, Danielle E. Berardi for excellent technical assistance, and Giya Abraham for cell culture.

Grants

This work was supported by NIH Grants HL 35549 and HL 57093.

Chapter 3

Interstitial Flow Induces MMP-13 Expression and Vascular SMC Migration in Collagen I Gels via an ERK1/2-Dependent and c-Jun-Mediated Mechanism

3.1 Abstract

The migration of vascular smooth muscle cells (SMC) and fibroblasts into the intima after vascular injury is a central process in vascular lesion formation. The elevation of transmural interstitial flow is also observed after damage to the vascular endothelium. We have shown previously that interstitial flow upregulates rat interstitial collagenase (MMP-13) expression which in turn promotes SMC and fibroblast migration in collagen I gels. In this study, we investigated further the mechanism of flow-induced MMP-13 expression. An ERK1/2 inhibitor (PD-98059) completely abolished interstitial flow-induced SMC migration and MMP-13 expression. Interstitial flow promoted ERK1/2 phosphorylation while PD-98059 abolished flow-induced activation. Silencing ERK1/2 completely abolished MMP-13 expression and SMC migration. In addition, interstitial flow increased the expression of AP-1 transcription factors (c-Jun and c-Fos), while PD-98059 attenuated flow-induced expression. Knocking down c-*jun* completely abolished flow-induced MMP-13 expression, while silencing c-*fos* did not affect MMP-13 expression. We also show that p38 MAPK does not play a significant role in flow-induced MMP-13 expression. Taken together, our data indicate that interstitial flow induces MMP-13 expression and SMC migration in collagen I gels via an ERK1/2-dependent and c-Jun-mediated mechanism and suggests that interstitial flow, ERK1/2 MAPK, c-Jun, and MMP-13 may play important roles in SMC migration and neointima formation after vascular injury.

Keywords: shear stress, matrix metalloproteinase, MAPK, AP-1, neointima formation

3.2 Introduction

Vascular smooth muscle cell (SMC) and fibroblast migration and proliferation in the intima play a major role in neointima formation after vascular injury. It is well known that growth factors and inflammatory cytokines can induce SMC migration through 3-dimensional (3-D) extracellular matrix (ECM) by stimulating secretion of matrix metalloproteinases (MMP) which are capable of digesting ECM [49, 97, 215]. For example, upregulated expression of MMP-1 in the early stages of atherosclerosis is associated with SMC migration [7, 12]. Because the major collagen components in the vascular wall are collagen type I and type III, and interstitial collagenase (MMP-1 in human and MMP-13 in rodents) is responsible for initial cleavage of collagen I and III [195], interstitial collagenase is believed to play an essential role in vascular SMC migration and vascular lesion formation [49] [135].

Transmural interstitial flow driven by the transmural pressure differential is a physiological fluid movement through vascular vessel interstitium that imposes fluid shear stress on parenchymal cells [184, 201]. The biological role of this small flow (shear stress) has not been well recognized [167, 182, 204]. However, during the early stages of vascular injury, the interstitial flow is elevated due to loss of the endothelial hydraulic resistance, and we hypothesized that this elevated flow could participate in vascular SMC and fibroblast migration and neointima formation [167]. Furthermore, in hypertension, the transmural interstitial flow is also increased due to the elevated transmural differential pressure in the large arteries, which also can lead to neointima formation [68, 101]. We have previously shown that interstitial flow can stimulate SMCs and fibroblasts to

express MMP-13, which can in turn facilitate cell migration in collagen I gels [167]. However, one of the remaining challenges is to determine the exact biomolecular signaling pathway (mechanism) of flow-induced MMP-13 expression.

Therefore, in this study, we investigated the underlying mechanism of interstitial flow-induced MMP-13 expression. The activation of mitogen-activated protein kinases (MAPKs) such as extracellular signal-regulated kinase-1 and -2 (ERK1/2), expression of activator protein-1 (AP-1) transcription factors such as c-Jun and c-Fos, and AP-1 DNA binding activity were examined. Gene silencing was also conducted to confirm the roles of ERK1/2 and AP-1 in regulation of MMP-13 expression. The results suggest that interstitial flow induces MMP-13 expression and SMC migration via an ERK1/2-dependent AP-1 (c-Jun) activation mechanism.

3.3 Materials and Methods

3.3.1 Collagen gel preparation and flow experiments. Rat aorta SMCs were isolated from male Sprague-Dawley rats weighing 150 g [50]. The procedure was approved by the City College/City University of New York Medical School Animal Care and Use Committee. As previously described [167], rat aortic SMC (passage 3-5) were suspended in rat tail collagen I (BD Science) gels (cell density: $2.5x10^5$ cells/ml; final gel concentration: 4 mg/ml), and pH was adjusted to 7.0 by mixing the appropriate amount of NaOH. For cell migration experiments, 200 μl of gel was loaded into each 12-well cell culture insert with 8 μm pores (BD Science). For RNA extraction and protein extraction experiments, 6-well cell culture inserts with 8 μm pores (BD Science) were used. In order

to keep the same level of shear stress, the same gel thickness was maintained in both the 6- and 12-well experiments, thus 1 ml of gel was used for a 6-well insert. The gels were incubated for 24 h to allow cell spreading. Gels were then subjected to interstitial flow driven by 1 cmH_2O pressure drop (shear stress was ~0.05 dyn/cm^2) for various time periods according to the specific experimental design. This shear stress level elicited the maximum enhancement of migration in our previous study [167]. For MAPK inhibition experiments, after 24 h of cell spreading in the collagen gel, the cells were treated with p38 MAPK inhibitor (InSolution™ SB-203580, SB, from Calbiochem), or ERK1/2 inhibitor (InSolution™ PD-98059, PD, from Calbiochem) for 1 h followed by various time periods of interstitial flow with or without inhibitors in the flow media.

3.3.2 Western blotting. Collagen gels were washed once with ice-cold PBS; then 2X lysis buffer was added immediately to the gels followed by sonication for 30 seconds on ice. The 2X lysis buffer was composed of 2X RIPA buffer (300 mM NaCl, 2% NP-40, 100 mM Tris, 0.2% Brij 35, 2 mM EDTA, pH 7.5) with a supplement of 2X protease inhibitor cocktail (Roche Diagnostics), 2X phosphatase inhibitor cocktail (Roche Diagnostics), 2 mM activated Na_3VO_4, and 2 mM PMSF. Lysates were centrifuged in a microfuge (14,000 rpm for 1 hour at 4°C), and then the supernatants were collected and the remaining gel pellets were discarded as previously described [50]. The supernatants were concentrated using an YM-10 Microcon centrifugal filter device (Millipore). Protein concentrations in supernatants were evaluated using a total protein assay (Bio-Rad). The protein samples were then boiled for 5 minutes after mixing with 4X sample buffer (400 mM Tris-HCl, 8% SDS, 40% glycerol, 0.04% bromphenol blue, and 20% β-

mercaptoethanol, pH 6.8) and stored at -80°C. Equal amounts of total protein per well were loaded onto 10% SDS-polyacrylamide gels. After electrophoresis, proteins were transferred to PVDF membranes (Bio-Rad) and blocked at room temperature with 2% Enhanced Chemiluminescence (ECL) Advance Blocking Agent (Amersham, GE Healthcare) in TBS-T [50]. The membranes were incubated overnight with a 1:1000 dilution of a specific rabbit primary antibody (monoclonal antibodies: ERK1/2, phospho-ERK1/2, phospho-p38 MAPK, c-Fos, and c-Jun; polyclonal antibodies: p38 MAPK, α-tubulin, and β-actin, all from Cell Signaling), followed by a 1.5-h room temperature incubation with an ECL horseradish peroxidase (HRP)-linked anti-rabbit IgG antibody (Amersham, GE Healthcare). The proteins on PVDF membranes were then detected using an ECL advanced Western blotting detection kit (Amersham, GE Healthcare) and the ChemiDoc XRS system with the Quantity One software (Bio-Rad). Some membranes were stripped using Restore™ Plus Western Blot Stripping Buffer (Thermo Scientific Pierce) for a subsequent detection.

3.3.3 Nuclear protein extraction and AP-1 DNA binding activity assay. Cells were released from collagen gels by 0.2% of collagenase I in growth medium and washed with ice-cold PBS as previously described [167]. To extract nuclear protein, cells were treated with NE-PER® nuclear and cytoplasmic extraction reagents (Thermo Scientific Pierce) by following the manufacturer's procedure. Because of the presence of EDTA, extracts were mixed with $CaCl_2$ to a final concentration of 5 mM to inactivate EDTA. 3 μg of nuclear extract per well was used for an AP-1 DNA binding activity assay using the AP-1 transcription factor microplate assay (Marligen) following the manufacturer's procedure.

3.3.4 RNA extraction and gene expression analysis. Total RNA was isolated from cells in collagen matrices using TRIzol® LS Reagent (Invitrogen) with the following modification. During RNA precipitation, high-salt (1.2 M Na-citrate / 0.8 M NaCl) was added together with isopropanol. Under these conditions, RNA can be effectively precipitated while contaminating polysaccharides and proteoglycans remain in the soluble form [27]. RNA samples were then converted to cDNA by reverse transcription (RT). For analyzing gene expression, the polymerase chain reaction (PCR) was performed using the following protocol: pre-denaturation at 95 ºC for 5 minutes, then either 40 cycles (for MMP-13) or 30 cycles (for c-*jun*, c-*fos*, and GAPDH) of denaturation at 94 ºC for 35 seconds, annealing at 52 ºC for 35 seconds, and extension at 72 ºC for 35 seconds, followed by a final extension at 72 ºC for 10 min. The amplified products were separated by electrophoresis in 2.5% agarose gels and photographed under UV light in the presence of ethidium bromide (EB). Quantitative real-time PCR (RT-qPCR) was also performed for c-*fos,* c-*jun,* and MMP-13 expression on the ABI PRISM® 7000 sequence detection system (Applied Biosystems). GAPDH served as an internal control. Reactions were performed in 30 µl reaction mixture volumes containing SYBR® Green PCR Master Mix (Applied Biosystems), cDNA and specific primer pairs. RT-qPCR programs were set to 2 minutes at 50°C and 10 minutes at 95°C followed by 45 cycles of 35 seconds at 95°C, 35 seconds at 52°C, and 40 seconds at 72°C. Following each PCR, dissociation curve analysis was used to assess the specificity of product amplification. Primer sequences are listed in Table 3-1.

Table 3-1. Primer sequences and product sizes for rat genes

Target gene	Primer sequence	Genbank locus	Size
GAPDH		NM_017008	232
Forward (372-390)	5'-TCTTCACCACCATGGAGAA-3'		
Reverse (603-585)	5'-ACTGTGGTCATGAGCCCTT-3'		
MMP-13		M60616	383
Forward (1016-1036)	5'-GACCTCATGTTCATCTTTAGA-3'		
Reverse (1398-1378)	5'-CACCACAATAAGGAATTCGTT-3'		
c-*fos*		X06769	239
Forward (1665-1684)	5'-GGAATTAACCTGGTGCTGGA-3'		
Reverse (1903-1884)	5'-TCAGACCACCTCAACAATGC-3'		
c-*jun*		X17163	291
Forward (2592-2611)	5'-GAAGTAGCCCCCAACCTCTC-3'		
Reverse (2882-2863)	5'-ATGGCTCTCAACTCAAGCGT-3'		

3.3.5 RNA interference. To silence ERK1/2, two ERK1 shRNAs and two ERK2 shRNAs which were subcloned into pSUPER vector (kindly donated by Dr. Michal Hetman) were co-transfected into SMCs. The ERK1/2 shRNA target sequences were:

shERK1-1, GACCGGATGTTAACCTTTA;

shERK1-2, ATGTCATAGGCATCCGAGA;

shERK2-1, GTACAGAGCTCCAGAAATT;

and shERK2-2, AGTTCGAGTTGCTATCAAG [74].

To silence c-*jun* and c-*fos*, two c-jun shRNAs and c-fos shRNAs which were subcloned into BS/U6 vector (kindly donated by Dr. Mingtao Li) were co-transfected into cells. The c-jun shRNA target sequences were:

shc-jun-a, ACAGGTGGCACAGCTTAAA;

and shc-jun-b: AGTCATGAACCACGTTAAC.

The c-fos shRNA target sequences were:

shc-fos-a, GGAGACAGATCAACTTGAA;

and shc-fos-b, GCTGAAGGCTGAACCCTTT [103, 211].

The transfections were conducted using Lipofectamine™ LTX and PLUS™ reagents (Invitrogen).

Data Analysis. Results are presented as mean ± SEM. Data sets were analyzed for statistical significance using a Student's t-test with a two-tailed distribution, and $P < 0.05$ was considered statistically significant. For comparison of more than two groups, we used one-way ANOVA followed by the t-test with Bonferroni correction, and $P < 0.05/N$ (N stands for number of comparisons) was considered statistically significant.

3.4 Results

3.4.1 Interstitial flow induces SMC migration and MMP-13 expression while PD-98059 abolishes the flow effects.

MAPKs are important mediators which regulate a variety of cellular processes, including gene expression, proliferation, survival, apoptosis, migration, and differentiation [146]. Therefore, the roles of ERK1/2 and p38 MAPK were examined in this study. As shown in Fig. 3-1, interstitial flow significantly induced vascular SMC migration by two-fold and ERK1/2 inhibitor (PD-98059) completely abolished flow-induced migration. Surprisingly, p38 MAPK inhibitor (SB-203580) markedly enhanced flow-induced migration. In no-flow control cases, PD-98059 did not affect SMC migration, while SB-203580 promoted SMC migration.

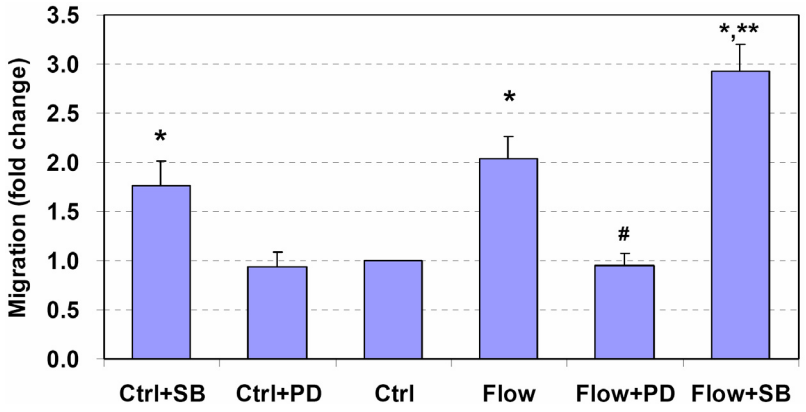

Figure 3-1. Effects of PD-98059 and SB-203580 on interstitial flow-induced vascular SMC migration. ERK1/2 inhibitor (PD-98059, PD) suppresses flow-induced SMC migration; and p38 MAPK inhibitor (SB-203580, SB) promotes SMC migration. After 24 h of cell spreading in collagen I gels, media was replaced with either fresh media, or 5 μM SB-203580, or 10 μM PD-98059 for 1 h, and then some gels were exposed to 1 cmH_2O of interstitial flow (~0.05 dyn/cm^2) either with or without inhibitors for 6 h followed by 48 h migration to 20 ng/ml PDGF-BB. The numbers of migrated cells to the undersides of cell culture inserts were counted. Other gels that were not exposed to flow served as no-flow controls (Ctrl). Data are presented as mean ± SEM, n= 6-8. * $P<0.05$ vs Ctrl; ** $P<0.02$ vs Ctrl+SB; # $P<0.005$ vs Flow.

We have previously shown that interstitial flow-induced cell migration in collagen I gels is controlled by MMP-13 [167]. Therefore, we examined the effects of interstitial flow and MAPK inhibitors on MMP-13 gene expression. As shown in Fig. 3-2, interstitial flow significantly induced MMP-13 gene expression in vascular SMC, and PD-98059 completely abolished flow-induced MMP-13 expression, while SB-203580 markedly enhanced flow-induced MMP-13 expression. In no-flow control cases, PD-98059 inhibited MMP-13 expression and SB-203580 slightly promoted MMP-13 gene expression. The combination of SMC migration data and MMP-13 expression data suggest that interstitial flow-induced cell migration and MMP-13 expression are ERK1/2-dependent, while p38 MAPK appears to play a downregulatory role.

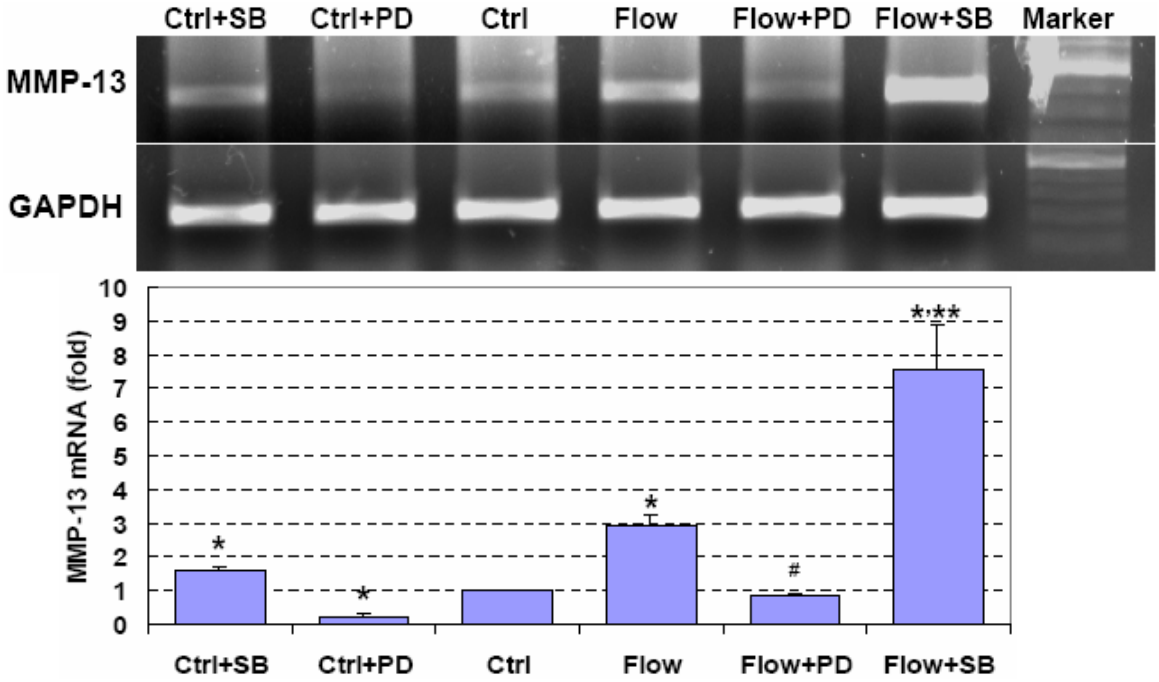

Figure 3-2. Effects of PD-98059 and SB-203580 on interstitial flow-induced MMP-13 expression. PD-98059 (PD) attenuates flow-induced MMP-13 expression; and SB-203580 (SB) promotes MMP-13 expression. After spreading out, cells in gels were pretreated with 5 μM SB or 10 μM PD for 1 h, and then exposed to interstitial flow either with or without MAPK inhibitors for 6 h. MMP-13 gene expression was checked by both RT-PCR and RT-qPCR. RT-qPCR data are presented as mean ± SEM in the bar graph, n= 4. * $P<0.05$ vs Ctrl; # $P<0.01$ vs Flow; ** $P<0.05$ vs Flow.

3.4.2 Interstitial flow induces ERK1/2 and p38 MAPK activation.

To further investigate whether the interstitial flow and MAPK inhibitors really affect ERK1/2 and p38 activation, Western blotting was used to analyze the levels of both phosphorylated and total ERK1/2 and p38 MAPK (shown in Fig. 3-3). During 60 min of exposure to interstitial flow, ERK1/2 was markedly activated as the phosphorylated ERK1/2 level increased greatly. PD-98059 dramatically inhibited ERK1/2 activation for no-flow (0 min) and flow (15-60 min) cases compared to the cases without addition of PD-98059. Interestingly, p38 MAPK inhibitor SB-203580 significantly enhanced ERK1/2 activation for no-flow (0 min) and flow (15-60 min) cases. This unexpected stimulatory role of SB-203580 on ERK1/2 activation has been reported elsewhere [45, 88, 145]. Sixty minutes of interstitial flow, with or without SB-203580 or PD-98059, had no effect on total ERK1/2.

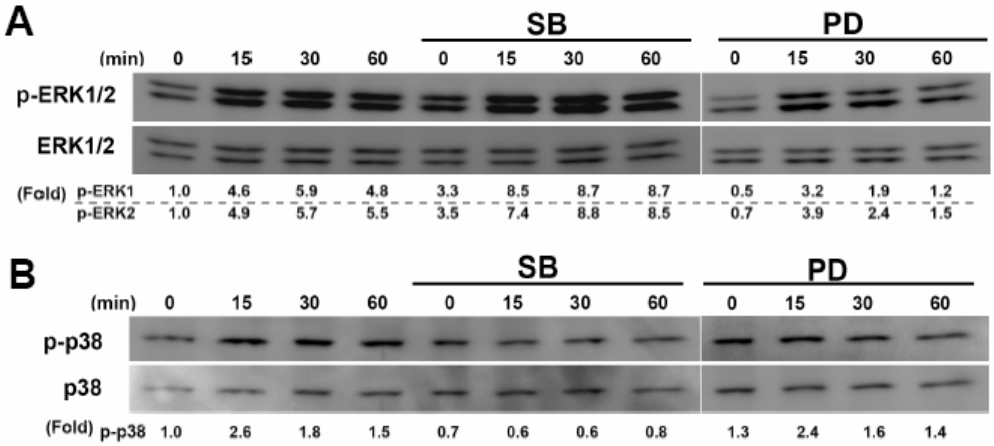

Figure 3-3. Interstitial flow induces ERK1/2 and p38 MAPK activation. *A*: PD markedly inhibited flow-induced ERK1/2 activation, and SB enhanced ERK1/2 activation. *B*: SB significantly inhibited flow-induced p38 activation, and PD did not affect p38 activation. After spreading out in gels, cells were pretreated with 5 μM SB or 10 μM PD for 1 h, and then exposed to interstitial flow either with or without inhibitors for 0 to 60 min. Total and phosphorylated ERK1/2 and p38 levels were analyzed by Western blotting. The experiments were run three times and similar results were observed. Fold change values are the ratios of phosphorylated MAPKs over their own total MAPKs, and then normalized to no-flow control cases without inhibitors, respectively.

As shown in Fig. 3-3*B*, interstitial flow markedly activated p38 MAPK. SB-203580 clearly inhibited flow-induced p38 MAPK activation, while PD-98059 did not affect p38 MAPK activation. Sixty minutes of interstitial flow, with or without SB-203580 or PD-98059, had no effect on total p38 MAPK.

3.4.3 Interstitial flow induces SMC migration and MMP-13 expression via ERK1/2

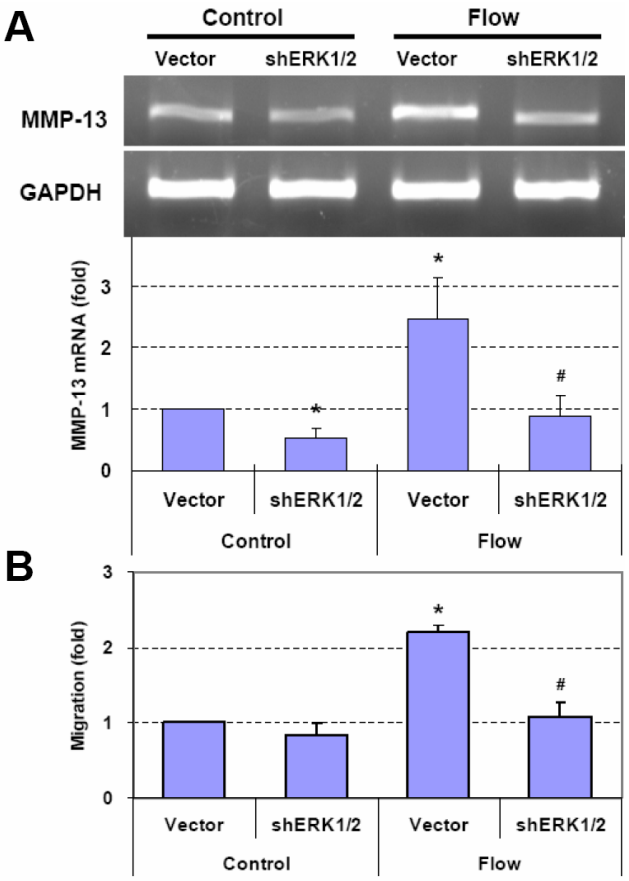

Figure 3-4. Silencing ERK1/2 abolished flow-induced MMP-13 expression (*A*) and cell migration (*B*). RT-PCR (gel panel in *A*) and RT-qPCR (bar graph in *A*) were used to measure MMP-13 gene expression. To silence both ERK1 and ERK2 at the same time, the same amount of each ERK1 and ERK2 short hairpin (sh)RNAs was co-transfected into SMCs at 10 μg of total plasmid DNA/2.5×10^6 cells (i.e. 2.5 μg of each of four ERK shRNAs were mixed together). 10 μg of pSUPER vector was used as vector control. After 24 h of transfection, cells were suspended into collagen gels for 24 h of spreading. Cells were then exposed to interstitial flow for 3 h either followed by 48 h migration to 20 ng/ml PDGF-BB or directly subjected to gene analysis. Data are presented as mean ± SEM. * $P<0.05$ vs vector-control; # $P<0.01$ vs vector-flow; n= 3-4.

Since the pharmacological inhibitors may also influence other protein kinases [35], to further confirm the predominant regulatory role of ERK1/2 in MMP-13 expression and cell migration, ERK1/2 shRNAs were transfected into cells. After knocking down of ERK1/2, both interstitial flow-induced MMP-13 expression (Fig. 3-4*A*) and cell migration (Fig. 3-4*B*) were completely abolished. In addition, the migration in no-flow control case (vector) was barely dependent on ERK1/2 (Figs. 3-1 and 3-4*B*), which is consistent with our previous observation that migration of SMC in the no-flow control case is independent of MMP-13 [167].

Taken together these data (cell migration, MMP-13 expression, MAPK activation and inhibition, and ERK1/2 gene knockdown) suggest that interstitial flow-induced cell migration and MMP-13 expression proceed through an ERK1/2-dependent pathway. ERK1/2 activation plays a much more direct and critical role in regulating MMP-13 expression than p38 MAPK does although the exact role of p38 MAPK is not clear.

3.4.4 Interstitial flow induces c-Jun and c-Fos expression through ERK1/2 activation

Transcription factors c-*jun* and c-*fos* are members of the AP-1 family and these immediate-early genes are targets of the ERK1/2 MAPK pathway [36]. To investigate whether interstitial flow-induced ERK1/2 phosphorylation affects AP-1 transcription factor (c-Jun and c-Fos) expression, we determined c-*jun* and c-*fos* gene expression by RT-qPCR and c-Jun and c-Fos protein expression by Western blotting. Interstitial flow dramatically induced c-*jun* and c-*fos* transient gene expression (Fig. 3-5*A*) within 15 min and then the elevated expression returned to the control level by 60 min. PD-98059 attenuated both c-*jun* and c-*fos* transient gene expression to their control levels. In the

presence of SB-203580, interstitial flow significantly induced c-*jun* and c-*fos* gene expression that remained relatively high level at 60 min although the peak level was not as high as the induction by interstitial flow alone (Fig. 3-5*A*). The change of c-*fos* expression was more pronounced than that of c-*jun*.

Similar trends were observed for AP-1 protein expression (Fig. 3-5*B*). Interstitial flow markedly induced c-Jun and c-Fos protein expression within 60 min. PD-98059 significantly reduced flow-induced c-Jun and c-Fos expression. SB-203580 raised c-Jun and c-Fos expression for both no-flow (0 min) and flow cases, but there appeared to be little flow-induction.

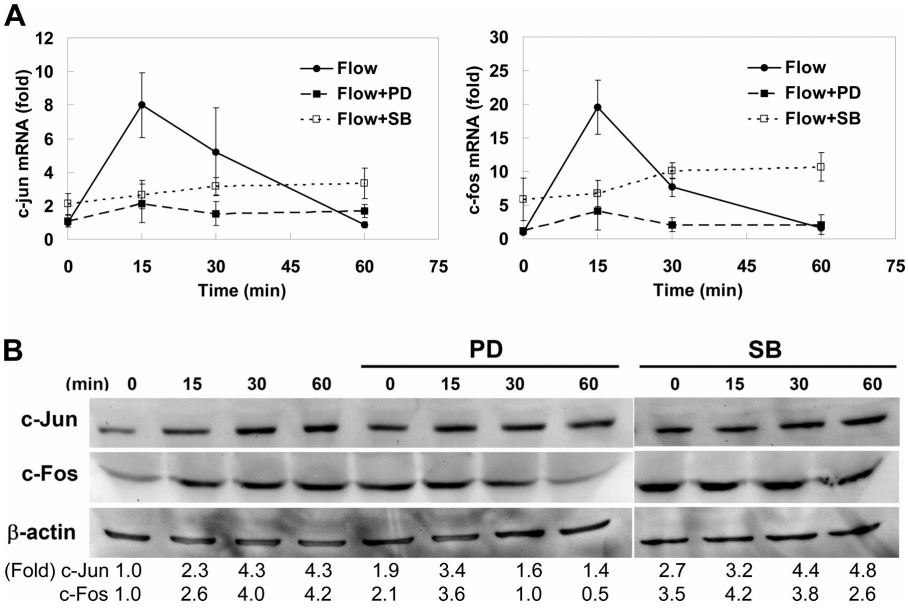

Figure 3-5. Interstitial flow induces AP-1 transcription factor expression through ERK1/2 activation. PD markedly inhibited flow-induced c-Jun and c-Fos expression, and SB promoted c-Jun and c-Fos expression at longer times (60 min). After spreading out, cells in gels were pretreated with 5 μM SB or 10 μM PD for 1 h, and then exposed to interstitial flow either with or without inhibitors for 0, 15, 30, or 60 min. β-actin served as internal control. *A*: mRNA expression of c-*fos* and c-*jun* were detected by real-time PCR (mean ± SEM, n= 3-5). *B*: A representative Western blot result for AP-1 protein expression. The experiments were run three times and similar results were observed. The quantifications for protein expression are shown as fold change.

3.4.5 Interstitial flow induces AP-1 DNA binding activity depending on ERK1/2 activation

To regulate target gene transcription, AP-1 transcription factors have to translocate from the cytoplasm into the nucleus and bind to specific sites on DNA (AP-1 site). As shown in Fig. 3-6, interstitial flow significantly increased AP-1 DNA binding activity by two-fold, and PD-98059 completely abolished flow-increased DNA binding activity, suggesting that increased DNA binding activity is ERK1/2-dependent. After treatment with SB-203580, the flow-induced AP-1 DNA binding activity was only slightly, but not significantly, higher than the flow only case (Fig. 3-6). This is not consistent with the fact that the MMP-13 gene expression was much higher in the case of flow with SB-203580 than in the flow only case (Fig. 3-2). However, it is possible that the sustained expression of AP-1 transcription factor stimulated by SB-203580 (Fig. 3-5) provided a sustained high level of DNA binding activity which maintained MMP-13 expression at a high level.

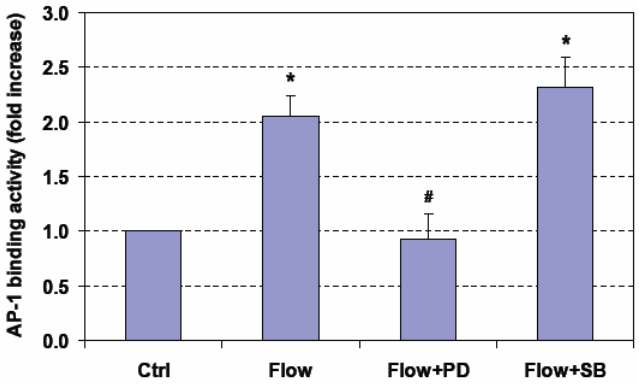

Figure 3-6. Interstitial flow induces AP-1 DNA binding activity via ERK1/2 activation. PD abolished flow-induced augmentation of AP-1 binding activity, while SB slightly enhanced flow-induced augmentation of AP-1 binding activity. After 24 h of cell spreading in collagen I gels, media was replaced with either fresh media, or 5 μM SB-203580, or 10 μM PD-98059 for 1 h, and then the gels were exposed to 1 cmH_2O of interstitial flow either with or without inhibitors for 3 h. After flow, cells were released from collagen gels by incubating with 0.2% collagenase I for 40 min. Nuclear proteins were then extracted followed by AP-1 DNA binding activity assay. Data are presented as mean ± SEM, n= 3. * $P<0.05$ vs Ctrl; # $P<0.02$ vs Flow.

3.4.6 Interstitial flow-induced MMP-13 expression is mediated by c-jun but not c-fos

To further investigate whether ERK1/2 regulated MMP-13 expression directly through AP-1, c-*jun* and c-*fos* genes were silenced by their shRNAs. As shown in Fig. 3-7, after knocking down c-*jun*, the flow-induced MMP-13 expression was completely abolished. Although interstitial flow significantly induced c-*fos* expression (Fig. 3-5), surprisingly, silencing of c-*fos* did not affect MMP-13 expression (Fig. 3-8). These data suggest that it was c-*jun* but not c-*fos* that mediated flow-induced MMP-13 expression through an ERK1/2-dependent pathway.

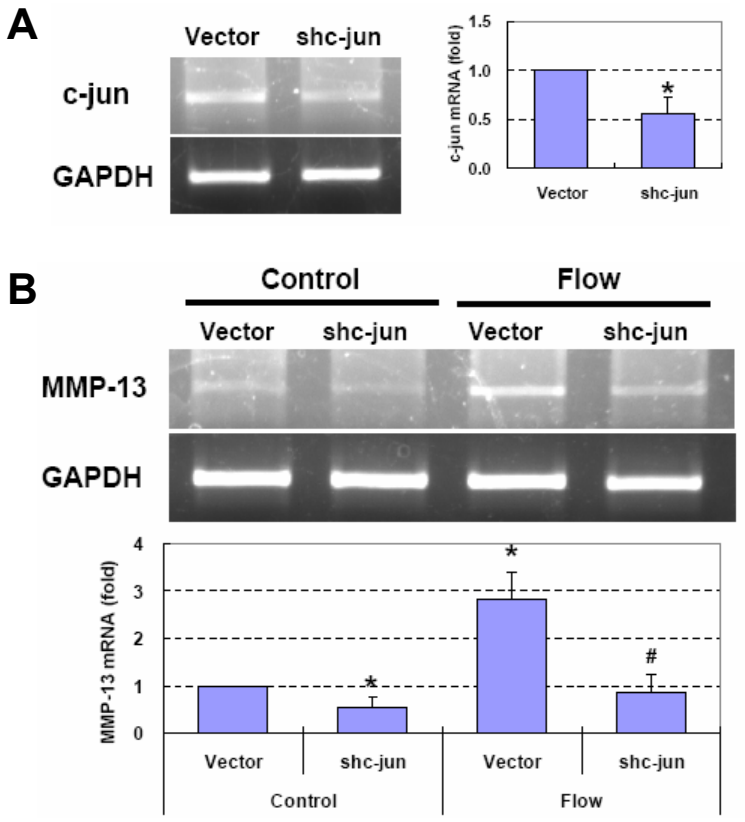

Figure 3-7. Interstitial flow induces MMP-13 expression depending on c-Jun. *A*: Cells that were transfected with c-*jun* shRNAs expressed less c-*jun* (gel panel: RT-PCR; bar graph: RT-qPCR). *B*: Silencing c-*jun* completely abolished flow-induced MMP-13 expression (gel panel: RT-PCR; bar graph: RT-qPCR). To silence c-*jun*, the same amounts of shc-jun-a and shc-jun-b shRNAs were co-transfected into SMCs at 10 μg of

total plasmid DNA/2.5×10^6 cells (i.e. 5 μg of each shRNA were mixed together). 10 μg of BS/U6 vector was used as vector control. After 24 h of transfection, cells were suspended into collagen gels and allowed to spread for 24 h before flow experiments. Gels were then exposed to interstitial flow for 3 h. Data in bar graphs are presented as mean ± SEM. In *A*, * P<0.005 vs vector, n= 3. In *B*, * P<0.02 vs vector-control; # P<0.01 vs vector-flow; n=3.

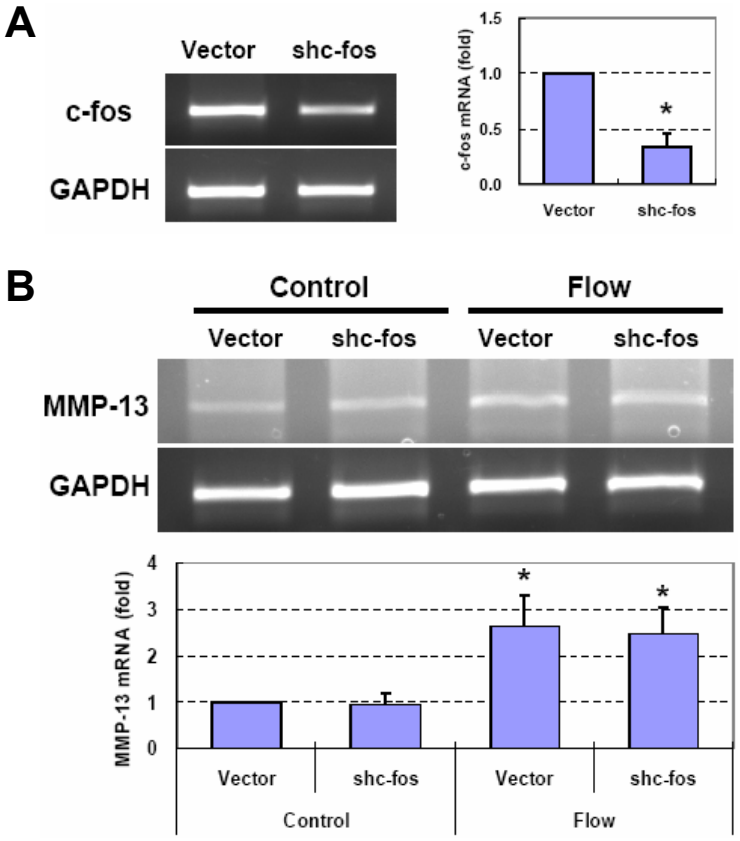

Figure 3-8. Interstitial flow-induced MMP-13 expression is independent of c-Fos. *A*: Cells that were transfected with c-fos shRNAs expressed much less c-*fos* (gel panel: RT-PCR; bar graph: RT-qPCR). *B*: Silencing c-*fos* barely affected flow-induced MMP-13 expression (gel panel: RT-PCR; bar graph: RT-qPCR). To silence c-*fos*, the same amounts of shc-fos-a and shc-fos-b shRNAs were co-transfected into SMCs at 10 μg of total plasmid DNA/2.5×10^6 cells (i.e. 5 μg of shc-fos-a and 5 μg of shc-fos-b were mixed together). 10 μg of BS/U6 vector was used as vector control. Transfection was conducted using Lipofectamine™ LTX and PLUS™ reagents (Invitrogen). After 24 h of transfection, cells were suspended into collagen gels and allowed to spread for 24 h before flow experiments. Gels were then exposed to 1 cmH_2O of interstitial flow for 3 h. Data in bar graphs are presented as mean ± SEM. In *A*, * P<0.001 vs vector, n= 3. In *B*, * P<0.02 vs vector-control, n=3.

3.5 Discussion

In the present study, we observed that interstitial flow activated both ERK1/2 and p38 MAPK; PD-98059 abolished flow-induced ERK1/2 activation; and in contrast, SB-203580 enhanced flow-induced ERK1/2 activation and abolished flow-induced p38 MAPK activation (Fig. 3-3). Interstitial flow also induced MMP-13 expression and SMC migration, and PD-98059 inhibited flow-induced MMP-13 expression and cell migration, while SB-203580 enhanced MMP-13 expression and cell migration although the activation of p38 MAPK was inhibited (Figs. 3-1 and 3-2). Silencing ERK1/2 completely abolished flow-induced MMP-13 expression and cell migration (Fig. 3-4). These findings indicate that interstitial flow-induced MMP-13 expression and cell migration proceed through an ERK1/2-dependent pathway. ERK1/2 activation plays a much more critical role in regulating flow-induced MMP-13 expression than p38 MAPK although the exact role of p38 MAPK remains unclear.

There is abundant evidence in the literature that induction of human interstitial collagenase (MMP-1) or rat interstitial collagenase (MMP-13) expression is related to the activation of MAPKs such as ERK1/2 and/or p38 MAPK [20, 110, 123, 142, 172]. Activation of ERK1/2 by chemical and physical factors such as mitogenic growth factors, proinflammatory cytokines, heat shock, ultraviolet (UV) light, and other factors often induce MMP-1 expression in many human cell types [20, 28, 38, 49, 110, 128]. In contrast, activation of p38 MAPK has opposing effects on human MMP-1 gene expression depending on the mode of induction [43]. For example, MMP-1 expression in human skin fibroblasts induced by tumor necrosis factor (TNF)-α is through AP-1-

dependent transcriptional activation via the ERK1/2 pathway and AP-1-independent enhancement via p38α MAPK by mRNA stabilization [142]; lipopolysaccharide (LPS)-induced monocyte human MMP-1 expression is regulated by both ERK1/2 and p38 MAPK [82]; while PDGF-BB and arsenite suppress human MMP-1 expression via p38 MAPK activation [43, 206]. One study has demonstrated that p38 α, one isoform of p38 MAPK, inhibits the ERK1/2 pathway [206]. Serotonin induces rat MMP-13 production via ERK1/2 pathway in uterine rat SMCs [172]. Macrophage migration inhibitory factor up-regulates MMP-13 mRNA of rat calvaria-derived osteoblasts via an ERK1/2 and AP-1 dependent but p38-independent pathway [123]. Thus in our study, the crosstalk between ERK1/2 and p38 MAPK might play a role in interstitial flow-induced rat interstitial collagenase (MMP-13) expression. However, although the role of p38 MAPK remains unclear, our data strongly suggest that ERK1/2 plays a predominant regulatory role in flow-induced rat MMP-13 expression.

In cardiovascular health and disease, it has been shown that the ERK1/2 MAPK plays an important role [113]. Increased ERK1/2 activation contributed to augmented vascular SMC proliferation and neointima formation with aging in a rabbit study [52]. The rapid activation of ERK1/2 after balloon injury of the rat carotid artery may be associated with vascular SMC migration and proliferation in vivo [67, 81]. Completely blocking ERK1/2 activation in balloon-injured carotid arteries can inhibit carotid neointima formation by suppressing SMC migration and proliferation after 2 weeks [53]. The evidence from in vitro studies has also shown that ERK1/2 activation plays a crucial role in cardiovascular cell proliferation, cell migration, and interstitial collagenase expression [28-30, 49, 110, 112, 139].

The activation of ERK1/2 MAPK can induce expression and activation of many transcription factors such as AP-1. AP-1 transcription factors have a variety of physiological and pathophysiological consequences through their regulation of target gene expression. The AP-1 DNA binding element plays a pivotal role in regulation of MMP expression since AP-1 sites are present throughout the MMP promoters [18, 199]. Jun proteins can form stable dimers that bind AP-1 DNA recognition elements (5'-TGAG/CTCA-3'). Fos proteins can bind DNA by forming heterodimers with Jun proteins (Jun:Fos) that are more stable than Jun:Jun dimers [161]. The ERK MAPK cascade is likely involved in the induction of the c-*fos* gene and in forming the Jun:Fos heterodimer [161]. In the present study, we observed that interstitial flow significantly promoted AP-1 (c-Jun and c-Fos) expression (Fig. 3-5). The increased expression and activation of c-Jun and c-Fos led to an elevated AP-1 DNA binding activity (Fig. 3-6), which could promote MMP-13 expression. Using an ERK1/2 specific inhibitor PD-98059, we further demonstrated that interstitial flow-induced AP-1 DNA binding activity is ERK1/2-dependent (Fig. 3-6). However, interestingly, RNA interference results suggest that it was c-*jun* but not c-*fos* that regulated MMP-13 expression (Figs. 3-7 and 3-8), although c-*fos* was definitely induced by flow. In addition, we observed that NF-κB did not play a major role in flow-induced MMP-1 expression and cell migration (data not shown).

Taken together, we described, for the first time, a mechanism of interstitial flow-induced rat interstitial collagenase (MMP-13) expression in vascular SMC in 3-D collagen I gels (shown in Fig. 3-9). Interstitial flow can, by an as yet to be determined mechanotransduction mechanism, induce ERK1/2 MAPK activation, which promotes

AP-1 transcription factor expression and AP-1 DNA binding activity, resulting in an elevated MMP-13 expression. Proteolysis of collagen by upregulated MMP-13 then facilitates SMC migration through collagen I. However, the mechanism by which vascular cells "sense" interstitial flow and then trigger ERK1/2 signaling pathway requires further investigation. Considering that cells in 3-D exhibit matrix adhesions all over their surface, cell-matrix adhesion and tethering through integrin-rich cell-matrix adhesions would be a potential mechanosensor [162, 167]. Another candidate would be the cell surface glycocalyx, which has been shown to mediate fluid shear stress-regulated vascular SMC contraction [4] and various endothelial cell functions [188].

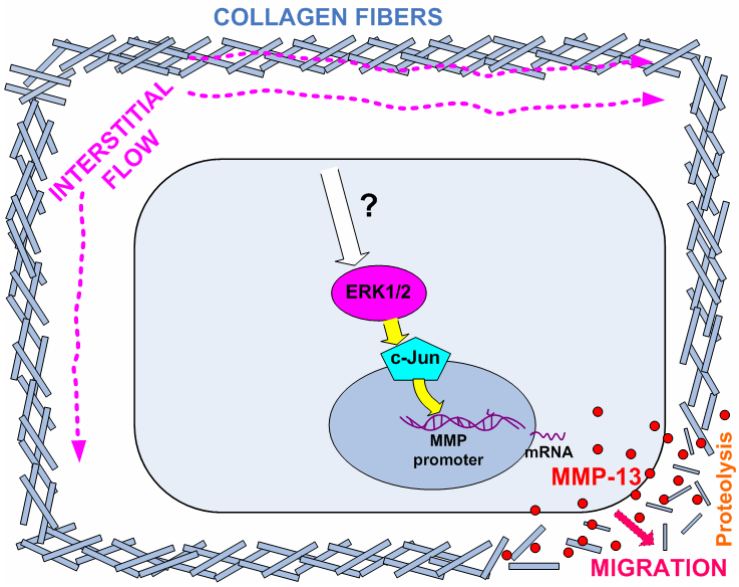

Figure 3-9. A proposed ERK1/2-c-Jun-dependent mechanism regulates flow-induced MMP-13 expression and cell motility. Interstitial flow stimulates the cell inducing ERK1/2 phosphorylation (mechanotransduction) which enhances AP-1 expression and AP-1 DNA binding activity, leading to an increased expression of rat interstitial collagenase (MMP-13). Upregulated MMP-13 digests collagen fibers and facilitates cell migration. One of the remaining questions is how cells "sense" interstitial flow and then activate the ERK1/2 pathway.

Transmural interstitial flow is elevated when the endothelium is injured due to chemical or mechanical stimuli or when the vascular hydraulic conductivity is enhanced by inflammation or hypertension. Thus elevated interstitial flow may be associated with vessel remodeling and neointima formation [143, 167]. The present study reveals a mechanism whereby altered interstitial flow during the early stages of vascular injury stimulates MMP expression and vascular SMC and fibroblast migration which can lead to neointima formation. These findings suggest that methods to control interstitial flow, or directly inhibit MMP expression, or suppress ERK1/2 MAPK activation may be able to limit neointima formation clinically after vascular injury.

ACKNOWLEDGEMENTS

The authors acknowledge financial support from NIH NHLBI grants RO1 HL 35549 and RO1 HL 57093. We thank Dr. Yongzhong Hou for valuable discussions and Hui Wang for cell migration assay.

Chapter 4

Heparan Sulfate Proteoglycan-Mediated FAK Activation Is Essential for Interstitial Flow Mechanotransduction Regulating ERK-Dependent MMP Expression and Cell Motility in 3-D

4.1 Abstract

Interstitial flow directly affects cells that reside in tissues and regulates tissue physiology and pathology by modulating important cellular processes including proliferation, differentiation, and migration. However, the structures that cells utilize to sense flow in a 3-dimensional (3-D) environment have not yet been elucidated. Previously, we have shown that interstitial flow upregulates rat interstitial collagenase (MMP-13) expression via activation of an ERK1/2-c-Jun signaling pathway, which in turn promotes cell motility in collagen I. Herein, we focused on uncovering the interstitial flow-induced mechanotransduction mechanism in 3-D. Inhibition or knockdown of focal adhesion kinase (FAK) inhibited flow-induced ERK1/2 activation, MMP-13 expression, and cell motility. Cleavage of cell surface heparan sulfate (HS) chains from proteoglycan (PG) core proteins by heparinase or disruption of HS biosynthesis by silencing *N*-deacetylase/*N*-sulfotransferase 1 (NDST1) also blocked flow-induced ERK1/2 activation, MMP-13 expression, and cell motility. Interstitial flow induced FAK phosphorylation at Tyr925, and this activation was blocked when HSPGs were disrupted. Removal of HS also attenuated FAK activation at Tyr397. Together, we demonstrate that cell surface HSPGs mediate interstitial flow-induced mechanotransduction that regulates MMP-13 expression and cell motility in 3-D via activation of a FAK-ERK1/2-c-Jun signaling cascade. This is the first study to describe the flow-induced mechanotransduction mechanism in cells in 3-D. This study will be of interest to understand the flow-related mechanisms in vascular remodeling and lesion formation and also tumor invasion.

Keywords: interstitial flow mechanotransduction, heparan sulfate proteoglycan, FAK

4.2 Introduction

In living tissues, many cell types including smooth muscle cells (SMCs), fibroblasts, bone cells, and tumor cells are exposed to interstitial fluid flow. Interstitial flow can modulate many cellular processes in 3-dimensional (3-D) microenvironment including proliferation, apoptosis, differentiation, and migration [149, 167, 182, 204]. Interstitial flow therefore plays important roles in tissue physiology and pathology. Transmural interstitial flow driven by the transmural pressure differential is a physiological fluid movement through vascular vessel interstitium that imposes fluid shear stress on vascular (SMCs) and fibroblasts [167, 201]. During the early stages of vascular injury or in hypertension, elevated transmural interstitial flow has been hypothesized to contribute to neointima formation by affecting SMC and fibroblast phenotype and motility [50, 143, 166, 167].

Interstitial fluid flow can affect cells in tissues both mechanically (via shear stress) and chemically (mass transport). To investigate effects of interstitial flow on biology of tissue interstitial cells including vascular cells, bone cells and tumor cells, application of fluid shear stress to cells cultured on 2-D substrates has been widely used [4, 23, 50, 208]. It is now well recognized that culturing cells in an in vitro 3-D extracellular matrix (ECM) better mimics in vivo cell physiology than traditional 2-D planar culture [32]. The interest in studying the biological effects of interstitial flow on cells in 3-D in vitro has increased substantially in the last decade. It has been reported that interstitial flow can induce cytokine release [204] and increase matrix metalloproteinase (MMP) expression and cell motility in 3-D collagen matrices [166, 167]. Interstitial flow can also promote tumor cell

migration, capillary morphogenesis, and stem cell differentiation in 3-D environments [61, 66, 170]. However, the mechanism by which cells in a 3-D microenvironment sense interstitial flow and convert this stimulation into cellular responses (mechanotransduction) that has not yet been well elucidated. Fluid shear stress-induced mechanotransduction in endothelial cells (ECs) on 2-D substrates has been well studied [6, 189]. Cells that are embedded in 3-D ECM have different patterns of cell-matrix adhesions [32] and elongated morphologies compared to cells seeded on 2-D substrates [15], which might give rise to different mechanotransduction pathways. Therefore, it is necessary to determine the mechanosensors for cells embedded in 3-D microenvironment when exposed to interstitial flow.

In 2-D studies, it has been suggested that cell surface glycocalyx components are responsible for sensing fluid shear stress on vascular ECs and SMCs [4, 47, 126, 188, 191]. The surfaces of eukaryotic cells, such as epithelial, cardiovascular and tumor cells, are decorated with a variety of membrane-bound macromolecules that constitute the glycocalyx. The glycocalyx consists primarily of proteoglycans and glycoproteins that are incorporated into the cell membrane. Proteoglycans contain a protein core (such as syndecans that transmembrane and can be attached to the cytoskeleton and glypicans that are anchored to the plasma membrane) with extended polysaccharide branches composed of glycosaminoglycans (GAGs) [4]. Heparan sulfate, chondroitin sulfate, and hyaluronan are the most dominant GAGs on most cell surface. Glycoproteins are also composed of a core protein but with much smaller sugar residues [4]. Glycocalyx components, especially heparan sulfate proteoglycans (HSPGs), have been demonstrated to play important roles in cellular recognition and signaling, cell growth, adhesion, spreading and

migration, and even in development, tumorigenesis, and vasculogenesis [14, 31, 44, 60]. Although, in 2-D, the role of glycocalyx (especially) HSPGs in flow-induced mechanotranduction have been well studied, there has been no report on the role of the glycocalyx in flow sensing in a 3-D microenvironment.

Focal adhesion kinase (FAK) is a widely expressed cytoplasmic protein tyrosine kinase (PTK) linked to integrin-mediated signaling. FAK is known to be a major mechanosensitive kinase that can be rapidly activated by a variety of mechanical stimuli and plays an important role in control of cell adhesion and migration [130]. It has been suggested that HSPGs (such as syndecan-1 and -4) can act cooperatively with integrins in creating signals for cell spreading and for assembly of focal adhesion plaques and stress fibers [75, 109, 151, 200]. Syndecan-4 can associate with FAK through the adaptor protein paxillin [37]. The association between syndecan-4 and paxillin is parallel to the association between integrin and paxillin, and this suggests the potential for syndecan-4 to mediate signaling events parallel to integrins [37]. In 2-D, it is well known that HSPGs on the apical side of the cells that do not bind to ECM can act as mechanosensors converting stimulation of fluid shear stress into biochemical responses [187, 188, 205]. On the basal side, HSPGs (such as syndecan-4) can bind to the substrate and modulate FAK and ERK1/2 activation in a manner similar to that of cells attached to ECM by integrin-based adhesions [11, 207]. This suggests that HSPG-mediated attachments are capable of functioning as another signaling pathway to transmit mechanical signals to the actin cytoskeleton and into cell nucleus.

We have shown previously that interstitial flow can activate an ERK1/2 MAPK and c-Jun signaling cascade leading to increased expression of MMP-13, which in turn

promotes vascular SMC and fibroblast migration in 3-D collagen I matrices [166]. Based on this background, we now demonstrate, for the first time, that cell surface HSPGs are mechanosensors for interstitial flow that leads to activation of the focal adhesion kinase (FAK) and ERK1/2-c-Jun signaling cascade, thus promoting MMP-13 expression and cell motility in 3-D ECM.

4.3 Materials and Methods

4.3.1 Collagen gel preparation and flow experiments. As previously described [166, 167], rat aortic SMC (passage 3-5) were suspended in rat tail collagen I (BD Science) gels (cell density: $2.5x10^5$ cells/ml; final gel concentration: 4 mg/ml), and pH was adjusted to 7.0 by mixing the appropriate amount of NaOH. For cell migration experiments, 200 μl of gel was loaded into each 12-well cell culture insert with 8 μm pores (BD Science). For RNA extraction and protein extraction experiments, 6-well cell culture inserts with 8 μm pores (BD Science) were used. In order to keep the same level of shear stress, the same gel thickness was maintained in both the 6- and 12-well experiments, thus 1 ml of gel was used for each 6-well insert. The gels were incubated for 24 h to allow cell spreading. Gels were then subjected to interstitial flow driven by a 1 cmH_2O pressure drop (shear stress was ~0.05 dyn/cm^2) for various time periods according to specific experimental designs.

For FAK inhibition and HSPGs cleavage experiments, before exposure to flow, the cells were treated either with 10 μM of FAK inhibitor PF-228 (Santa Cruz Biotechnology) or 6.7 IU/L heparinase III (IBEX Technologies, Montreal, Canada) in growth medium for 2.5 hours. Gels were then exposed to flow. Flow medium contained either 10 μM of PF-228 for FAK inhibition experiments or 1 IU/L heparinase III for HSPGs cleavage experiments.

4.3.2 RNA interference. To silence FAK, two FAK short hairpin (sh) RNAs and one control shRNA were used (gift from Dr. Tadashi Yamamoto). The sequences specific for

rat FAK mRNA were: FAK#1, 5'-GGTCCAGACCAATCACTAT-3' and FAK#2, 5'-GCAGTTTGCCAACCTTAAT-3'. A non-silencing control sequence was: 5'-TTCTCCGAACGTGTCACGT-3'. The annealed nucleotides were inserted into pSIREN-RetroQ vector [65]. In order to disrupt heparan sulfate biosynthesis, a rat N-deacetylase/N-sulfotransferase 1 (NDST1) shRNA was used. The target sequence for rat NDST1 was: 5'-CTTACTGTGCTCCTCAATCCTATCAGCGT-3', which was subcloned into pGFP-V-RS vector (Origene, MD). The transfections were conducted using Lipofectamine™ LTX and PLUS™ reagents (Invitrogen).

4.3.3 Immunostaining. To assess the cleavage of heparan sulfate glycosaminoglycans (HS-GAGs) by heparinase III, primary antibody HepSS-1 (US Biological) and secondary antibody Alexa Fluor 350 goat anti-mouse IgM (Invitrogen) were used to stain cell HS-GAGs. Briefly, cells were seeded in a 24-well plate for 2 days and then treated with 6.7 IU/L heparinase III for 1 hour, followed by fixation with 4% paraformaldehyde and blocking with 4% BSA in PBS. Then cells were incubated with primary antibody HepSS-1 (1:200 dilution in PBS with 4% BSA) for 2 hours and secondary antibody anti-mouse IgM (1:100 dilution) for 2 hours at room temperature. Finally cells were mounted by mounting medium containing propidium iodide (PI) (Vector Laboratories). For the NDST1 knockdown experiment, the same staining procedure was followed to evaluate the disruption of heparan sulfate biosynthesis by shNDST1. To visualize the influence of heparinase III on cell morphology in 3-D collagen gels, cells were stained with Calcein AM (invitrogen).

4.3.4 Western blotting. Protein samples were collected and western blots were performed as described previously [166]. Collagen gels were washed once with ice-cold PBS, then 2X lysis buffer was added immediately to the gels followed by sonication for 30 seconds on ice. The 2X lysis buffer was composed of 2X RIPA buffer (300 mM NaCl, 2% NP-40, 100 mM Tris, 0.2% Brij 35, 2 mM EDTA, pH 7.5) with a supplement of 2X protease inhibitor cocktail (Roche Diagnostics), 2X phosphatase inhibitor cocktail (Roche Diagnostics), 2 mM activated Na_3VO_4, and 2 mM PMSF. Lysates were centrifuged in a microfuge (12,000 g for 1 hour at 4°C), and then the supernatants were collected and the remaining gel pellets were discarded. The supernatants were concentrated using Centrifugal Filter Units (Millipore). Protein concentrations in supernatants were evaluated using Protein Determination Kit (Cayman Chemical). The protein samples were then boiled for 5 minutes after mixing with 4X sample buffer (400 mM Tris-HCl, 8% SDS, 40% glycerol, 0.04% bromphenol blue, and 20% β-mercaptoethanol, pH 6.8) and stored at -80°C. Protein samples were loaded onto 10% Tris-HCl Ready Gels (Bio-Rad). After electrophoresis, proteins were transferred to PVDF membranes (Bio-Rad) and blocked at room temperature with 2% Enhanced Chemiluminescence (ECL) Advance Blocking Agent (Amersham, GE Healthcare) in TBS-T [50]. The membranes were incubated overnight with a 1:1000 dilution of a specific rabbit primary antibody (monoclonal antibodies: ERK1/2, phospho-ERK1/2; polyclonal antibodies: FAK, phospho-FAK (Tyr397), phospho-FAK (Tyr925), α-tubulin, and β-actin. All antibodies were purchased from Cell Signaling), followed by a 1.5-h room temperature incubation with an ECL horseradish peroxidase (HRP)-linked anti-rabbit IgG antibody (1:1000) (Amersham, GE Healthcare). The proteins on PVDF membranes were then detected

using Immobilon Western Chemiluminescent HRP Substrate (Millipore) and the ChemiDoc XRS system with the Quantity One software (Bio-Rad). Some membranes were stripped using Restore™ Plus Western Blot Stripping Buffer (Thermo Scientific Pierce) for subsequent detections.

4.3.5 RNA extraction and gene expression analysis. Cells in collagen gels were directly lysed by TRIzol® LS Reagent (Invitrogen) and the insoluble materials were removed by centrifugation at 12,000 x g for 10 minutes at 4°C. Chloroform was added for phase separation followed by RNA isolation using the RNeasy Mini Kit (Qiagen). RNA samples were then converted to cDNA by reverse transcription (RT). For analyzing gene expression, the polymerase chain reaction (PCR) was performed using the following protocol as previously described [166]: pre-denaturation at 95 ºC for 5 minutes, then either 30 cycles (for MMP-13) or 28 cycles (for GAPDH) of denaturation at 94 ºC for 35 seconds, annealing at 52 ºC for 35 seconds, and extension at 72 ºC for 35 seconds, followed by a final extension at 72 ºC for 10 min. The amplified products were separated by electrophoresis in 2.5% agarose gels and photographed under UV light in the presence of ethidium bromide (EB). Quantitative real-time PCR (RT-qPCR) was also performed for MMP-13 expression on the ABI PRISM® 7000 sequence detection system (Applied Biosystems). GAPDH served as an internal control. Reactions were performed in 25 µl reaction mixture volumes containing ABsolute Blue QPCR SYBR Green ROX Mix (Thermo Scientific), cDNA, and specific primer pairs. Real-time PCR protocol was set to 15 minutes at 95°C followed by 45 cycles of 30 seconds at 95°C, 30 seconds at 55°C, and 30 seconds at 72°C. The fluorescent data were collected at 76°C. The dissociation curve

analysis was used to assess the specificity of product amplification. Primer sequences are listed in Table 4-1.

Table 4-1. Primer sequences for rat genes

Target gene	Primer sequence	GenBank Locus	Size
MMP-13		NM_133530	71
Forward (1124-1145)	5'-TCTGACCTGGGATTTCCAAAAG-3'		
Reverse (1194-1175)	5'-GTCTTCCCCGTGTCCTCAAA-3'		
NDST1		NM_024361	258
Forward (3188-3207)	5'- CCCAGCCAGCCAGGAGCAAC-3'		
Reverse (3445-3426)	5'- GGGCAGGACTGGCCGAACAC-3'		
FAK		NM_013081	232
Forward (3405-3424)	5'- CTGCTGAACTCCGACTTGGG-3'		
Reverse (3636-3317)	5'- CCCAAAGGGCAGAAAGCCAT-3'		
GAPDH		NM_017008	232
Forward (372-390)	5'-TCTTCACCACCATGGAGAA-3'		
Reverse (603-585)	5'-ACTGTGGTCATGAGCCCTT-3'		

Data Analysis. Results are presented as mean ± SEM. Data sets were analyzed for statistical significance using a Student's t-test with a two-tailed distribution, and $P < 0.05$ was considered statistically significant.

4.4 Results

4.4.1 Interstitial flow-induced MMP-13 expression and cell motility depend on HSPGs.

Heparan sulfate glycosaminoglycans (HS-GAGs) are abundantly presented on the surfaces of vascular SMCs and can be substantially depleted by a selective enzyme, heparinase III (upper panel of Fig. 4-1*A*). Heparan sulfate production can be effectively suppressed by silencing *N*-deacetylase/*N*-sulfotransferase 1 (NDST1), an enzyme that modulates heparan sulfate biosynthesis (lower panel of Fig. 4-1*A*). Elimination of heparan sulfate disrupted cell surface HSPGs, providing a possibility to determine the mechanotransduction role of HSPGs in sensing fluid flow [4, 47]. To investigate whether the HSPGs were responsible for sensing 3-D interstitial flow, heparinase III and NDST1 short hairpin RNA (shRNA) were used to disrupt cell surface HSPGs. Cleavage of HS-GAGs by heparinase completely abolished flow-induced MMP-13 expression (Fig. 4-1*B*), resulting in a significant reduction in flow-induced cell motility (Fig. 4-1*C*). Heparinase also reduced MMP-13 expression and cell motility in the no-flow control case (Figs. 4-1*B* and 4-1*C*). Knockdown of NDST1 abolished the augmentation of MMP-13 expression and cell motility induced by interstitial flow (Fig. 4-1*B* and 4-1*C*). NDST1 gene expression was reduced by NDST1 shRNA (Fig. 4-1*D*). It appears that shNDST1 and heparinase III had similar effects on MMP-13 expression and cell motility.

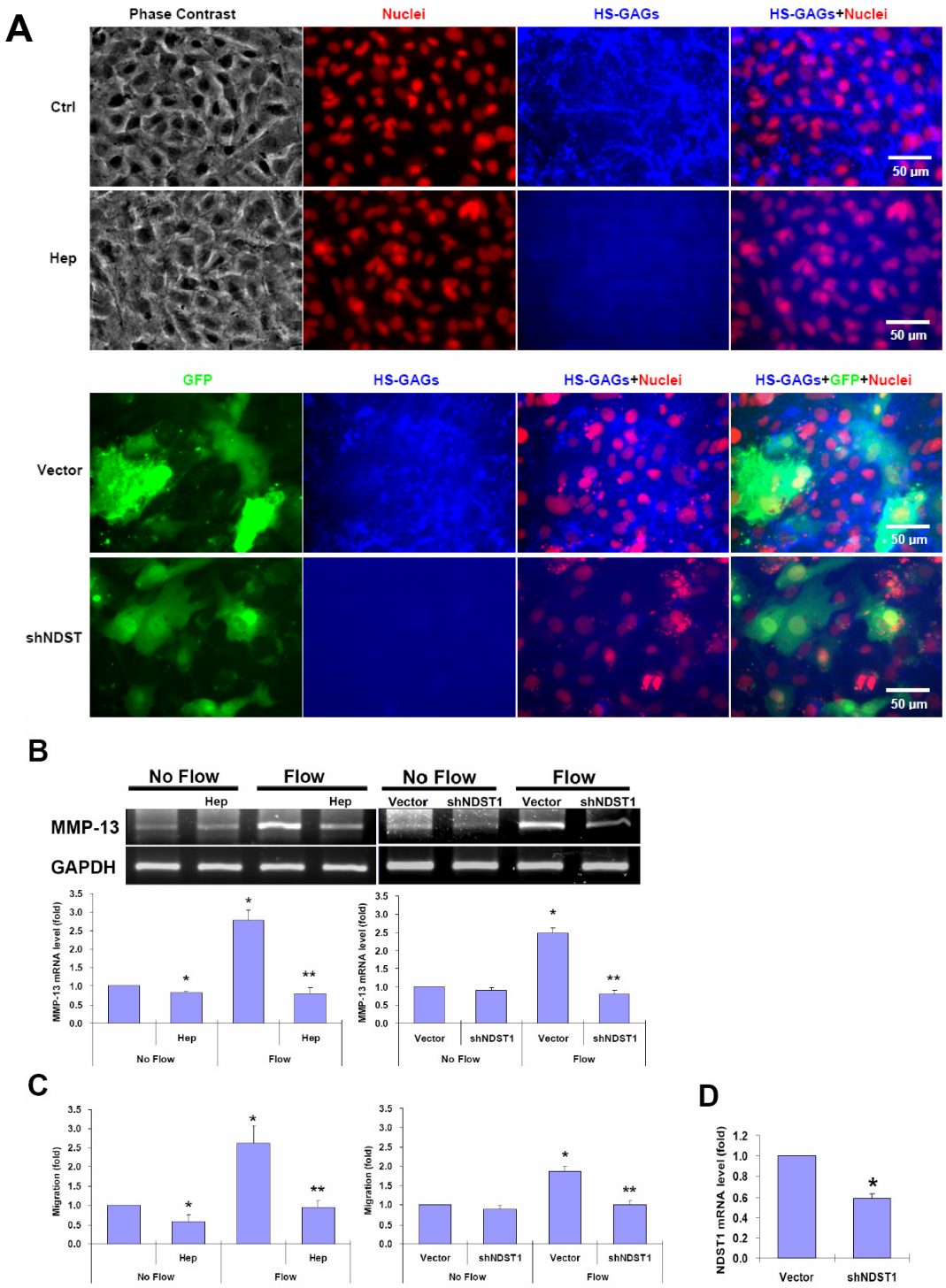

Figure 4-1. Interstitial flow promotes MMP-13 expression and cell motility dependent on heparan sulfate proteoglycans (HSPGs). (*A*) Immunostaining to show that HSPGs present on the surfaces of cells cultured on 2-D; Both heparinase III (Hep) and NDST1 shRNA (shNDST1) successfully eliminated HS glycosaminoglycans (HS-GAGs); Blue: HS-GAGs; Red: PI for nuclei; Green: GFP. (*B*) Cleavage of HS-GAGs by Hep (left panel) or disruption of HS biosynthesis by shNDST1 (right panel) abolished

flow-induced MMP-13 expression (gel panel data were obtained by traditional RT-PCR; bar graph data were obtained by RT-qPCR). (*C*) Flow-induced cell motility was abolished by disruption of HSPGs by Hep or shNDST1. (*D*) NDST1 was successfully suppressed by shNDST1. For Hep treatment experiments, after spreading in collagen gels, cells were treated with 6.7 IU/L Heparinase III, and then incubated for 2.5 h, followed by 4.5 h of exposure to interstitial flow. After flow, some gels were subjected to RNA extraction and RT-(q)PCR, and other gels were subjected to cell motility test experiment. RT-qPCR data and migration are presented as mean ± SEM, n= 3-4. * $P<0.05$ vs No-flow controls; ** $P<0.05$ vs Flow cases.

4.4.2 Interstitial flow-induced MMP-13 expression and cell motility depend on FAK.

FAK is a major mechanosensitive kinase that can be rapidly activated by a variety of mechanical stimuli to regulate cell adhesion and migration [130]. Therefore, we investigated whether FAK was involved in flow-induced MMP-13 expression and cell motility in our 3-D system. It has been reported that a FAK inhibitor PF-228 selectively inhibits FAK phosphorylation at Tyr397 and inhibits cell migration concomitant with the inhibition of focal adhesion turnover [175]. In this study, PF-228 significantly attenuated but not completely abolished flow-induced MMP-13 expression (Fig. 4-2*A*) and completely abolished flow-induced cell motility (Fig. 4-2*B*). To further elucidate the role of FAK, shRNA was used to silence FAK. After FAK knockdown, flow-induced MMP-13 expression was substantially inhibited (Fig. 4-2*A*) and cell motility was completely abolished to a level even lower than the control case (Fig. 4-2*B*). In the no-flow control cases, PF-228 slightly reduced MMP-13 expression but not cell motility, while shRNA of FAK significantly suppressed cell motility but not MMP-13 expression (Fig. 4-2*A* and *B*). Transfection of cells with FAK shRNA reduces total FAK expression, resulting in less focal adhesion turnover and thus less cell motility. Addition of inhibitor PF-228 inhibits FAK phosphorylation at Tyr397, but do not affect total amount of FAK. Therefore, our data suggest that FAK activation at Tyr397 and focal adhesion turnover are critical for

cell migration; and there must be FAK phosphorylation at other tyrosine sites played an important role for MMP-13 expression besides Tyr397, because FAK shRNA completely abolished flow-induced MMP-13 expression but PF-228 did not. Baseline migration in the no-flow controls barely depended on FAK, which is consistent with previous results that baseline migration is independent of MMP and ERK1/2 [166, 167].

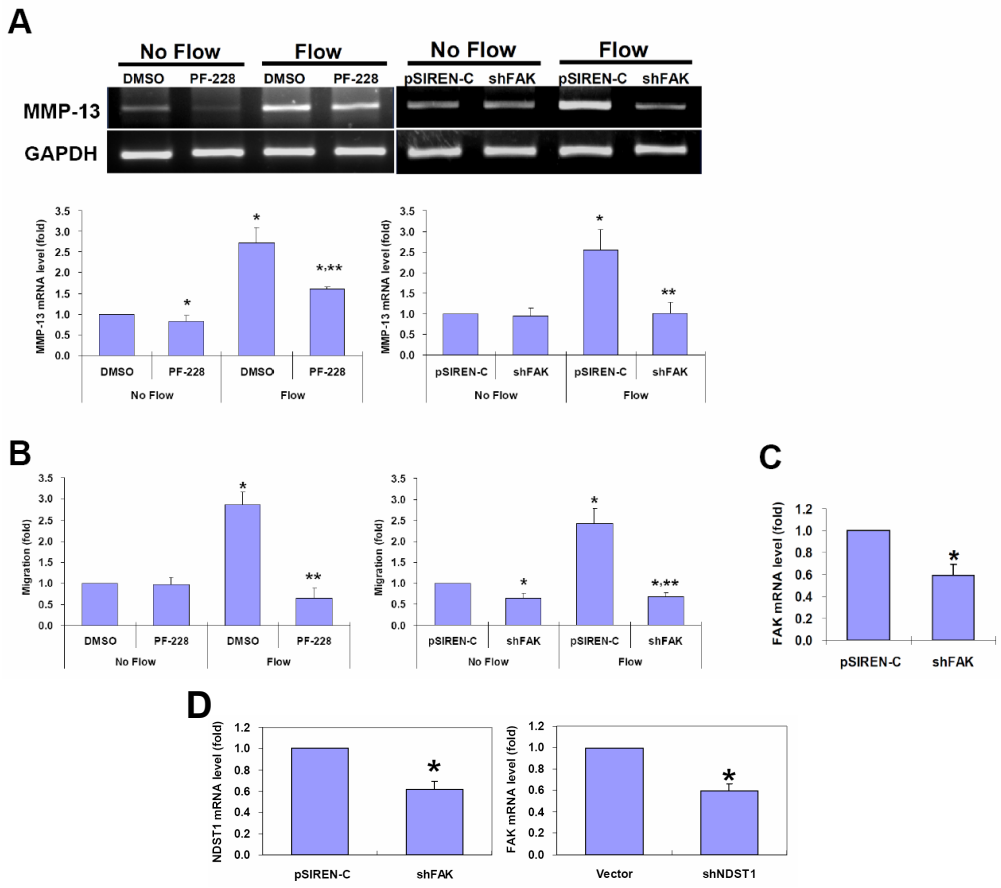

Figure 4-2. Interstitial flow promotes MMP-13 expression and cell motility dependent on focal adhesion kinase (FAK). (*A*) Inhibition of FAK by PF-228 (left panel) or knockdown of FAK by FAK shRNA (shFAK, right panel) abolished interstitial flow-induced MMP-13 expression (gel panel data were obtained by traditional RT-PCR; bar graph data were obtained by RT-qPCR). (*B*) Interstitial flow-induced cell motility was abolished by inhibition of FAK by PF-228 or silencing FAK by shFAK. (*C*) FAK expression was reduced by shFAK. (*D*) FAK knockdown inhibited NDST1 gene expression; NDST1 knockdown suppressed FAK gene expression. Before flow experiments, cells were incubated with DMSO or 10 μM PF-228 in medium for 2 h. RT-qPCR data and cell migration data are presented as mean ± SEM in the bar graph, n= 3-4. * P<0.05 vs No-flow controls; ** P<0.05 vs Flow cases.

Interestingly, knocking down either NDST1 or FAK gene suppressed the other gene (Fig. 4-2*D*), suggesting HSPGs and FAK may interact with each other. We speculate that HSPG production promotes cell-matrix adhesion formation, while cell-matrix adhesion formation enhances cell spreading which may promote HSPG production.

4.4.3 FAK and HSPGs mediate flow-induced ERK1/2 activation.

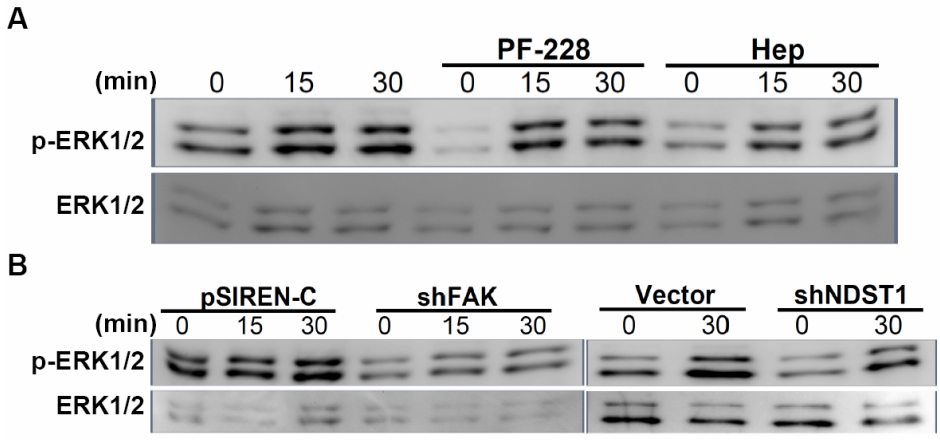

Figure 4-3. Interstitial flow-induced ERK1/2 activation depends on both FAK and HSPGs. (*A*) Western blots showed that inhibition of FAK by PF-228 and disruption of HSPGs by heparinase (Hep) reduced ERK1/2 phosphorylation; Cells in gels were pretreated with 10 μM of PF-228 or 6.7 IU/L of heparinase for 2.5 h before exposed to flow. (*B*) Western blots showed that silencing FAK by shFAK or disrupting HSPGs by shNDST1 significantly reduced flow-induced ERK1/2 activation. The gel panels are representative images from three independent experiments.

We have previously demonstrated that interstitial flow-induced MMP-13 expression depends on activation of the ERK1/2-c-Jun signaling cascade [166]. We also showed that flow-induced MMP-13 upregulation depends on both FAK and HSPGs (above). Therefore, we further investigated whether FAK and HSPGs regulate flow-induced ERK1/2 activation using Western blotting (Fig. 4-3). Flow significantly stimulated ERK1/2 phosphorylation, and PF-228 dramatically reduced ERK1/2 phosphorylation in the no-flow control case, and partially but significantly attenuated flow-induced ERK1/2

activation under flow (Fig. 4-3*A*). Knockdown of FAK significantly reduced ERK1/2 activation in the no-flow control case and substantially inhibited flow-induced ERK1/2 activation (Fig. 4-3*B*). Cleavage of HSPGs by heparinase significantly inhibited ERK1/2 phosphorylation in the no-flow control and also inhibited flow-induced ERK1/2 activation (Fig. 4-3*A*). Disruption of HSPGs by silencing NDST1 also significantly reduced flow-induced ERK1/2 activation (Fig. 4-3*B*). These results suggest that both FAK and HSPGs play crucial roles in ERK1/2 activation to regulate MMP-13 expression.

4.4.4 HSPGs are interstitial flow mechanosensors mediating FAK and ERK1/2 activation.

Since both knockdown of FAK and removal of HSPGs abolished flow-induced ERK1/2 activation and MMP-13 expression, these data suggest that the mechanosensitive signaling pathways mediated by FAK and by HSPGs regulating ERK1/2 activation should be in a serial, not parallel pattern. Therefore, we hypothesized that HSPGs are flow sensors and signal transducers which sense and transmit interstitial flow stimuli to activate FAK and its downstream signaling cascade. To test this hypothesis, we simply eliminated cell surface HSPGs using heparinase and then investigated whether flow-induced activations of FAK and ERK1/2 were affected. The results are shown in Fig. 4-4. Removal of HSPGs significantly reduced FAK phosphrylation at Tyr397, leading to a marked reduction in ERK1/2 activation. Surprisingly, flow did not affect FAK phosphorylation at Tyr397 as the level of phosphorylated Tyr397 did not change with flow exposure time. However, flow dramatically elevated phosphorylation of FAK at Tyr925 and ERK1/2 and these activations were markedly attenuated by cleavage of HSPGs. These data together with MMP-13 expression, cell migration and ERK1/2

activation data (Figs. 4-2 and 4-3) imply that phosphorylation of FAK at Tyr397 play a role in baseline ERK1/2 activation and MMP-13 expression, while activation of FAK at Tyr925 is crucial for flow-induced ERK1/2 activation, MMP-13 expression, and cell motility. Disruption of HSPGs attenuated interstitial flow-induced activation of FAK Tyr925 and ERK1/2, suggesting that HSPGs are mechanosensors in mediating interstitial flow-induced signaling activation and MMP expression.

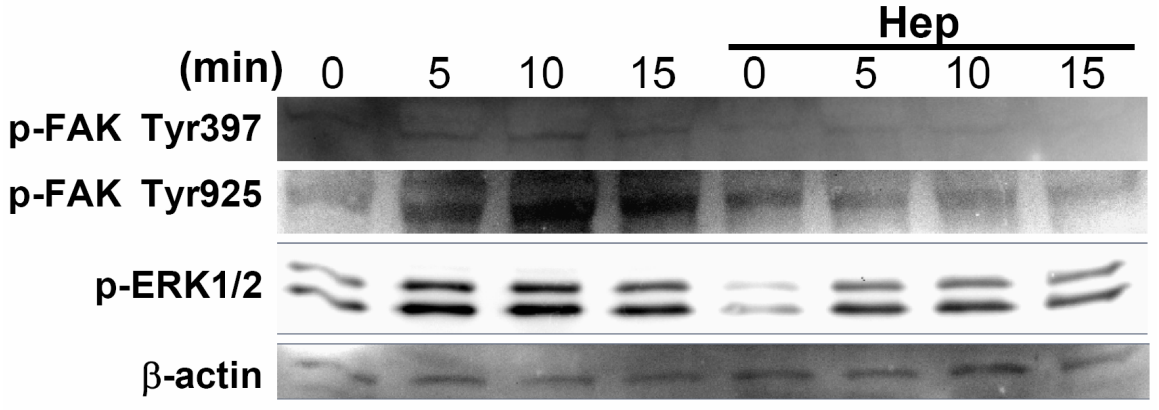

Figure 4-4. HSPGs mediate flow-induced activation of FAK Tyr925 and ERK1/2. Cells in gels were pretreated with heparinase for 2.5 h to remove cell surface HSPGs. Removal of HSPGs reduced FAK phosphorylation at Tyr397, but interstitial flow did not affect Tyr397 phosphorylation. Flow promoted Tyr925 and ERK1/2 phosphorylation, and cleavage of HSPGs blocked the flow effects. The gel panels are representative images from three independent experiments. β-actin serves as an internal control.

4.4.5 Heparinase but not shNDST1 induces cell contraction in 3-D.

We also observed that after cleavage of HS-GAGs by incubating cells with heparinase, cells tended to be slightly contracted (see Fig. 4-5*A*). This is probably a result of cell adhesions to collagen fibers being loosened by removal of HS-GAGs. It is known that HSPGs can promote cell-matrix adhesion formation and increase the strength of adhesions to ECM [14]. HSPGs themselves can also tether to ECM binding domains with HS chains serving as secondary cell-matrix adhesions [14]. Thus, depletion of HS-GAGs

reduced HSPGs ligation to ECM and released some of the cell-matrix attachments that causing cell contraction (Fig. 4-5*A*). However, when we disrupted HSPGs by knocking down NDST1, we did not see significant differences in cell morphology (i.e. attachment and spreading) in 3-D collagen gels between vector control cells and NDST1 knockdown cells (Fig. 4-5*B*), suggesting integrin-based cell-matrix adhesions were still formed. Therefore, we conclude that HSPGs played a crucial role in mediating interstitial flow signal to activate FAK-ERK1/2 and their downstream cascade, eventually leading to an increase in MMP-13 expression and cell motility.

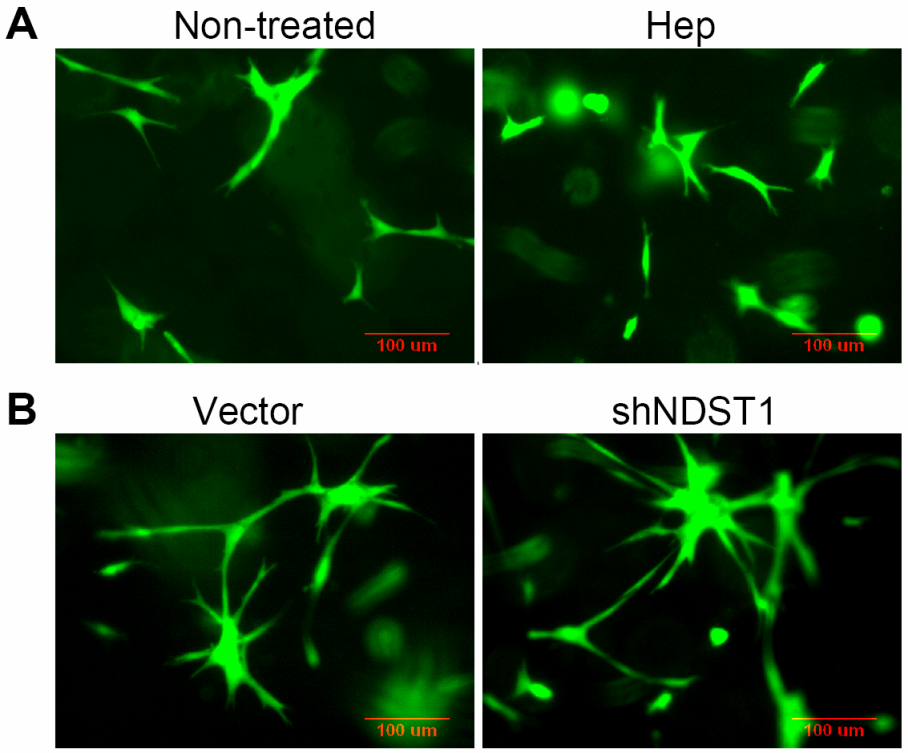

Figure 4-5. Effects of heparinase and NDST1 shRNA on SMC morphology in 3-D collagen gels. Disruption of HSPGs with heparinase III induced slight cell contraction in 3-D (*A*), while knockdown of NDST1 did not affect cell morphology (adhesion and spreading) in collagen gels (*B*). For heparinase treatment experiments, after 24 h of cell spreading, cells were incubated with 6.7 IU/L heparinase for 2.5 h. Cells were stained with Calcein AM (Invitrogen) in green. Images are the representative pictures from three independent experiments.

4.5 Discussion

Fluid flow in the tissue interstitium is very low due to the resistance of ECM fibrils and cells [86]. It has been shown, however, that such low fluid flow can affect cytokine release, vascular and tumor cell migration, capillary morphogenesis, and stem cell differentiation [61, 66, 166, 167, 170, 204]. But, how cells sense this subtle fluid flow in a 3-D environment remains largely unknown. Thus, the aim of this study was to determine the interstitial flow sensors and transducers for cells in 3-D ECM. We showed, for the first time, that HSPG-mediated activation of the FAK-ERK-c-Jun signaling cascade plays the major mechanotransduction role in interstitial flow-induced MMP-13 expression and SMC motility in a 3-D matrix.

HSPGs are present all over the cell surface, binding extracellular ligands and forming signaling complexes with receptors. The binding of cell surface HSPGs to ECM components can immobilize the proteoglycans, enabling HSPG core proteins to interact with the actin cytoskeleton [14, 17]. Therefore, cell surface HSPGs can act as both coreceptors and mechanosensors in most ECM and cytoskeleton interactions. In the absence of integrins, binding of HSPGs to ECM can support cell attachment and spreading through reorganization of the actin cytoskeleton and can also mediate solid strain-induced mechanotransduction [11, 14, 151]. It has been suggested that HSPGs play important roles in EC and tumor cell migration and/or invasion [24, 108]. In the present 3-D study, we showed that cleavage of HS-GAGs significantly reduced MMP-13 expression and cell motility in the no-flow control case and completely abolished flow-induced MMP-13 expression and cell motility (Fig. 4-1). This finding is opposite to that

of a previous 2-D study which showed that HSPG disruption enhanced EC migration by decreasing stress fibers and the size of focal adhesions, and increased EC migration speed under flow conditions [108], suggesting that cells in 3-D use distinct mechanotransduction and migration mechanisms compared with cells on 2-D. Differences in cell surface HSPGs organization and cell-matrix interactions may contribute to the distinct flow responses.

Appropriate cell-matrix adhesions are critical for cells and tissues to maintain function. Focal adhesions are macromolecular contact complexes between cells and ECM, which are composed of transmembrane receptors (such as HSPGs and integrins), structural molecules (such as actin, tensin, and α-actinin), and signaling molecules (such as FAK) [207]. FAK is a non-receptor protein tyrosine kinase (PTK) which is involved in integrin downstream signaling. Stimulation of a number of cell surface receptors, including integrins and G protein-coupled receptors, can cause FAK autophosphrylation at Tyr397. Phosphorylation at Tyr397 generates a binding site for Src family PTKs. Recruitment of Src family kinases induces FAK phosphorylation at Tyr925. Phosphorylation at Tyr925 creates a binding site for the growth factor receptor-bound-2 (Grb2) domain and triggers Ras/MAPK cascade activation [154]. FAK plays a central role in mediating cell migration. Silencing of FAK blocks agonist-induced upregulation of MMP, EC motility, and vascular tube formation [34]. FAK can mediate ERK-dependent eosinophil migration [26]. FAK also plays pivotal roles in tumor cell migration, and has been suggested as a target for cancer therapy [131]. Shear stress-induced ERK activation in ECs depends on FAK in 2-D [92]. Furthermore, centrifugal force can induce cytokine production through activation of FAK and ERK pathways [64]. In this study, we

showed that inhibition or knockdown of FAK suppressed interstitial flow-induced MMP-13 expression and cell motility (Fig. 4-2) due to inhibition of ERK1/2 phosphorylation (Fig. 4-3), suggesting that FAK is the cytoplasmic signal mediator of interstitial flow-induced ERK1/2 activation in cells in 3-D.

Studies have shown that in 2-D, shear stress can induce phosphorylation of FAK at Tyr397 in ECs [90, 92], probably mediated by HSPGs on the apical surface of the cells transmitting shear force through actin filaments to focal adhesions on the basal side, where adhesions were assembled for cell directional migration [108]. Other studies have shown that cyclic strain can induce FAK phosphorylation at both Tyr397 and Tyr925 [19, 25], however, strain-induced activation of the ERK pathway is mediated by activation of FAK at Tyr925 but not Tyr397 [25]. Interestingly, FAK phosphorylation at Tyr397 is not required for FAK phosphorylation at Tyr925 in response to strain [25]. The Tyr925 site is within the focal adhesion targeting (FAT) domain of FAK and binds to paxillin which connects to integrin [25, 106] or proteoglycan (such as syndecan-4) [37], while Tyr397 locates farther away from paxillin and normally is activated by integrin clustering [106] or syndecan-4 ligation to ECM [207]. Therefore, we speculate that phosphorylation at Tyr397 is mainly caused by the stimulation of signals (mechanical or chemical) that regulates cell-matrix adhesion formation and turnover, while activation at Tyr925 most likely directly relates to signal (mechanical or chemical) transmission from ECM to cytoskeleton that modulates intracellular signaling events.

When cells are embedded in 3-D, we do not know whether all of the HSPGs on the surfaces are bound to ECM ligands or only a fraction of them. This makes it difficult to evaluate whether all of the HSPGs on the cell surface are involved in flow-induced

mechanotransduction, or only those HSPGs bound to the ECM, or those HSPGs not bound to the ECM. However, after we cleaved HSPGs with heparinase, without exposing cells to flow, phosphorylation of both FAK Tyr397 and ERK1/2, MMP-13 expression, and cell motility were significantly attenuated compared to the case without enzyme treatment (see Figs. 4-1, 4-3, and 4-4). Reduced FAK phosphorylation at Tyr397 probably was due to reduced HSPG (syndecan-4) ligation to collagen fibers [207] and/or decreased cell-matrix adhesion assembly (integrin clustering) caused by disruption of cell adhesion to the ECM by heparinase (Fig. 4-5*A*), resulting in lower cell motility (Fig. 4-1*C*). Interestingly, interstitial flow significantly enhanced FAK phosphorylation at Tyr925, but not Tyr397 (Fig. 4-4), suggesting that flow-induced MMP expression and ERK1/2 activation are dependent on FAK phosphorylation at Tyr925. While disruption of HSPGs by heparinase abolished interstitial flow-induced Tyr925 phosphorylation and ERK activation (Fig. 4-4), and inhibition of heparan sulfate production by knockdown of NDST1 did not affect cell spreading (Fig. 4-5*B*), suggesting that mechanotransduction is mainly HSPG-dependent. Studies have shown that HSPG syndecan-4 can modulate FAK phosphorylation [207] and that syndecan-4-mediated cell adhesion to the ECM can be an alternative signaling pathway to the integrin-based signaling cascade [11]. Since interstitial flow-induced mechanotransduction is mediated by FAK, the HSPGs that function as flow sensors in 3-D might be directly located at the sites of cell adhesions to the ECM, where HSPGs (specially syndecan-4) are able to pass signals to FAK [37]. It is not known whether FAK can also link to HSPGs that are not bound to the ECM. When cells are embedded in 3-D, cell-matrix adhesions form all around the cell surface, however, the level of phosphorylated FAK at Tyr397 is lower than on 2-D [15, 32],

suggesting that integrin-based signaling may be less than it is on 2-D. Thus, it is possible that cell surface HSPG-mediated signaling (such as the flow-induced Tyr925 phosphorylation in this study) compensates the loss of function from integrins.

Integrins consist of αβ heterodimers with large extracellular and short cytoplasmic domains. The molecular weights of α and β subunits are 110-128 kDa and 81-87 kDa respectively [109]. To adhere to the ECM, integrin extracellular domains directly attach to the binding sites in the ECM and cytoplasmic domains interact with the cytoskeleton. The length of integrin-mediated adhesion (gap between cell membrane and ECM substrate surface) is around 15 nm [69, 213]. When exposed to solid strains, integrin-based adhesions can be easily deformed due to the relative motion between the ECM and cell membrane, resulting in activation of integrin signaling. Because of this, integrin-mediated focal adhesions have been widely suggested to be mechanosensors for solid strain [16]. Unlike integrins, HSPGs (especially syndecans) contain a relatively shorter transmembrane core protein with several long and flexible HS-GAG chains extended into the extracellular space [109]. Monomeric syndecan core proteins range in size from 20 to 45 kDa [122]. In mediating cell adhesion, syndecans form stable homodimers and bind to the heparin/heparan sulfate binding sites on the relatively rigid collagen fibers with the long and flexible heparan sulfate chains and the cytoplasmic domains on core proteins interact with the cytoskeleton [109].

The core proteins of HSPGs do not bind directly to the ECM. The binding is realized by the heparan sulfate chains. Noting that the pore size of collagen gels in vitro is around 0.5-1.0 μm [138, 204] and the space between two adjacent collagen fibers in the media of human aortas is greater than 50 nm (estimated from [40, 41]), there is plenty of space for

HS-GAG chains (diameter < 1 nm, [188, 205]) and even HSPG core proteins (5-10 nm, estimated from [150]) to be deformed.

The HS-GAG chains are rather long and flexible and may be deformed by shear flow. We therefore spectulate that HSPG-mediated attachments are more flexible and sensitive to flow than integrin-mediated adhesions. When exposed to interstitial flow, the flexible heparan sulfate chains can be deformed causing HSPG core protein deformation that is transmitted to the cytoskeleton, leading to activation of the FAK-mediated signaling cascade. When exposed to interstitial flow, on the other hand, there is not much relative motion between the cell membrane and the ECM. Since integrin-mediated bonding is rather rigid, the flow-induced displacement of integrin-mediated adhesion bonds should be much less than that of HSPG-mediated adhesions, implying less mechanotransduction through integrins than HSPGs. However, we observed that cells could not spread out in collagen I gels when β1 integrins were blocked by a specific antibody (see Fig. 6-2), suggesting that cell spreading through HSPG chain ligation alone is minimal and integrin-mediated adhesions are indispensable for spreading and maintaining cytoskeleton rigidity. This cytoskeletal organization is important for mechanosignal sensing and transduction [203]. Synthesizing all of the above information, we conclude that, by colocalizing within integrin-mediated cell-matrix adhesion complexes, HSPGs play a major role in sensing interstitial flow and mediating the mechanotransduction through FAK activation in 3-D.

Previously we showed that interstitial flow-enhanced MMP-13 expression and cell motility depends on activation of the ERK1/2-c-Jun signaling pathway [166]. In the present study, we further showed that in 3-D, cell surface HSPG-mediated FAK

phosphorylation is responsible for ERK1/2 activation, although which HSPG core proteins are responsible for force transmission to FAK remains to be determined. Taking these results together, we propose, for the first time, that HSPG-mediated FAK activation is essential for interstitial flow-induced mechanotransduction (shown in Fig. 4-6). Interstitial flow can, by a HSPG-mediated mechanotransduction mechanism, with the presence of integrin-mediated adhesions, induce FAK activation, which further activates the ERK1/2-c-Jun signaling cascade, resulting in an elevated MMP-13 expression and SMC motility. Once vascular injury occurs in vivo, this interstitial flow-induced mechanotransduction mechanism can be used by SMCs and fibroblasts to migrate into the intima where the cells contribute to neointima formation. This hypothesis is partly supported by a recent study that shows ERK1/2-dependent c-Jun activation regulates shear- and injury-induced MMP expression, vein graft stenosis, and intimal hyperplasia [119]. Our hypothesis should be examined by more sophisticated in vivo experiments.

In conclusion, for the first time, we reveal a HSPG-mediated mechanotransduction pathway by which cells sense interstitial flow in a 3-D ECM and activate FAK and its downstream effectors. This study may shed light on mechanotransduction mechanisms in 3-D interstitial flow-related models of capillary morphogenesis, tumor invasion, and cell differentiation, in addition to cell migration.

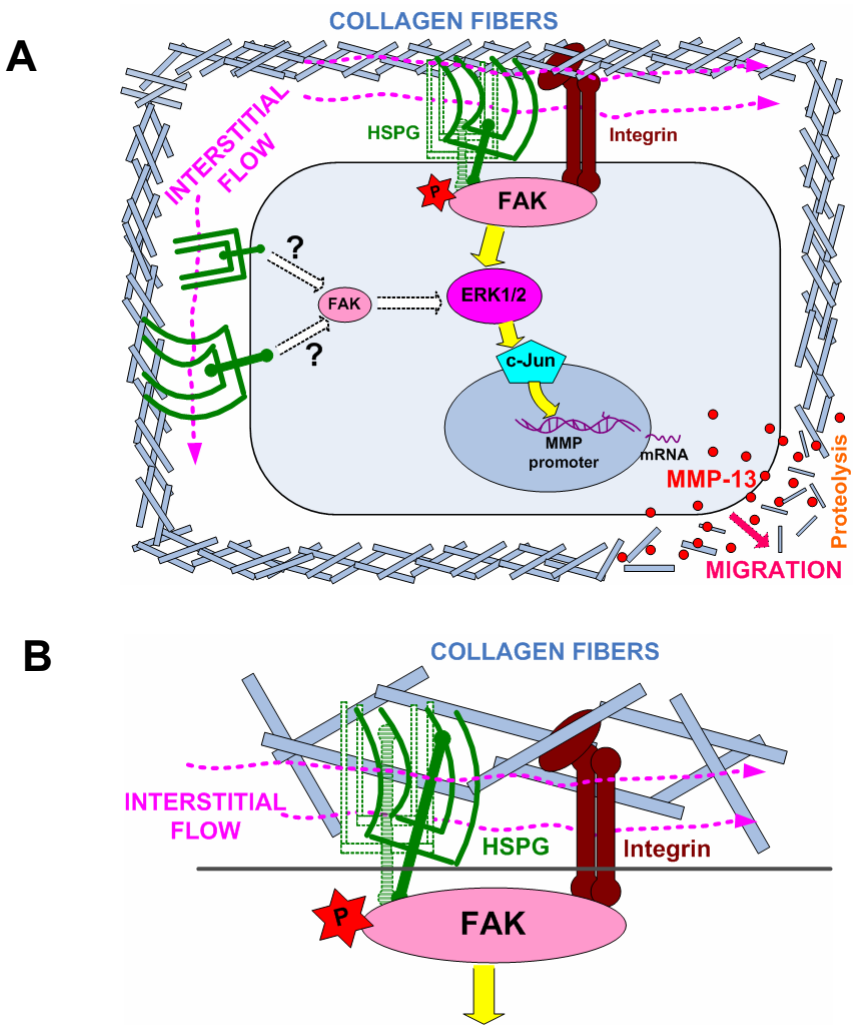

Figure 4-6. A proposed mechanotransduction mechanism for interstitial flow on cells via HSPG-mediated FAK activation in 3-D. Cell surface HSPGs colocalized with integrin-mediated cell-matrix adhesions are responsible for sensing flow. Interstitial flow stimulation causes HSPG deformation which activates FAK and induces ERK1/2-c-Jun signal cascade activation, leading to an increase in MMP-13 expression and cell motility. The core proteins of HSPGs do not bind to the ECM directly. The core proteins can be deformed in the large ECM spaces as the result of shear flow forces on the HS-GAG chains. Either core proteins do not extend into the ECM spaces (A) or they do (B). Integrin-mediated cell adhesions are important for mechanotransduction, but integrins do not play a major flow sensing role because integrin-collagen bonds are rather rigid and there is not much strain between cell membrane and the ECM. Some HSPGs may bind the ECM but do not cooperate with integrins (lower left in A), and other HSPGs may not bind the ECM (upper left in A). It is unlikely that these two types of HSPGs connect with FAK, and thus they do not play a major role in flow-induced mechanotransduction.

ACKNOWLEDGEMENTS

The authors acknowledge financial support from NIH NHLBI grants RO1 HL 57093 and RO1 HL 094889. We thank Henry Qazi and Dr. Limary Cancel for valuable discussions.

Chapter 5

Fluid Flow Shear Stress Modulation of Smooth Muscle Cell Marker Genes in 2-D and 3-D Depends on Mechanotransduction by Heparan Sulfate Proteoglycans and ERK1/2 Activation

5.1 Abstract

Vascular SMC phenotypic switching, migration, and proliferation play central roles in vascular repair, remodeling, and lesion formation in response to vascular injury. During vascular injury, SMCs may be directly exposed to altered luminal blood flow or transmural interstitial flow which may modulate SMC gene expression. In this study, we examined the influences of both laminar flow and interstitial flow on SMC marker gene expression in both SMCs and myofibroblasts (MFBs). Exposure to 8 dyn/cm^2 laminar flow shear stress (2-dimensional, 2-D) for 15 h significantly reduced expression of α-SMA, SM22, SM-MHC, smoothelin, and calponin. Cells suspended in collagen gels were exposed to interstitial flow shear stress (~0.05 dyn/cm^2, 3-D), and after 6 h of exposure, expression of SM-MHC, smoothelin, and calponin were significantly reduced, while expression of α-SMA and SM22 were markedly enhanced. PD98059 and heparinase III significantly blocked the effects of laminar flow on gene expression. PD98059 and heparinase also dramatically attenuated the effects of interstitial flow on SM-MHC, smoothelin, and calponin, but enhanced flow-induced expression of α-SMA and SM22. SMCs and MFBs have similar responses to fluid flow. Silencing ERK1/2 completely blocked both laminar flow and interstitial flow effects on SMC marker gene expression. Western blotting showed that both fluid flow types induced ERK1/2 activation which was inhibited by cleavage of heparan sulfate proteoglycans (HSPGs). Our results suggest that HSPG-mediated ERK1/2 activation is an important mechanotransduction pathway modulating SMC marker gene expression when SMC and MFB are exposed to flow.

Keywords: interstitial flow mechanotransduction, smooth muscle cell, myofibroblast, differentiation, phenotype, heparan sulfate proteoglycan, ERK1/2

5.2 Introduction

The major functions of vascular SMCs are to maintain and regulate blood vessel tone, blood pressure, and blood flow distribution. SMCs retain remarkable plasticity and can undergo phenotypic modulation between contractile state and synthetic state in response to alterations in local environmental cues [125, 140]. The phenotype of SMC is a continuum, not a discrete set of phenotypic states. The terms "contractile" and "synthetic" refer to relative positions along this continuum, indicating cell functions and marker expression that are associated with either a contractile or a synthetic function [178]. In response to injury, SMCs can dramatically increase proliferation, motility, and secretion capacity, and play critical roles in vascular repair and remodeling [125, 140]. However, if the responses are excessive, SMCs may also contribute to vascular lesion formation by migrating from the media into the intima under abnormal environmental conditions [125, 167]. Besides SMCs, adventitial fibroblasts (FBs) and their activated counterpart myofibroblasts (MFBs) are also involved in intimal lesion formation [152, 163].

SMCs and FBs/MFBs normally reside in a 3-dimensional (3-D) environment composed of extracellular matrix (ECM) components mainly collagen I and III. Most in vitro studies have investigated responses of SMCs to chemical or mechanical stimuli by culturing them on 2-D substrates. However, it has been shown that 3-D culture systems are a better representation of the in vivo environment than conventional 2-D systems [140, 178]. In a 3-D collagen gel, SMCs are less proliferative and more quiescent compared with SMCs cultured in 2-D on a collagen matrix [93, 204].

The contractile SMCs in the media are exposed to a physiological interstitial flow driven by the transmural pressure drop [184, 201]. However, during vascular injury,

SMCs may be exposed to elevated interstitial flow after damage to the vascular endothelium [167], and the superficial layer of SMCs may even be directly exposed to luminal blood flow where the intima is denuded. During the early stages of injury, shear stresses (luminal blood flow and transmural interstitial flow) on SMCs are elevated, and have been hypothesized to contribute to neointima formation [50, 143, 167]. In some 2-D studies, fluid shear stress has reduced cell proliferation [180, 196] and induced apoptosis [46]. Other 2-D studies, however, have shown that shear stress can reduce expression of SMC marker genes [9, 202] and promote SMC proliferation [9, 57]. In addition, SMC and MFB have different migratory response to laminar flow (2-D) and interstitial flow (3-D) [50, 51, 167].

To date, no studies have shown whether interstitial flow affects SMC and MFB phenotype in 3-D, and the mechanisms by which SMC and MFB sense fluid flow shear stress and modulate their phenotype remain unclear. Given that switching SMC from contractile to synthetic phenotype will increase cell proliferation and motility, we therefore postulate that there can be some shared mechanisms between cell phenotypic modulation and migration. We have already shown that ERK1/2 signaling plays a key role in interstitial flow-induced SMC motility [166]. In this study, we investigated how laminar flow and interstitial flow affect the expression of SMC marker genes and the potential role of ERK1/2. In addition, it has been suggested that cell surface glycocalyx heparan sulfate proteoglycans (HSPGs) are shear stress sensors for endothelial cells (ECs) and SMCs in 2-D [4, 47]. There has been no study to show whether or not the glycocalyx functions as an intersitial flow sensor in 3-D. Therefore we also examined the role of HSPGs in mechanotransduction in both 2-D and 3-D.

5.3 Materials and methods

5.3.1 2-D and 3-D cell culture. Rat aortic SMCs and MFBs were obtained and cultured as previously described [50]. For 2-D experiments: SMCs and MFBs were seeded on fibronectin coated (30 ug/insert) 6-well format cell culture inserts with 0.4 μm pore size (1.5×10^5 cells/insert) and cultured for 24 h with 2 ml of growth medium in the inserts and 3 ml of growth medium in the companion well. For 3-D experiments: SMCs and MFBs were suspended in rat tail collagen I (BD Science) gels and plated in 6-well cell culture inserts with 8 μm pore size (cell density: $2.5x10^5$ cells/ml; final gel concentration: 4 mg/ml); cells were then cultured for 24 h with 2 ml growth medium in the bottom well [166].

5.3.2 Fluid flow shear stress experiment. 2-D laminar flow: a rotating disk shear rod device was used [51], and the average shear stress of 8 dyn/cm^2 was applied to cells cultured in the inserts for 15 h. 3-D interstitial flow: cells in 3-D collagen gels were subjected to interstitial flow as previously described [167] for 6 h, which was driven by a 1 cmH_2O pressure differential (~0.05 dyn/cm^2).

5.3.3 ERK1/2 inhibition and HSPG cleavage. PD98059 (Calbiochem) was used for ERK1/2 inhibition and heparinase III (IBEX Technologies, Montreal, Canada) was used for HSPG cleavage. After 24 h spreading in 2-D or 3-D, cells were pre-incubated with 10 μM of PD98059 or 6.7 IU/L of heparinase III for 3 h in growth medium. Cells were then subjected to flow experiments as described above.

5.3.4 RNA interference. To silence ERK1/2, two ERK1 short hairpin (sh) RNAs and two ERK2 shRNAs which were subcloned into pSUPER vector (kindly donated by Dr. Michal Hetman) and were co-transfected into SMCs. The ERK1/2 shRNA target sequences were:

shERK1-1, GACCGGATGTTAACCTTTA;

shERK1-2, ATGTCATAGGCATCCGAGA;

shERK2-1, GTACAGAGCTCCAGAAATT;

and shERK2-2, AGTTCGAGTTGCTATCAAG [74, 166].

The transfections were conducted using Lipofectamine™ LTX and PLUS™ reagents (Invitrogen).

5.3.5 RNA extraction and gene expression analysis. 2-D experiments: 0.5 ml of TRIzol® LS Reagent (Invitrogen) was added to cell culture inserts and incubated for 5 min with gentle pipette mixing; samples were then transferred to microcentrifuge tubes for further RNA extraction. 3-D experiments: Cells in collagen gels were directly lysed by TRIzol and the insoluble materials were removed by centrifugation at 12,000 x g for 10 minutes at 4°C. Chloroform was added for phase separation followed by RNA isolation using the Purelink RNA Mini Kit (Invitrogen). RNA samples were then converted to cDNA by reverse transcription (RT). For analyzing gene expression, quantitative polymerase chain reaction (qPCR) was performed using the following protocol as previously described [166]: GAPDH served as an internal control; reactions were performed in 25 µl reaction mixture volumes containing ABsolute Blue QPCR SYBR Green ROX Mix (Thermo Scientific), cDNA and specific primer pairs; real-time

PCR protocol was set to 15 minutes at 95°C followed by 45 cycles of 30 seconds at 95°C, 30 seconds at 55°C, and 30 seconds at 72°C; the fluorescent data were collected at 80°C; the dissociation curve analysis was used to assess the specificity of product amplification. Primer sequences are listed in Table 5-1.

Table 5-1. Primer sequences for rat SMC marker genes

Gene	Forward sequence (5'-3')	Reverse sequence (5'-3')	GenBank Locus	Reference
α-SMA	GATCACCATCGGGAATGAACGC	CTTAGAAGCATTTGCGGTGGAC	NM_031004.2	[129]
SM22	TGTTCCAGACTGTTGACCTC	GTGATACCTCAAAGCTGTCC	NM_031549.2	[194]
SM-MHC	AAGCAGCTCAAGAGGCAG	AAGGAACAAATGAAGCCTCGTT	NM_001170600.1	[98]
SMTN	TCGGAGTGCTGGTGAATAC	CCCTGTTTCTCTTCCTCTGG	NM_001013049.2	[141]
Calponin	ACAAAAGGAAACAAAGTCAAT	GGGCAGCCCATACACCGTCAT	NM_031747.1	[121]
GAPDH	TCTTCACCACCATGGAGAA	ACTGTGGTCATGAGCCCTT	NM_017008	[167]

5.3.6 Immunofluorescence staining. To assess the cleavage of heparan sulfate glycosaminoglycans (HS-GAG) by heparinase III, primary antibody HepSS-1 (US Biological) and secondary antibody Alexa Fluor 350 goat anti-mouse IgM (Invitrogen) were used to stain HS-GAGs. Briefly, SMCs were seeded in plate wells for 2 days and then treated with 6.7 IU/L heparinase III for 1 hour, followed by fixation with 4% paraformaldehyde and blocking with 4% BSA in PBS. Then cells were incubated with primary antibody HepSS-1 (1:200 dilution in PBS with 4% BSA) for 2 hours and secondary antibody anti-mouse IgM (1:100 dilution) for 2 hours at room temperature. Finally, cells were mounted with mounting medium containing propidium iodide (PI) (Vector Laboratories) and covered by coverslips.

5.3.7 Protein extraction and Western blotting. Protein extraction from 2-D: briefly, after washing cells in inserts with ice-cold PBS, 1X lysis buffer was added and cell scrapers were used to remove cells from inserts; samples were sonicated for 30 s and rocked for 15 min; supernatants were collected and cell pellets were discarded by centrifugation. Protein extraction from 3-D collagen gels was described previously in detail [166]: briefly, 2X lysis buffer (with a supplement of 2X protease inhibitor cocktail and 2X phosphatase inhibitor cocktail , 2 mM activated Na_3VO_4, and 2 mM PMSF) was added immediately to the gels followed by sonication for 45 s on ice; lysates were centrifuged at 12,000 g for 1 hour at 4°C, and then the supernatants were collected and the remaining gel pellets were discarded; the supernatants were concentrated using Centrifugal Filter Units (Millipore); the protein samples were boiled for 5 minutes after mixing with 4X sample buffer and then subjected to SDS-PAGE; proteins were transferred to PVDF membranes and incubated with specific primary antibodies (ERK1/2 and phospho-ERK1/2, from cell signaling), followed by incubation with an ECL horseradish peroxidase (HRP)-linked anti-rabbit IgG antibody (Amersham, GE Healthcare); the proteins on PVDF membranes were then detected using Immobilon Western Chemiluminescent HRP Substrate (Millipore) and the ChemiDoc XRS system with the Quantity One software (Bio-Rad); some membranes were stripped using Restore™ Plus Western Blot Stripping Buffer (Thermo Scientific Pierce) for a subsequent detection.

Data Analysis. Results are presented as mean ± SEM. Data sets were analyzed for statistical significance using a Student's t-test with a two-tailed distribution, and $P < 0.05$ was considered statistically significant.

5.4 Results

5.4.1 2-D Laminar flow reduces SMC marker gene expression in SMCs and MFBs

To investigate the effect of laminar shear stress (2-D) on SMC marker expression in SMCs and MFBs, cells were cultured in inserts (6-well format with 0.4 μm pore size; 1.5×10^5 cells/filter) for 24 h. Cells were then exposed to 8 dyn/cm^2 (average) shear stress applied by a rotating disk shear rod for 15 h. The mRNA levels were measured by RT-qPCR, and are shown in Fig. 5-1. Exposure to 8 dyn/cm^2 of laminar shear stress significantly reduced α-smooth muscle actin (α-SMA), smooth muscle protein 22 (SM22 also called as transgelin), smooth muscle myosin heavy chain (SM-MHC), smoothelin (SMTN), and calponin gene expression in both SMCs (Fig. 5-1A) and MFBs (Fig. 5-1B).

5.4.2 Interstitial flow attenuates SM-MHC, SMTN, and calponin expression but enhances α-SMA and SM22 expression in 3-D

To evaluate the influence of interstitial flow on SMC marker expression, SMCs and MFBs were suspended in collagen I gels and plated in cell culture inserts (6-well format with 8 μm pore size; gel concentration: 4 mg/ml; cell density: 2.5×10^5 cells/ml). After spreading in gels for 24 h, cells were then subjected to interstitial flow driven by 1 cmH_2O pressure differential (~0.05 dyn/cm^2) for 6 h. The expression of SMC markers was assessed by RT-qPCR and shown in Fig. 5-2. Just like laminar flow in 2-D, interstitial flow in 3-D also significantly reduced SMC marker SM-MHC, SMTN, and calponin gene expression in both SMCs and MFBs (Fig. 5-2). However, unlike laminar flow, interstitial flow markedly promoted α-SMA and SM22 expression in both cell types.

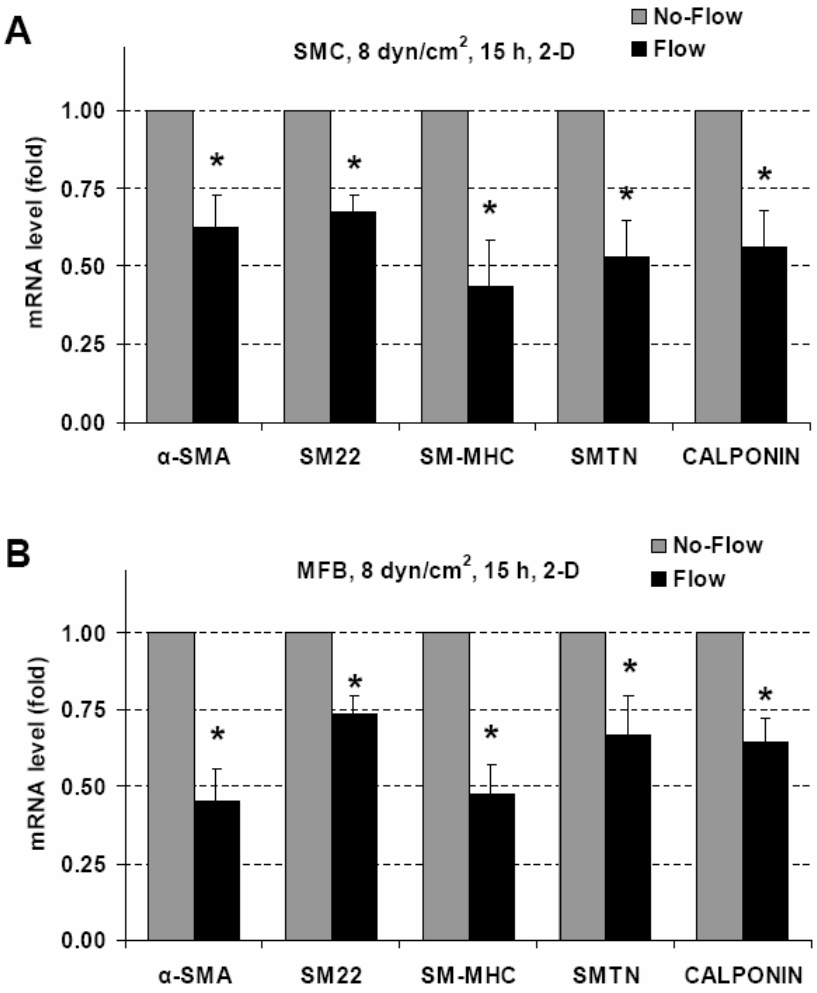

Figure 5-1. Laminar flow down-regulates expression of SMC marker genes in both SMCs (A) and MFBs (B) in 2-D. SMCs and MFBs were exposed to 8 dyn/cm^2 laminar shear stress for 15 h. Expression of SMC marker genes (α-SMA, SM22, SM-MHC, smoothelin (SMTN), and calponin) were analyzed by RT-qPCR. The gene expression was normalized to its companion No-Flow control case. All the data are presented as mean ± SEM. * $P<0.05$ vs corresponding No-Flow control; n=4-6.

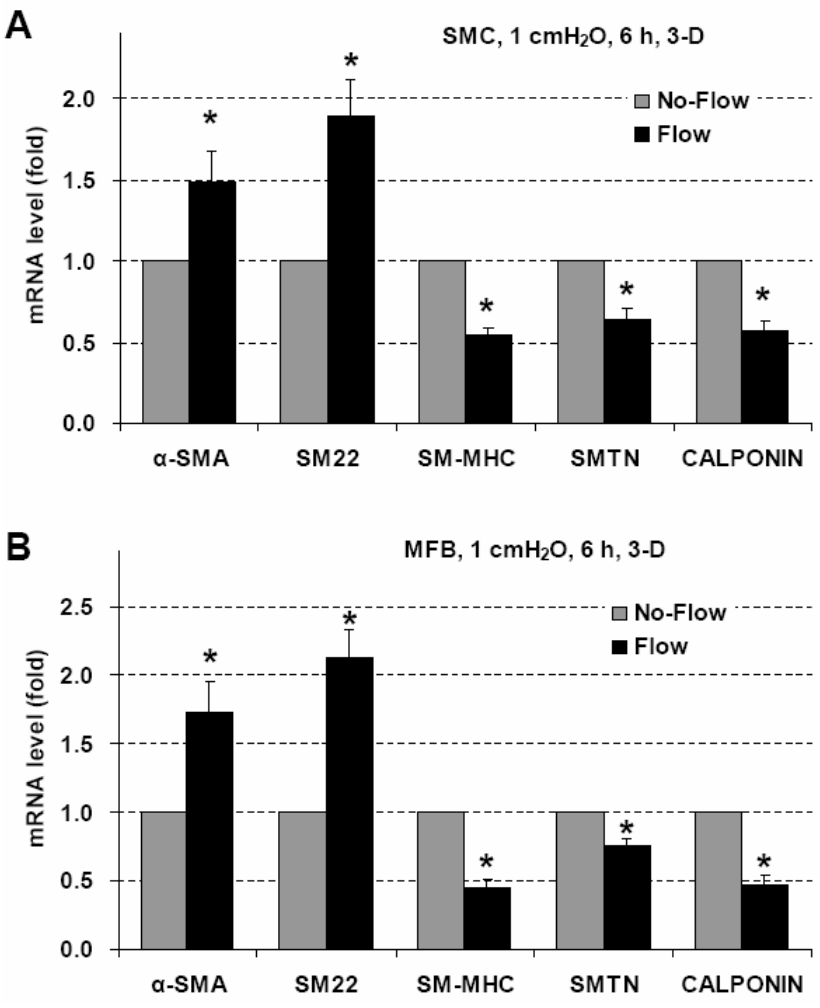

Figure 5-2. Interstitial flow attenuates gene expression of SM-MHC, smoothelin, and calponin, but promotes expression of α-SMA and SM22 in both SMCs (A) and MFBs (B) in 3-D. SMCs and MFBs were exposed to interstitial fluid flow driven by 1 cmH_2O pressure differential (~0.05 dyn/cm^2 shear stress [167]) for 6 h. Gene expression was analyzed by RT-qPCR and normalized to its own No-Flow control case. All the data are presented as mean ± SEM. * $P<0.05$ vs corresponding No-Flow control; n=4-6.

5.4.3 Both PD98059 and heparinase III block laminar flow-induced reduction in SMC marker expression 2-D

To investigate the underlying mechanisms by which laminar flow attenuated SMC marker expression, PD98059 was used to inhibit ERK1/2 activation and heparinase III was used to cleave cell surface heparan sulfate glycosaminoglycans (HS GAGs) from

heparan sulfate proteoglycans (HSPGs). Cells were pre-incubated with 10 μM of PD98059 or 6.7 IU/L of heparinase for 3 h followed by exposure to laminar flow for 15 h. Flow medium contained 10 μM of PD98059 for ERK inhibition experiments, and flow medium contained 1.0 IU/L heparinase for HSPG cleavage experiments. RT-qPCR results are shown in Fig. 5-3. After treatment with PD98059 or heparinase, reduction in gene expression in SMCs and MFBs caused by laminar flow were significantly blocked in both cell types. These data suggest that ERK1/2 MAPK and cell surface HSPGs played important roles in laminar flow-induced decreases in SMC marker expression.

5.4.4 Both PD98059 and heparinase III block interstitial flow-induced reduction in SM-MHC, SMTN, and calponin expression, but enhance flow-induced α-SMA or SM22 expression in 3-D

To examine whether the effects of interstitial flow on SMC marker gene expression were also related to ERK1/2 and HSPGs, cells were pre-incubated with 10 μM of PD98059 or 6.7 IU/L of heparinase for 3 h followed by exposure to interstitial flow for 6 h. Flow medium contained 10 μM of PD98059 for ERK inhibition experiments, and flow medium contained 1 IU/L heparinase for HSPG cleavage experiments. As shown in Fig. 4, inhibition of ERK1/2 or cleavage of HSPGs eliminated interstitial flow-induced decreases in SM-MHC, SMTN, and calponin expression in both SMCs and MFBs. However, either inhibition of ERK1/2 or removal of HSPGs did not attenuate interstitial flow-induced α-SMA and SM22 expression. Instead, expression of α-SMA and SM22 was further enhanced. These data suggest that ERK1/2 and HSPGs were involved in interstitial flow-mediated SMC marker expression.

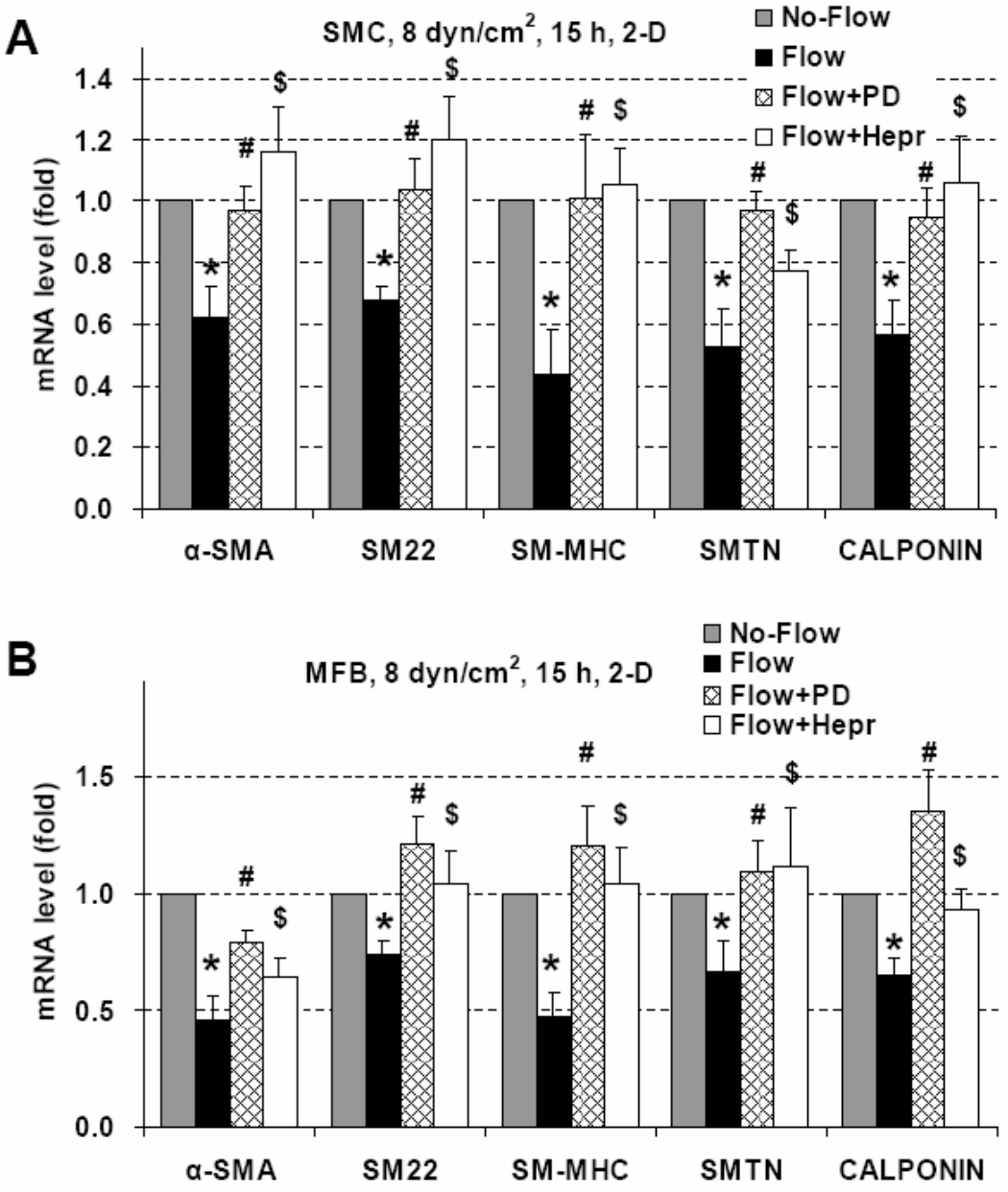

Figure 5-3. PD98059 and heparinase III reverse laminar flow-induced reductions in expression of SMC marker genes in both SMCs (A) and MFBs (B) in 2-D. The cells were pretreated with PD98059 (PD) or heparinase III (Hepr) for 3 h, and then exposed to 8 dyn/cm^2 laminar shear stress for 15 h. Gene expression was analyzed by RT-qPCR and normalized to its own Flow without PD or Hepr treated case. All the data are presented as mean ± SEM. * P<0.05 vs corresponding No-Flow control; #P<0.05 vs corresponding Flow case; $ P<0.05 vs corresponding Flow case; n=4-5.

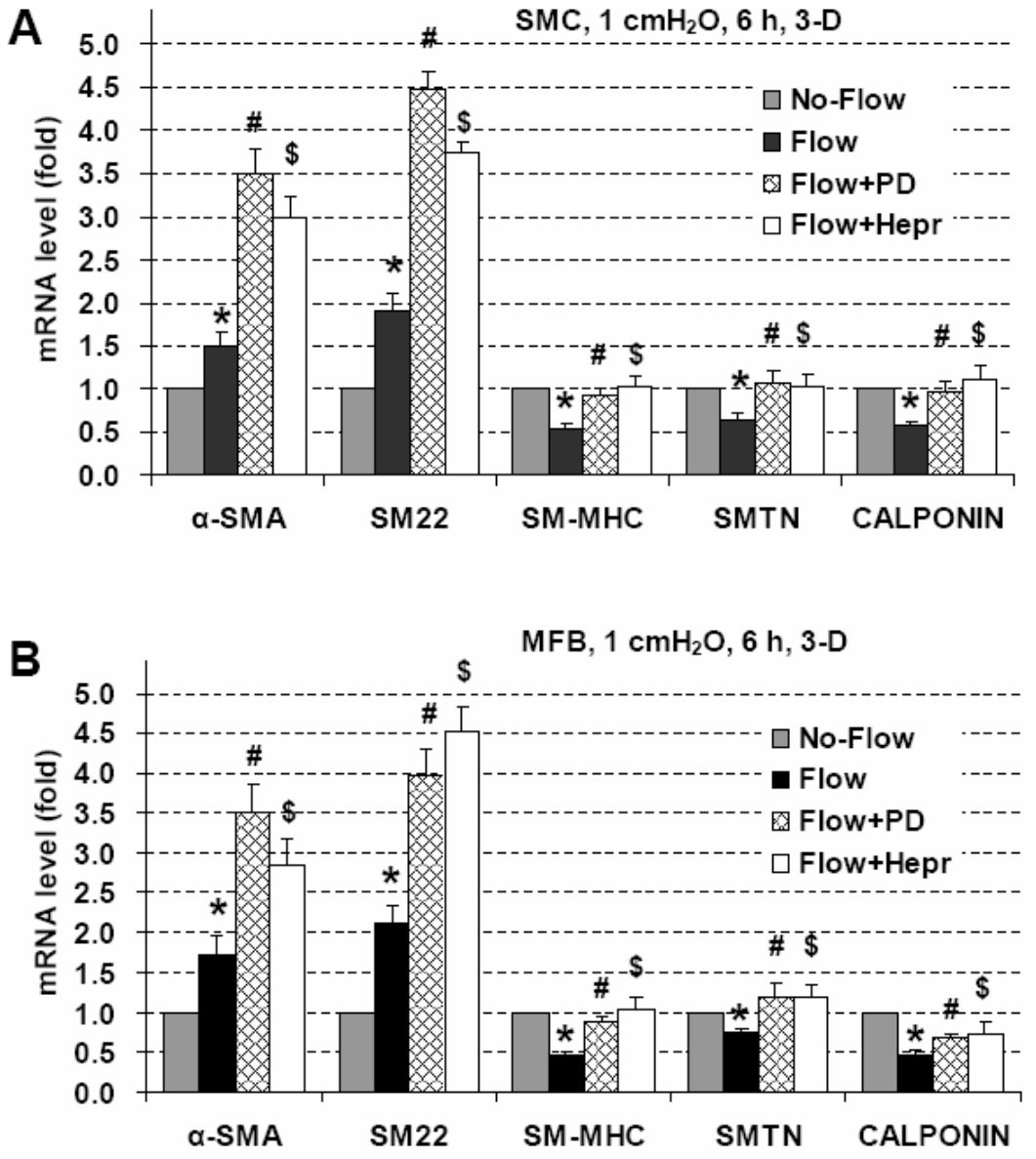

Figure 5-4. PD98059 and heparinase III reverse interstitial flow-induced reductions in SM-MHC, smoothelin, and calponin expression, but further enhance interstitial flow-induced α-SMA and SM22 expression in both SMCs (A) and MFBs (B) in 3-D. The cells were pretreated with PD98059 (PD) or heparinase III (Hepr) for 3 h, and then exposed to interstitial flow (1 cmH_2O) for 6 h. Gene expression was analyzed by RT-qPCR and normalized to its own Flow without PD or Hepr treated case. All the data are presented as mean ± SEM. * $P<0.05$ vs corresponding No-Flow control; #$P<0.05$ vs corresponding Flow case; \$ $P<0.05$ vs corresponding Flow case; n=4-5.

5.4.5 Knocking down ERK1/2 attenuates effects of both laminar flow and interstitial flow on SMC marker expression

Since PD98059 may have cellular effects other than inhibition of ERK1/2, shRNA specific to ERK1/2 was used. Due to the high similarity in SMC marker gene expression between SMCs and MFBs when they were exposed to either laminar flow or interstitial flow, ERK1/2 gene knockdown was only performed in SMCs. Knockdown of ERK1/2 significantly reversed laminar flow-induced down-regulation of SMC marker gene expression in 2-D (Fig. 5-5A). Silencing of ERK1/2 also significantly inhibited interstitial flow effects on SMC marker expression in 3-D: reduced expression of SM-MHC, SMTN, and calponin were significantly reversed with ERK1/2 knockdown; while increased expression of both α-SMA and SM22 were markedly inhibited (Fig. 5-5B). These results suggest that regulation of SMC marker gene expression by fluid flow is dependent on the ERK1/2 signaling pathway.

However, interstitial flow-induced upregulation of α-SMA and SM22 was not attenuated by PD98059 or heparinase in 3-D (Fig. 5-4) but blocked by ERK1/2 knockdown, indicating that besides affecting ERK1/2, PD98059 and removal of HSPGs also had effects on other cellular signal pathways which increased expression of α-SMA and SM22.

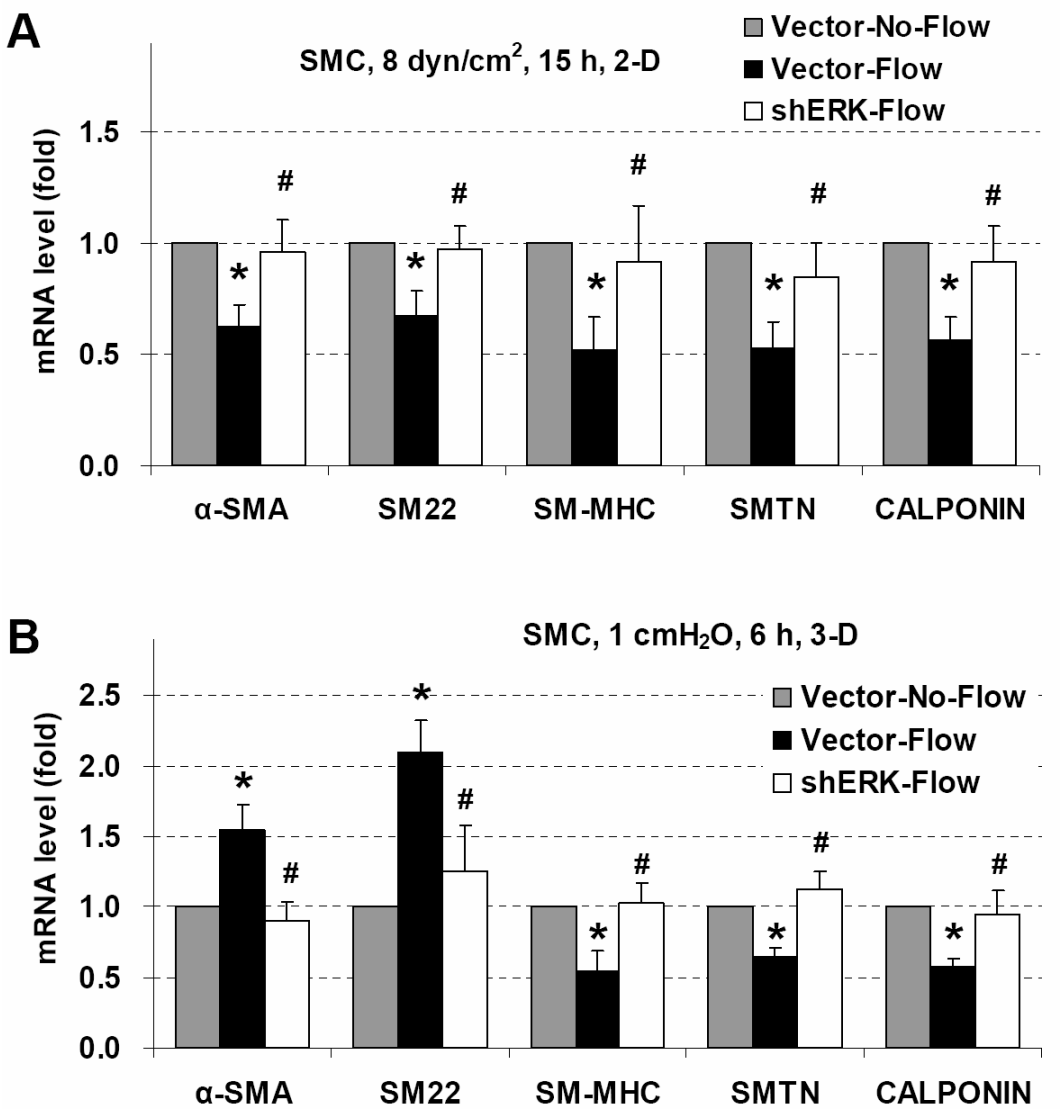

Figure 5-5. Knockdown of ERK1/2 reverses effects of both laminar flow (A) and interstitial flow (B) on expression of SMC marker genes. The cells were transfected with ERK1/2 shRNAs or shRNA vectors. All the data were presented as mean ± SEM. * P<0.05 vs corresponding No-Flow control; #P<0.05 vs corresponding Vector-Flow case; n=4.

5.4.6 Heparan sulfate proteoglycans are mechanosensors for fluid flow-induced and ERK-mediated cell phenotypic modulation

The efficiency of heparinase III in cleaving cell surface HSPG GAGs was evaluated by immunostaining. Fig. 5-6 shows that SMC surfaces contain abundant HSPGs and that using heparinase III can substantially cleave cell surface HS GAGs. Removal of HSPGs reversed most of the flow effects, suggesting that HSPGs might be involved in ERK1/2 activation. To examine whether the fluid flow affected ERK1/2 activation and the role of cell surface HSPGs, Western blotting was used to determine ERK1/2 phosphorylation. The results are shown in Fig. 5-7. Both laminar flow (2-D) and interstitial flow (3-D) dramatically induced ERK1/2 phosphorylation, and PD98059 significantly inhibited fluid flow-induced ERK1/2 activation. After removal of HSPGs, however, activation of ERK1/2 induced by fluid flow was significantly attenuated as well. These results suggest that ERK1/2 activation was mediated by cell surface HSPGs. Although PD98059 and heparinase had different effects on the expression of some SMC marker genes in 3-D (Fig. 5-4) compared with 2-D (Fig. 5-3), knockdown of ERK1/2 abolished flow effects in both 2-D and 3-D (Fig. 5-5). In addition, both PD98059 and removal of HS-GAGs suppressed flow induced ERK1/2 activation in 2-D and 3-D (Fig. 5-7), suggesting that besides displaying some other cellular effects, HSPGs are essential in mediating flow induced ERK1/2 activation. Therefore, we conclude that the effects of laminar flow and interstitial flow on expression of SMC marker genes depend on ERK1/2 activation via a mechanotransduction mechanism mediated by HSPGs.

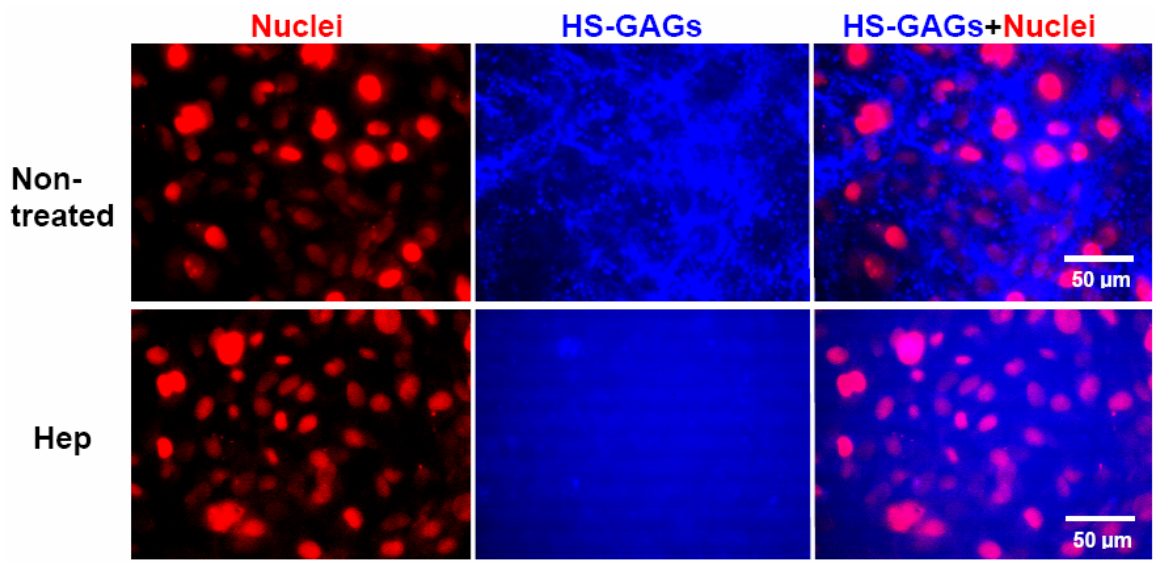

Figure 5-6. Cleavage of heparan sulfate glycosaminglycans (HS-GAGs) by heparinase III. SMCs were grown on the plate for 2 days, and then incubated with 6.7 IU/L heparinase III (Hep) for 1 h followed by immunostaining for HS-GAGs. The surfaces of SMCs present abundant HS-GAGs (blue), which was successfully cleaved by heparinase III. Cell nuclei were stained by propidium iodide shown in red.

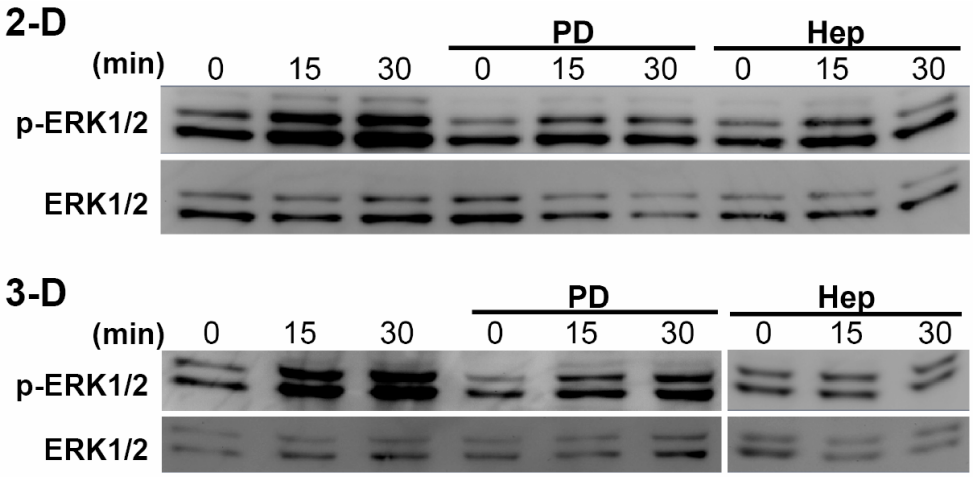

Figure 5-7. PD98059 and heparinase III suppress both laminar flow and interstitial flow-induced ERK1/2 activation. Cells in 2-D or 3-D were pretreated with ERK1/2 inhibitor PD98059 (PD) or heparinase III (Hep) and then exposed to laminar flow or interstitial flow for 0 to 30 min. Cells were lysed and proteins were extracted for Western blotting. Gel panels were representative Western blots from three independent experiments, where similar results were found.

5.5 Discussion

In the present study, we demonstrated that laminar flow and interstitial flow significantly affect expression of SMC marker genes (α-SMA, SM22, SM-MHC, smoothelin, and calponin): laminar flow reduces expression of all five SMC marker genes in SMCs and MFBs on a 2-D substrate; interstitial flow attenuates gene expression of SM-MHC, smoothelin, and calponin, but enhances expression for α-SMA and SM22. The influences of laminar flow and interstitial flow on expression of SMC marker genes are mediated by activation of ERK1/2 MAPK. In addition, cell surface glycocalyx HSPGs play a major role in mechanotransduction of fluid flow-induced ERK1/2 activation. SMCs and MFBs have the same pattern of phenotypic modulation in response to fluid flow.

Vascular SMC dedifferentiation, migration, proliferation, and protein secretion play central roles in both vascular remodeling and vascular lesion formation [125]. Phenotypic modulation (switching) is one of the key events for SMCs to be engaged in vascular repair, remodeling, and disease. In response to vascular injury, contractile SMCs are capable of transiently modulating their phenotype to a highly synthetic state with increasing ability to migrate into wound sites. In vivo, SMCs continuously encounter mechanical stimuli that play important roles in governing cell function and phenotype [178]. Surgical intervention such as balloon angioplasty or stent implantation can denude endothelial cells and damage the intima, leaving SMCs directly exposed to luminal blood flow shear stress. In hypertension, SMCs and FBs/MFBs are not only exposed to tensile stress (stretch), but also exposed to elevated interstitial flow driven by augmented transmural pressure [166, 167]. Therefore, in the early stages of vascular injury, shear

stress induced either by luminal blood flow or by transmural flow may alter the phenotype of SMCs and FBs/MFBs. In the present in vitro study, we show that both laminar flow (2-D) and interstitial flow (3-D) affect expression of SMC marker genes in SMCs and MFBs.

Other studies have shown that FBs can differentiate into MFBs followed by further differentiation into SMC like cells [152]. Vascular SMCs, FBs, and MFBs therefore share common characteristics and functions. α-SMA is widely expressed in both SMCs and MFBs and regulates cell contractility when it is incorporated within actin filaments to form stress fibers. SM22 is highly expressed in SMCs, FBs, and MFBs [84]. SM22 colocalizes with α-SMA and may play a role in actin filament remodeling , but it is not essential for SM development and its function still remains unknown [85]. Calponin is also expressed in SMCs and FBs/MFBs. SM-MHC and smoothelin are better SMC markers, and smoothelin is only expressed in mature and fully differentiated SMCs [197]. Although it has been suggested that some SMC marker proteins such as SM-MHC and smoothelin are not expressed in MFBs or immature SMCs [152], we still detected the expression of these genes by RT-qPCR.

Laminar flow reduces expression of all studied SMC marker genes, consistent with several studies [9, 202]. Other 2-D studies, however, have shown that shear stress can reduce cell proliferation [180, 196] and induce apoptosis [46]. The controversy about different effects of shear stress on SMC proliferation probably is due to the level of shear stress and the patterns of shear stress that were applied to cells, and also the species and phenotypic states of SMCs that were used. In this study, 3-D interstitial flow attenuates expression of SM-MHC, smoothelin, and calponin genes, but enhances expression for α-

SMA and SM22. The disparity between 2-D and 3-D suggests the microenvironmental cues that cells receive are important for phenotype modulation. In conventional 2-D cultures, decreased cell proliferation is generally associated with the contractile state. In 3-D, SMC proliferation and cytokine secretion are reduced, suggesting that cells are more contractile compared with 2-D. However, α-SMA expression is also reduced in 3-D [93, 178]. This seeming contradiction may well explain the differences in gene expression between cells in 2-D and 3-D in response to flow. SMCs cultured in a 3-D collagen matrix express diminished α-SMA, and exhibit less phosphorylation of focal adhesion kinase [32, 93] and less spreading. It has been suggested that incorporation of α-SMA into stress fibers directly correlates with the strength of cell-matrix adhesion and is crucial for cell contractility and cell spreading [63]. In our study, when exposed to interstitial flow, cell proliferation and spreading are increased (data not shown), and therefore more cell-matrix adhesions are required, which could induce α-SMA and SM22 expression to promote stress fiber formation and cell-matrix adhesion formation. This is consistent with another study that has shown that interstitial flow can increase α-SMA expression and promote FB differentiation into MFB and their proliferation in 3-D collagen gels [117]. It has been suggested that laminar flow shear stress can induce SMC to decrease expression of SMC markers and increase expression of endothelial cell (EC) markers which transdifferetiate SMCs into ECs [202]. Because a 3-D environment is suitable for SMC and MFB physiology and a 2-D system is more suitable for ECs to perform their function, another explanation for our observations is that reduction in SMC marker expression on 2-D substrates turns SMCs/MFBs into more EC like cells; while

interstitial flow only modulates SMC/MFB in 3-D from a more contractile phenotype to a more synthetic state.

α-SMA and SM22 are not SMC specific markers and are present in many cell types. Their roles generally are related to stress fiber formation and cell contractility, which may regulate cell motility. This hypothesis may well explain the difference in flow-induced migration between 2-D and 3-D that we have observed before: in 2-D studies, laminar flow inhibits SMC and MFB migration [50, 51], while in 3-D, interstitial flow-induced upregulation of α-SMA and SM22 may enhance SMC and MFB motility [167].

In 3-D, unlike SM-MHC, smoothelin and calponin, α-SMA and SM22 were upregulated by interstitial flow and that could not be reversed by PD98059 or heparinase; instead, their expression was further enhanced (Fig. 5-4). However, the interstitial flow-upregulated expression could be abolished by knockdown of ERK1/2 (Fig. 5-5), indicating that besides affecting ERK1/2, PD98059 and removal of HSPGs by heparinase also affected other cellular signaling pathways which induced expression of α-SMA and SM22. We observed that treatment with PD98059 and heparinase caused cells to contract slightly in 3-D gels (data not shown). The chemical inhibitor PD98059 displays toxicity to cells, and HSPGs (such as syndecans) can mediate cell attachment to ECM [75]. Thus, cleavage of HSPG GAGs by heparinase reduces cell attachment to ECM. Also note that proliferation of SMC/MFB in 3-D was reduced compared with 2-D. Treatment with PD98059 and heparinase further reduced cell proliferation and decreased cell attachment to ECM in 3-D. When exposed to interstitial flow, cells tended to be more proliferative, spreading out to regain attachments to ECM, which likely required an increase in

expression of α-SMA and SM22. The distinct effects of PD98059 and heparinase on cells in 2-D and 3-D suggest that cell physiology is different between 2-D and 3-D.

MAPKs are important mediators which regulate a variety of cellular processes, including gene expression, proliferation, survival, apoptosis, migration, and differentiation [146]. In cardiovascular health and disease, it has been shown that the ERK1/2 MAPK pathway plays an important role [113]. Increased ERK1/2 activation contributed to augmented vascular SMC proliferation and neointima formation with aging in a rabbit study [52]. The rapid activation of ERK1/2 after balloon injury of the rat carotid artery may be associated with vascular SMC migration and proliferation in vivo [67, 79, 81]. The evidence from in vitro studies has also shown that ERK1/2 activation plays a crucial role in cardiovascular cell proliferation and cell migration [9, 166]. The increase in SMC proliferation and migration is associated with a phenotypic switching from the contractile state to the synthetic state, which is regulated by sustained phosphorylation of ERK1/2 [148]. Our results suggest that besides the role in regulating cell proliferation as reported in the literature, ERK1/2 also plays a central role in both laminar flow and interstitial flow-induced cell phenotype modulation.

In 2-D studies, it has been suggested that the cell surface glycocalyx is responsible for sensing fluid flow shear stress on vascular ECs and SMCs [4, 47, 188]. In 3-D, HSPGs, which are present all over the cell surface, bind extracellular ligands and form signaling complexes with receptors. Binding of cell surface HSPGs to ECM components can immobilize the proteoglycans, enabling HSPG core proteins to interact with the actin cytoskeleton [14]. Therefore, the cell surface HSPGs can act as both coreceptors and mechanosensors in ECM-cytoskeleton interactions. In the present study, we demonstrated

that cell surface HSPGs are flow sensors by which cells can sense laminar flow and interstitial flow stimuli and then undergo phenotypic modulation through ERK1/2 activation.

We have shown previously that 1-6 h of interstitial flow driven by 1 cmH_2O (~0.05 dyn/cm^2) can dramatically enhance cell motility and MMP expression [167]. In the present study, we again show that this short exposure to interstitial flow also has great impact on the expression of cell phenotypic genes. The unique 3-D cell-matrix structure may play the key role. In the more physiological 3-D system, the cells exhibit matrix adhesions all over their surface, and 3-D cell-matrix interactions enhance cell biological activity [32]. Thus the mechanosignal of interstitial flow on the glycocalyx can be significantly amplified by interactions between the cell cytoskeleton and matrix through cell-matrix adhesions.

In summary, we have shown, for the first time, that both laminar flow and interstitial flow are capable of modulating SMC and MFB phenotype into a more synthetic state via HSPG-mediated ERK1/2 activation - a mechanotransduction mechanism. Fluid flow-induced phenotype modulations are somewhat different in 2-D and 3-D: fluid flow down-regulates both α-SMA and SM22 in 2-D, but promotes their expression for cell spreading in 3-D; however, fluid flow reduces expression of more specific SMC markers (such as SM-MHC and smoothelin) in both 2-D and 3-D. On the other hand, interstitial flow can induce FB differentiation into MFB in 3-D [117]. Together with the fact that laminar flow inhibits SMC and MFB migration in 2-D [50, 51] and interstitial flow enhances SMC, FB, and MFB motility in 3-D [166, 167], our study may indicate that during vascular injury, in response to the alterations of interstitial flow in the local environment, SMCs in the

media can shift their phenotype from a contractile state to a more synthetic state and FBs in the adventitia can modulate their phenotype from a quiescent state to an activated state and differentiate into MFBs. Under the sustained stimulation of interstitial flow, the synthetic SMCs and activated FB and MFB gain higher motility and migrate into the intima or wound sites. While for the superficial layer of SMCs in the injury regions, the luminal blood flow directly promotes their dedifferentiation into a more proliferative state and inhibits their migration. SMCs and MFBs in the intima or injury sites can proliferate, secrete ECM proteins, and increase stress fiber contractility by expressing α-SMA under interstitial flow, which therefore contribute to wound closure and healing, vascular remodeling, or vascular lesion formation. This study also suggests that ERK1/2 and HSPGs may be the potential targets for regulation of cell phenotype and inhibition of vascular lesion formation.

ACKNOWLEDGEMENTS

The authors acknowledge financial support from NIH NHLBI grants RO1 HL 57093 and RO1 HL 094889. We thank Giya Abraham for the hard work and great contribution. We thank Sandra V. Lopez-Quintero and Henry Qazi for great help on the shear appartus setup and Hui Wang for RNA extraction.

Chapter 6

General Conclusions and Future Directions

6.1 General conclusions

In vivo, when the endothelium of an artery is injured, the interstitial fluid flow on vascular SMC and fibroblast is elevated due to the reduced flow resistance. During the damage period, SMCs and fibroblasts will be exposed to elevated interstitial flow. After damage of the intima, SMCs in the superficial layer may be directly exposed to luminal blood flow. In response to vascular injury, contractile SMCs in the media and quiescent fibroblasts in the adventitia of vessel wall can rapidly modulate their phenotypic states, increase proliferation rates, synthetic capacities, and motilities. The activated cells then migrate into injury sites (such as in the intima) where they contribute to vascular repair, remodeling, or vascular lesion formation depending on the characteristics of microenvironmental cues. Therefore, our hypothesis has been that the alterations of fluid flow during vascular injury modulate SMC and fibroblast phenotype and motility. Through a series of novel experimental methods, we have generated several primary findings that are summarized below.

6.1.1 Summary on the effects of flow on MMP expression and cell motility

1) Interstitial flow can promote vascular SMC and fibroblast motility in 3-D collagen I gels by upregulation of MMP-13 expression.
2) However, if the interstitial flow is too high, it will suppress cell motility by enhancing TIMP-1 expression and inducing cell apoptosis, although MMP-13 gene expression still remains elevated. High intensity flow driven by high pressure may also cause collagen gel compaction which can impair cell function.

3) Flow-induced upregulation of MMP-13 is mediated by activation of ERK1/2 MAPK and a downstream transcription factor (activating protein-1, AP-1) (c-Jun). Activation of AP-1 increases DNA binding activity, which promotes MMP-13 expression.

4) Interstitial flow also induces activation of p38 MAPK and AP-1 transcription factor c-Fos, however, both p38 MAPK and c-Fos play minor roles in flow-induced MMP-13 expression.

5) By chemical inhibitor and gene silencing, we have shown that focal adhesion kinase (FAK) is the mechanosensitive kinase that mediates interstitial flow-induced ERK1/2 activation.

6) We further found that cell surface heparan sulfate proteoglycan (HSPG)-mediated activation of focal adhesion kinase (FAK) plays an essential role in promoting MMP-13 expression in 3-D.

6.1.2 Summary on flow modulation of SMC and MFB phenotype

In the cell differentiation study, we have shown that laminar flow shear stress (8 dyn/cm^2 for 15 h) in 2-D attenuates gene expression of SMC marker α-SMA, SM22, SM-MHC, smoothelin, and calponin. In 3-D, interstitial flow (driven by 1 cmH_2O, ~0.05 dyn/cm^2 for 6 h) also downregulates gene expression of SM-MHC, smoothelin, and calponin, but enhances expression of α-SMA and SM22 genes. We further have shown that HSPG-mediated ERK1/2 activation plays a mechanotransduction role in modulating SMC marker gene expression induced by laminar flow (2-D) and interstitial flow (3-D).

A recent study has shown that ERK1/2- and c-Jun N-terminal kinase (JNK)-dependent c-Jun activation regulates shear- and injury-inducible early growth response-1 (egr-1) expression, vein graft stenosis after autologous end-to-side transplantation in rabbits, and intimal hyperplasia in human saphenous veins [119]. The activation of c-Jun is independent of p38 MAPK. The activation of c-Jun stimulates SMC proliferation and MMP expression. DNAzyme targeting c-Jun attenuates SMC growth, wound repair, and reduces intimal thickening [119]. These data demonstrate that strategies targeting c-Jun may be useful for the prevention of vein graft stenosis. In our in vitro 3-D study, we also demonstrated that interstitial flow induces MMP expression and promotes SMC migration via activation of an ERK1/2-dependent and c-Jun-mediated mechanism and this process is independent of p38 MAPK. The mechanism by which SMCs sense the interstitial flow signal in our in vitro 3-D study is very similar to the in vivo study. Therefore, our findings suggest that interstitial fluid flow is involved in regulating vascular cell phenotype and motility in vivo and that contribute to vascular remodeling and lesion formation. This has been the first study to investigate the effects of interstitial fluid flow on vascular wall cell migration, and also the first study to explore the underlying mechanotransduction mechanism induced by interstitial flow in 3-D [165-168]. Our primary observations support the hypothesis that we have made.

6.1.3 Conclusions

Our study may indicate that during vascular injury, in response to the alterations of interstitial flow in the local environment, SMCs in the media can shift their phenotype from a contractile state to a more synthetic state and FBs in the adventitia can modulate

their phenotype from a quiescent state to an activated state and differentiate into MFBs. Under the sustained stimulation of interstitial flow, the synthetic SMCs and activated FB and MFB gain higher motility and migrate into the intima or wound sites. While for the superficial layer of SMCs in the injury regions, the luminal blood flow directly promotes their dedifferentiation into a more proliferative state and inhibits their migration. SMCs and MFBs in the intima or injury sites can proliferate, secrete ECM proteins, and increase stress fiber contractility by expressing α-SMA under interstitial flow, which therefore contribute to wound closure and healing, vascular remodeling, or vascular lesion formation. The contribution of interstitial flow to vascular lesion formation after vascular injury has been summarized in Fig. 6-1.

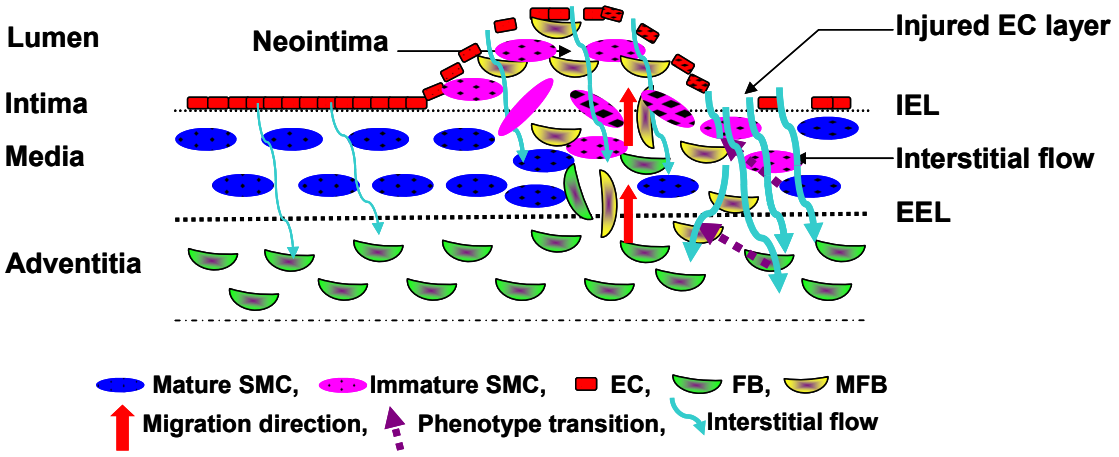

Figure 6-1. A model for contribution of interstitial flow to vascular lesion formation after vascular injury. In response to elevated interstitial flow after EC damage, adventitial FBs modulate their phenotype from a quiescent state to a more activated state and differentiate into MFB; medial SMCs switch their phenotype from a contractile state to a more synthetic and proliferative state. Under interstitial flow, the activated cells then gain higher motility and migrate into the intima or injury sites where they proliferate, secrete abundant new ECM, and eventually contribute to vascular lesion formation. For simplicity, the involvements of inflammatory cells and cytokines and many other factors in vascular lesion formation are not shown in this cartoon. SMC: smooth muscle cell; EC: endothelial cell; FB: fibroblast; MFB: myofibroblast; IEL: internal elastic lamina; EEL: external elastic lamina.

6.1.4 Clinical significance and potential implications

All in all, we have explored the novel concept that interstitial flow affects vascular cells in the interstitium by modulating cell phenotype and motility. Therefore, interstitial flow-mediated events coupled to inflammatory responses present at sites of vascular injury would collectively contribute to vascular repair and lesion formation. The effects of interstitial flow on vascular remodeling and lesion formation have important clinical implications. In the regions of vascular injury, such as at the site of vessel repair by angioplasty and at the anastomoses of a vascular graft with the native artery, if we can control transmural interstitial flow, modify the surface glycocalyx, target signaling molecules (FAK, ERK1/2, and c-Jun), or modulate MMP expression, we will be able to promote wound healing or limit vascular lesion formation.

This study also sheds light on putative fluid flow-induced mechanotransduction mechanisms involving HSPGs and FAK in other fields including tumor cell invasion and stem cell differentiation. It has been suggested that both FAK and HSPGs play critical roles in regulating tumor initiation, progression, and metastasis and also stem cell differentiation [17, 58, 78, 120, 153]. FAK is a key regulator of cardiogenesis in mouse embryonic stem (ES) cells and FAK signaling within embryoid bodies can direct stem cell lineage commitment [58]. HS-GAGs, composed of N- and O-sulfated polysaccharide chains covalently bound to core proteins ubiquitously expressed on the cell surface and in the extracellular matrix (ECM), play a critical role in regulating tumor initiation, progression, and metastasis [95, 153]. Treatment of primary tumors with heparinase III inhibits FAK and ERK1/2 activation [96]. HS-GAGs, depending on their location (anchored at the cell surface or soluble as free GAGs), the signaling molecules they

associate with, and their fine structures, can either promote or inhibit the tumorigenic process [95]. HSPGs are also present throughout embryonic development and could potentially modulate signals maintaining pluripotency and initiating differentiation [83]. HSPGs are critical coreceptors for signals inducing embryonic stem (ES) cell differentiation. Genetic targeting of *N*-deacetylase/*N*-sulfotransferase 1 and 2 (NDST1 and NDST2), two enzymes required for N-sulfation of proteoglycans, blocks ESC differentiation [83]. Differentiation of embryonic stem cells into endothelial cells in an in vitro embryoid body is paralleled by an amplification of HS-GAG sulfation, which correlates with the levels of the enzyme NDST1 [60]. Knockdown of NDST1 by shRNA or modification of HS-GAGs in ES cells with heparinases or sodium chlorate inhibits differentiation of embryonic stem cells into endothelial cells [60]. Tumor cells and ES cells in vivo are exposed to interstitial fluid flow, and therefore the effects of interstitial flow and the potential roles of FAK and HSPGs should be determined.

6.2 Future directions

Vascular remodeling and lesion formation in vivo is very complicated, involving not only elevated flow, but also inflammatory cells and other factors. However, using a 3-D collagen I gel system as a model of physiological interstitial flow, we, for the first time, have been able to observe the fascinating and potentially significant influences of interstitial flow on cell migration and differentiation. Our results suggest a possible mechanism whereby vessel injury enhances interstitial flow that activates vascular SMC and FB and thus further contributes to vascular remodeling or lesion formation.

6.2.1 Future considerations for improvement of 3-D interstitial flow system

Since beside type I collagen, there are many other components (such as elastin, proteoglycans, collagen II, III, IV, and etc) in the blood vessel wall extracellular matrix in vivo, our 3-D collagen I only model is somewhat limited compared with real vessel wall matrix. This component-limited matrix may affect different MMP expression and activation. Therefore, our hypotheses should be tested in the following modified models:

1) A more sophisticated 3-D system that uses mixed matrix to better mimic vessel wall ECM.
2) A system using cocultured endothelial cells (ECs) on the surface of 3-D matrix with SMC inside will better recapitulate in vivo conditioins. This system will allow us to create vascular injury on ECs and then test our hypothesis.
3) The hypotheses should also be examined in a model more relevant to the in vivo situation such as an intact perfused vessel or in animal models.

6.2.2 Future considerations for the study of mechanotranduction

In the mechanotransduction study, we have shown that cell surface heparan sulfate proteoglycans (HSPGs) are responsible for mediating interstitial flow-induced activation of FAK and the downstream ERK1/2 signal cascade. To date there is only one study that has shown that the HSPG, syndecan-4, can bind to paxillin which is the substrate for FAK. Syndecan-4 is the only HSPG that colocalizes with focal adhesions. Syndecan-4 itself can mediate cell-matrix adhesion. However, whether other cell surface HSPGs that are not bound to ECM can mediate FAK/ERK activation remains unknown and needs to be clarified. Future work also should examine whether syndecan-4 is the major HSPG that mediates interstitial flow mechanotransduction.

In addition, the integrin-mediated focal adhesions are well-known mechanosensitive pathways, and FAK is one of the important components of focal adhesion. HSPG syndecan-4-mediated adhesions are parallel to integrin-based adhesions. However, HSPG syndecans must work synergistically with integrins to regulate cell adhesion. If one either blocks integrin or removes syndecan-4, the adhesions via the companion molecule (syndecan-4 or integrin) will be disrupted, which makes it almost impossible to dissect these two signaling paths from each other. For example, Fig. 6-2 shows that blockage of integrin β1 completely inhibits SMC spreading in collagen I gels. The difference in morphology also affects cell physiology as MMP-13 expression is dramatically altered (see Table 6-1). Therefore using an integrin blocking antibody is not a feasible method. Thus the the degree of involvement of integrin-based adhesion remains to be investigated.

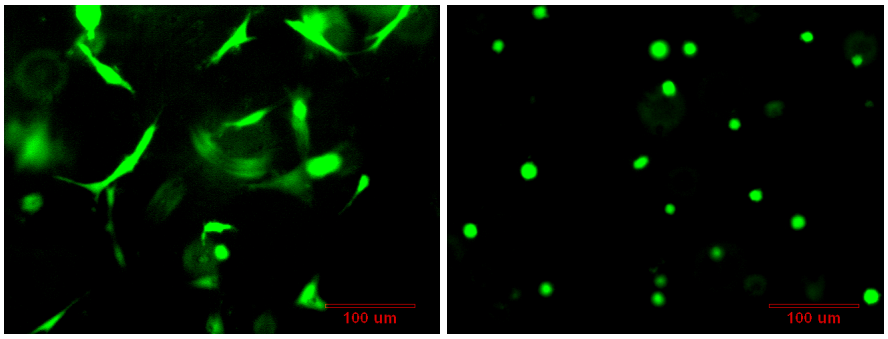

Figure 6-2. Integrin β1 antibody blocks cell spreading in 3-D collagen I gels. A) Non-treated cells. B) Integrin β1 antibody treated cells. Cells were pretreated with 40 μg/ml of integrin β1 antibody (NA/LE Hamster Anti-Rat CD29, clone Ha2/5, BD Pharmingen, #555002) for 15 min to neutralize integrin β1. Cells were then suspended in collagen I gel, 4 mg/ml, $0.25x10^6$ cells/ml and plated into 6-well inserts, and then incubated for 24 h followed by Calcein AM staining. The growth medium in companion wells contains 20 μg/ml Ha2/5 antibody.

Table 6-1. Effect of interstitial flow on MMP-13 gene expression in cells with or without treatment by integrin β1 antibody.

	No-Flow	Flow	No-Flow + Ab	Flow + Ab
MMP-13	1	3.2* ± 0.7	46.3* ± 4.6	38.2*,# ± 7.7

Cells were treated as described in the caption of Fig. 6-2, and then exposed to interstitial flow for 6 h. Total RNA was extracted by adding Trizol directly to collagen gels, and purified using Qiagen RNeasy mini-kit. * $P < 0.05$ vs No-Flow; # $P > 0.05$ vs No-Flow+Ab.

6.2.3 Future directions in the flow-induced differentiation study

We have demonstrated that laminar flow shear stress in 2-D attenuates gene expression of SMC markers α-SMA, SM22, SM-MHC, smoothelin, and calponin. In 3-D, interstitial flow also downregulates gene expression of SM-MHC, smoothelin, and calponin, but enhances expression of α-SMA and SM22 genes. PD98059 and heparinase III also enhances α-SMA and SM22 gene expression. We have postulated that the 3-D environment may affect cell phenotype which may cause these different responses. However, the exact mechanism should be further addressed.

We further showed that HSPG-mediated ERK1/2 activation plays a mechanotransduction role in modulating SMC marker gene expression induced by laminar flow (2-D) and interstitial flow (3-D). Based on the studies of interstitial flow-induced MMP expression and cell migration, the activation of FAK seems important for regulating the ERK1/2-c-Jun signaling cascade. Therefore, whether FAK and c-Jun also are involved in flow induced SMC phenotype modulation needs to be examined. However, the difficulty of this problem is that either a chemical inhibitor or siRNA by themselves may affect cell phenotype, which may block or amplify the flow effects. Therefore, more sophisticated methods will be required to study the effect of fluid flow on cell phenotype.

The multifunctional cytokine, transforming growth factor-β1 (TGF-β1) is a well-characterized mediator that regulates vascular cell growth and differentiation and is involved in the induction of intimal thickening [2, 73, 125]. Therefore, the possible involvement of TGF-β1 in this study should be assessed.

REFERENCES

1. **Abedi H and Zachary I.** Signalling mechanisms in the regulation of vascular cell migration. *Cardiovasc Res* 30: 544-556, 1995.

2. **Agrotis A, Kalinina N, and Bobik A.** Transforming growth factor-beta, cell signaling and cardiovascular disorders. *Curr Vasc Pharmacol* 3: 55-61, 2005.

3. **Aimes RT and Quigley JP.** Matrix metalloproteinase-2 is an interstitial collagenase. Inhibitor-free enzyme catalyzes the cleavage of collagen fibrils and soluble native type I collagen generating the specific 3/4- and 1/4-length fragments. *J Biol Chem* 270: 5872-5876, 1995.

4. **Ainslie KM, Garanich JS, Dull RO, and Tarbell JM.** Vascular smooth muscle cell glycocalyx influences shear stress-mediated contractile response. *J Appl Physiol* 98: 242-249, 2005.

5. **Alberts B, Johnson A, Lewis J, Raff M, Roberts K, and Walter P.** Molecular Biology of the Cell (4th ed.): Garland Science, 2002.

6. **Ando J and Yamamoto K.** Vascular mechanobiology: endothelial cell responses to fluid shear stress. *Circ J* 73: 1983-1992, 2009.

7. **Aoyagi M, Yamamoto M, Azuma H, Nagashima G, Niimi Y, Tamaki M, Hirakawa K, and Yamamoto K.** Immunolocalization of matrix metalloproteinases in rabbit carotid arteries after balloon denudation. *Histochem Cell Biol* 109: 97-102, 1998.

8. **Arnoczky SP, Tian T, Lavagnino M, and Gardner K.** Ex vivo static tensile loading inhibits MMP-1 expression in rat tail tendon cells through a cytoskeletally based mechanotransduction mechanism. *J Orthop Res* 22: 328-333, 2004.

9. **Asada H, Paszkowiak J, Teso D, Alvi K, Thorisson A, Frattini JC, Kudo FA, Sumpio BE, and Dardik A.** Sustained orbital shear stress stimulates smooth muscle cell proliferation via the extracellular signal-regulated protein kinase 1/2 pathway. *J Vasc Surg* 42: 772-780, 2005.

10. **Baldwin AL, Wilson LM, Gradus-Pizlo I, Wilensky R, and March K.** Effect of atherosclerosis on transmural convection an arterial ultrastructure. Implications for local intravascular drug delivery. *Arterioscler Thromb Vasc Biol* 17: 3365-3375, 1997.

11. **Bellin RM, Kubicek JD, Frigault MJ, Kamien AJ, Steward RL, Jr., Barnes HM, Digiacomo MB, Duncan LJ, Edgerly CK, Morse EM, Park CY, Fredberg JJ, Cheng CM, and LeDuc PR.** Defining the role of syndecan-4 in mechanotransduction using surface-modification approaches. *Proc Natl Acad Sci U S A* 106: 22102-22107, 2009.

12. **Bendeck MP, Irvin C, Reidy M, Smith L, Mulholland D, Horton M, and Giachelli CM.** Smooth muscle cell matrix metalloproteinase production is stimulated via alpha(v)beta(3) integrin. *Arterioscler Thromb Vasc Biol* 20: 1467-1472, 2000.

13. **Bendeck MP, Zempo N, Clowes AW, Galardy RE, and Reidy MA.** Smooth muscle cell migration and matrix metalloproteinase expression after arterial injury in the rat. *Circ Res* 75: 539-545, 1994.

14. **Bernfield M, Gotte M, Park PW, Reizes O, Fitzgerald ML, Lincecum J, and Zako M.** Functions of cell surface heparan sulfate proteoglycans. *Annu Rev Biochem* 68: 729-777, 1999.

15. **Berrier AL and Yamada KM.** Cell-matrix adhesion. *J Cell Physiol* 213: 565-573, 2007.

16. **Bershadsky A, Kozlov M, and Geiger B.** Adhesion-mediated mechanosensitivity: a time to experiment, and a time to theorize. *Curr Opin Cell Biol* 18: 472-481, 2006.

17. **Bishop JR, Schuksz M, and Esko JD.** Heparan sulphate proteoglycans fine-tune mammalian physiology. *Nature* 446: 1030-1037, 2007.

18. **Borden P and Heller RA.** Transcriptional control of matrix metalloproteinases and the tissue inhibitors of matrix metalloproteinases. *Crit Rev Eukaryot Gene Expr* 7: 159-178, 1997.

19. **Boutahar N, Guignandon A, Vico L, and Lafage-Proust MH.** Mechanical strain on osteoblasts activates autophosphorylation of focal adhesion kinase and proline-rich tyrosine kinase 2 tyrosine sites involved in ERK activation. *J Biol Chem* 279: 30588-30599, 2004.

20. **Brauchle M, Gluck D, Di Padova F, Han J, and Gram H.** Independent role of p38 and ERK1/2 mitogen-activated kinases in the upregulation of matrix metalloproteinase-1. *Exp Cell Res* 258: 135-144, 2000.

21. **Brooke BS, Karnik SK, and Li DY.** Extracellular matrix in vascular morphogenesis and disease: structure versus signal. *Trends Cell Biol* 13: 51-56, 2003.

22. **Carragher NO and Frame MC.** Focal adhesion and actin dynamics: a place where kinases and proteases meet to promote invasion. *Trends Cell Biol* 14: 241-249, 2004.

23. **Chang SF, Chang CA, Lee DY, Lee PL, Yeh YM, Yeh CR, Cheng CK, Chien S, and Chiu JJ.** Tumor cell cycle arrest induced by shear stress: Roles of integrins and Smad. *Proc Natl Acad Sci U S A* 105: 3927-3932, 2008.

24. **Charni F, Friand V, Haddad O, Hlawaty H, Martin L, Vassy R, Oudar O, Gattegno L, Charnaux N, and Sutton A.** Syndecan-1 and syndecan-4 are involved

in RANTES/CCL5-induced migration and invasion of human hepatoma cells. *Biochim Biophys Acta* 1790: 1314-1326, 2009.

25. **Chaturvedi LS, Gayer CP, Marsh HM, and Basson MD.** Repetitive deformation activates Src-independent FAK-dependent ERK motogenic signals in human Caco-2 intestinal epithelial cells. *Am J Physiol Cell Physiol* 294: C1350-1361, 2008.

26. **Cheung PF, Wong CK, Ip WK, and Lam CW.** FAK-mediated activation of ERK for eosinophil migration: a novel mechanism for infection-induced allergic inflammation. *Int Immunol* 20: 353-363, 2008.

27. **Chomczynski P and Mackey K.** Short technical reports. Modification of the TRI reagent procedure for isolation of RNA from polysaccharide- and proteoglycan-rich sources. *Biotechniques* 19: 942-945, 1995.

28. **Cortez DM, Feldman MD, Mummidi S, Valente AJ, Steffensen B, Vincenti M, Barnes JL, and Chandrasekar B.** IL-17 stimulates MMP-1 expression in primary human cardiac fibroblasts via p38 MAPK- and ERK1/2-dependent C/EBP-beta , NF-kappaB, and AP-1 activation. *Am J Physiol Heart Circ Physiol* 293: H3356-3365, 2007.

29. **Cospedal R, Abedi H, and Zachary I.** Platelet-derived growth factor-BB (PDGF-BB) regulation of migration and focal adhesion kinase phosphorylation in rabbit aortic vascular smooth muscle cells: roles of phosphatidylinositol 3-kinase and mitogen-activated protein kinases. *Cardiovasc Res* 41: 708-721, 1999.

30. **Cospedal R, Lobo M, and Zachary I.** Differential regulation of extracellular signal-regulated protein kinases (ERKs) 1 and 2 by cAMP and dissociation of ERK inhibition from anti-mitogenic effects in rabbit vascular smooth muscle cells. *Biochem J* 342 (Pt 2): 407-414, 1999.

31. **Couchman JR, Chen L, and Woods A.** Syndecans and cell adhesion. *Int Rev Cytol* 207: 113-150, 2001.

32. **Cukierman E, Pankov R, Stevens DR, and Yamada KM.** Taking cell-matrix adhesions to the third dimension. *Science* 294: 1708-1712, 2001.

33. **Daniels JT, Limb GA, Saarialho-Kere U, Murphy G, and Khaw PT.** Human corneal epithelial cells require MMP-1 for HGF-mediated migration on collagen I. *Invest Ophthalmol Vis Sci* 44: 1048-1055, 2003.

34. **Das A, Yaqoob U, Mehta D, and Shah VH.** FXR promotes endothelial cell motility through coordinated regulation of FAK and MMP-9. *Arterioscler Thromb Vasc Biol* 29: 562-570, 2009.

35. **Davies SP, Reddy H, Caivano M, and Cohen P.** Specificity and mechanism of action of some commonly used protein kinase inhibitors. *Biochem J* 351: 95-105, 2000.

36. **Delaney J, Chiarello R, Villar D, Kandalam U, Castejon AM, and Clark MA.** Regulation of c-fos, c-jun and c-myc gene expression by angiotensin II in primary cultured rat astrocytes: role of ERK1/2 MAP kinases. *Neurochem Res* 33: 545-550, 2008.

37. **Denhez F, Wilcox-Adelman SA, Baciu PC, Saoncella S, Lee S, French B, Neveu W, and Goetinck PF.** Syndesmos, a syndecan-4 cytoplasmic domain interactor, binds to the focal adhesion adaptor proteins paxillin and Hic-5. *J Biol Chem* 277: 12270-12274, 2002.

38. **Di Girolamo N, Coroneo MT, and Wakefield D.** UVB-elicited induction of MMP-1 expression in human ocular surface epithelial cells is mediated through the ERK1/2 MAPK-dependent pathway. *Invest Ophthalmol Vis Sci* 44: 4705-4714, 2003.

39. **Diamond SL.** Engineering design of optimal strategies for blood clot dissolution. *Annu Rev Biomed Eng* 1: 427-462, 1999.

40. **Dingemans KP, Jansen N, and Becker AE.** Ultrastructure of the normal human aortic media. *Virchows Arch A Pathol Anat Histol* 392: 199-216, 1981.

41. **Dingemans KP, Teeling P, Lagendijk JH, and Becker AE.** Extracellular matrix of the human aortic media: an ultrastructural histochemical and immunohistochemical study of the adult aortic media. *Anat Rec* 258: 1-14, 2000.

42. **Dzau VJ, Braun-Dullaeus RC, and Sedding DG.** Vascular proliferation and atherosclerosis: new perspectives and therapeutic strategies. *Nat Med* 8: 1249-1256, 2002.

43. **Endo H, Utani A, and Shinkai H.** Activation of p38 MAPK suppresses matrix metalloproteinase-1 gene expression induced by platelet-derived growth factor. *Arch Dermatol Res* 294: 552-558, 2003.

44. **Esko JD and Selleck SB.** Order out of chaos: assembly of ligand binding sites in heparan sulfate. *Annu Rev Biochem* 71: 435-471, 2002.

45. **Fatima S, Khandekar Z, Parmentier JH, and Malik KU.** Cytosolic phospholipase A2 activation by the p38 kinase inhibitor SB203580 in rabbit aortic smooth muscle cells. *J Pharmacol Exp Ther* 298: 331-338, 2001.

46. **Fitzgerald TN, Shepherd BR, Asada H, Teso D, Muto A, Fancher T, Pimiento JM, Maloney SP, and Dardik A.** Laminar shear stress stimulates vascular smooth muscle cell apoptosis via the Akt pathway. *J Cell Physiol* 216: 389-395, 2008.

47. **Florian JA, Kosky JR, Ainslie K, Pang Z, Dull RO, and Tarbell JM.** Heparan sulfate proteoglycan is a mechanosensor on endothelial cells. *Circ Res* 93: e136-142, 2003.

48. **Galis ZS and Khatri JJ.** Matrix metalloproteinases in vascular remodeling and atherogenesis: the good, the bad, and the ugly. *Circ Res* 90: 251-262, 2002.

49. **Game BA, Maldonado A, He L, and Huang Y.** Pioglitazone inhibits MMP-1 expression in vascular smooth muscle cells through a mitogen-activated protein kinase-independent mechanism. *Atherosclerosis* 178: 249-256, 2005.

50. **Garanich JS, Mathura RA, Shi ZD, and Tarbell JM.** Effects of fluid shear stress on adventitial fibroblast migration: implications for flow-mediated mechanisms of arterialization and intimal hyperplasia. *Am J Physiol Heart Circ Physiol* 292: H3128-3135, 2007.

51. **Garanich JS, Pahakis M, and Tarbell JM.** Shear stress inhibits smooth muscle cell migration via nitric oxide-mediated downregulation of matrix metalloproteinase-2 activity. *Am J Physiol Heart Circ Physiol* 288: H2244-2252, 2005.

52. **Gennaro G, Menard C, Giasson E, Michaud SE, Palasis M, Meloche S, and Rivard A.** Role of p44/p42 MAP kinase in the age-dependent increase in vascular smooth muscle cell proliferation and neointimal formation. *Arterioscler Thromb Vasc Biol* 23: 204-210, 2003.

53. **Gennaro G, Menard C, Michaud SE, Deblois D, and Rivard A.** Inhibition of vascular smooth muscle cell proliferation and neointimal formation in injured arteries by a novel, oral mitogen-activated protein kinase/extracellular signal-regulated kinase inhibitor. *Circulation* 110: 3367-3371, 2004.

54. **Gibbs DF, Warner RL, Weiss SJ, Johnson KJ, and Varani J.** Characterization of matrix metalloproteinases produced by rat alveolar macrophages. *Am J Respir Cell Mol Biol* 20: 1136-1144, 1999.

55. **Gogly B, Groult N, Hornebeck W, Godeau G, and Pellat B.** Collagen zymography as a sensitive and specific technique for the determination of subpicogram levels of interstitial collagenase. *Anal Biochem* 255: 211-216, 1998.

56. **Griffith LG and Swartz MA.** Capturing complex 3D tissue physiology in vitro. *Nat Rev Mol Cell Biol* 7: 211-224, 2006.

57. **Haga M, Yamashita A, Paszkowiak J, Sumpio BE, and Dardik A.** Oscillatory shear stress increases smooth muscle cell proliferation and Akt phosphorylation. *J Vasc Surg* 37: 1277-1284, 2003.

58. **Hakuno D, Takahashi T, Lammerding J, and Lee RT.** Focal adhesion kinase signaling regulates cardiogenesis of embryonic stem cells. *J Biol Chem* 280: 39534-39544, 2005.

59. **Hamamdzic D, Harley RA, Hazen-Martin D, and LeRoy EC.** MCMV induces neointima in IFN-gammaR-/- mice: intimal cell apoptosis and persistent proliferation of myofibroblasts. *BMC Musculoskelet Disord* 2: 3, 2001.

60. **Harfouche R, Hentschel DM, Piecewicz S, Basu S, Print C, Eavarone D, Kiziltepe T, Sasisekharan R, and Sengupta S.** Glycome and transcriptome regulation of vasculogenesis. *Circulation* 120: 1883-1892, 2009.

61. **Hernandez Vera R, Genove E, Alvarez L, Borros S, Kamm R, Lauffenburger D, and Semino CE.** Interstitial fluid flow intensity modulates endothelial sprouting in restricted Src-activated cell clusters during capillary morphogenesis. *Tissue Eng Part A* 15: 175-185, 2009.

62. **Herrmann J, Samee S, Chade A, Rodriguez Porcel M, Lerman LO, and Lerman A.** Differential effect of experimental hypertension and hypercholesterolemia on adventitial remodeling. *Arterioscler Thromb Vasc Biol* 25: 447-453, 2005.

63. **Hinz B, Dugina V, Ballestrem C, Wehrle-Haller B, and Chaponnier C.** Alpha-smooth muscle actin is crucial for focal adhesion maturation in myofibroblasts. *Mol Biol Cell* 14: 2508-2519, 2003.

64. **Hong SY, Jeon YM, Lee HJ, Kim JG, Baek JA, and Lee JC.** Activation of RhoA and FAK induces ERK-mediated osteopontin expression in mechanical force-subjected periodontal ligament fibroblasts. *Mol Cell Biochem* 335: 263-272, 2010.

65. **Hoshina N, Tezuka T, Yokoyama K, Kozuka-Hata H, Oyama M, and Yamamoto T.** Focal adhesion kinase regulates laminin-induced oligodendroglial process outgrowth. *Genes Cells* 12: 1245-1254, 2007.

66. **Hosseinkhani H, Inatsugu Y, Hiraoka Y, Inoue S, and Tabata Y.** Perfusion culture enhances osteogenic differentiation of rat mesenchymal stem cells in collagen sponge reinforced with poly(glycolic Acid) fiber. *Tissue Eng* 11: 1476-1488, 2005.

67. **Hu Y, Cheng L, Hochleitner BW, and Xu Q.** Activation of mitogen-activated protein kinases (ERK/JNK) and AP-1 transcription factor in rat carotid arteries after balloon injury. *Arterioscler Thromb Vasc Biol* 17: 2808-2816, 1997.

68. **Humbert M, Morrell NW, Archer SL, Stenmark KR, MacLean MR, Lang IM, Christman BW, Weir EK, Eickelberg O, Voelkel NF, and Rabinovitch M.** Cellular and molecular pathobiology of pulmonary arterial hypertension. *J Am Coll Cardiol* 43: 13S-24S, 2004.

69. **Hynes RO.** Integrins: versatility, modulation, and signaling in cell adhesion. *Cell* 69: 11-25, 1992.

70. **James TW, Wagner R, White LA, Zwolak RM, and Brinckerhoff CE.** Induction of collagenase and stromelysin gene expression by mechanical injury in a vascular smooth muscle-derived cell line. *J Cell Physiol* 157: 426-437, 1993.

71. **Kang H, Bayless KJ, and Kaunas R.** Fluid shear stress modulates endothelial cell invasion into three-dimensional collagen matrices. *Am J Physiol Heart Circ Physiol* 295: H2087-2097, 2008.

72. **Karakiulakis G, Papakonstantinou E, Aletras AJ, Tamm M, and Roth M.** Cell type-specific effect of hypoxia and platelet-derived growth factor-BB on extracellular matrix turnover and its consequences for lung remodeling. *J Biol Chem* 282: 908-915, 2007.

73. **Khan R, Agrotis A, and Bobik A.** Understanding the role of transforming growth factor-beta1 in intimal thickening after vascular injury. *Cardiovasc Res* 74: 223-234, 2007.

74. **Kharebava G, Makonchuk D, Kalita KB, Zheng JJ, and Hetman M.** Requirement of 3-phosphoinositide-dependent protein kinase-1 for BDNF-mediated neuronal survival. *J Neurosci* 28: 11409-11420, 2008.

75. **Kirkpatrick CA and Selleck SB.** Heparan sulfate proteoglycans at a glance. *J Cell Sci* 120: 1829-1832, 2007.

76. **Kohler TR and Jawien A.** Flow affects development of intimal hyperplasia after arterial injury in rats. *Arterioscler Thromb* 12: 963-971, 1992.

77. **Kong HJ, Polte TR, Alsberg E, and Mooney DJ.** FRET measurements of cell-traction forces and nano-scale clustering of adhesion ligands varied by substrate stiffness. *Proc Natl Acad Sci U S A* 102: 4300-4305, 2005.

78. **Kornberg LJ.** Focal adhesion kinase and its potential involvement in tumor invasion and metastasis. *Head Neck* 20: 745-752, 1998.

79. **Koyama H, Olson NE, and Reidy MA.** Cell signaling in injured rat arteries. *Thromb Haemost* 82: 806-809, 1999.

80. **Kuzuya M and Iguchi A.** Role of matrix metalloproteinases in vascular remodeling. *J Atheroscler Thromb* 10: 275-282, 2003.

81. **Lai K, Wang H, Lee WS, Jain MK, Lee ME, and Haber E.** Mitogen-activated protein kinase phosphatase-1 in rat arterial smooth muscle cell proliferation. *J Clin Invest* 98: 1560-1567, 1996.

82. **Lai WC, Zhou M, Shankavaram U, Peng G, and Wahl LM.** Differential regulation of lipopolysaccharide-induced monocyte matrix metalloproteinase (MMP)-1 and MMP-9 by p38 and extracellular signal-regulated kinase 1/2 mitogen-activated protein kinases. *J Immunol* 170: 6244-6249, 2003.

83. **Lanner F, Lee KL, Sohl M, Holmborn K, Yang H, Wilbertz J, Poellinger L, Rossant J, and Farnebo F.** Heparan sulfation-dependent fibroblast growth factor signaling maintains embryonic stem cells primed for differentiation in a heterogeneous state. *Stem Cells* 28: 191-200, 2010.

84. **Lawson D, Harrison M, and Shapland C.** Fibroblast transgelin and smooth muscle SM22alpha are the same protein, the expression of which is down-regulated in many cell lines. *Cell Motil Cytoskeleton* 38: 250-257, 1997.

85. **Leguillette R, Laviolette M, Bergeron C, Zitouni N, Kogut P, Solway J, Kachmar L, Hamid Q, and Lauzon AM.** Myosin, transgelin, and myosin light chain kinase: expression and function in asthma. *Am J Respir Crit Care Med* 179: 194-204, 2009.

86. **Levick JR.** Flow through interstitium and other fibrous matrices. *Q J Exp Physiol* 72: 409-437, 1987.

87. **Li G, Chen SJ, Oparil S, Chen YF, and Thompson JA.** Direct in vivo evidence demonstrating neointimal migration of adventitial fibroblasts after balloon injury of rat carotid arteries. *Circulation* 101: 1362-1365, 2000.

88. **Li J, Gorospe M, Barnes J, and Liu Y.** Tumor promoter arsenite stimulates histone H3 phosphoacetylation of proto-oncogenes c-fos and c-jun chromatin in human diploid fibroblasts. *J Biol Chem* 278: 13183-13191, 2003.

89. **Li L, Couse TL, Deleon H, Xu CP, Wilcox JN, and Chaikof EL.** Regulation of syndecan-4 expression with mechanical stress during the development of angioplasty-induced intimal thickening. *J Vasc Surg* 36: 361-370, 2002.

90. **Li S, Butler P, Wang Y, Hu Y, Han DC, Usami S, Guan JL, and Chien S.** The role of the dynamics of focal adhesion kinase in the mechanotaxis of endothelial cells. *Proc Natl Acad Sci U S A* 99: 3546-3551, 2002.

91. **Li S, Guan JL, and Chien S.** Biochemistry and biomechanics of cell motility. *Annu Rev Biomed Eng* 7: 105-150, 2005.

92. **Li S, Kim M, Hu YL, Jalali S, Schlaepfer DD, Hunter T, Chien S, and Shyy JY.** Fluid shear stress activation of focal adhesion kinase. Linking to mitogen-activated protein kinases. *J Biol Chem* 272: 30455-30462, 1997.

93. **Li S, Lao J, Chen BP, Li YS, Zhao Y, Chu J, Chen KD, Tsou TC, Peck K, and Chien S.** Genomic analysis of smooth muscle cells in 3-dimensional collagen matrix. *Faseb J* 17: 97-99, 2003.

94. **Lijnen HR, Lupu F, Moons L, Carmeliet P, Goulding D, and Collen D.** Temporal and topographic matrix metalloproteinase expression after vascular injury in mice. *Thromb Haemost* 81: 799-807, 1999.

95. **Liu D, Shriver Z, Qi Y, Venkataraman G, and Sasisekharan R.** Dynamic regulation of tumor growth and metastasis by heparan sulfate glycosaminoglycans. *Semin Thromb Hemost* 28: 67-78, 2002.

96. **Liu D, Shriver Z, Venkataraman G, El Shabrawi Y, and Sasisekharan R.** Tumor cell surface heparan sulfate as cryptic promoters or inhibitors of tumor growth and metastasis. *Proc Natl Acad Sci U S A* 99: 568-573, 2002.

97. **Lovdahl C, Thyberg J, and Hultgardh-Nilsson A.** The synthetic metalloproteinase inhibitor batimastat suppresses injury-induced phosphorylation of MAP kinase ERK1/ERK2 and phenotypic modification of arterial smooth muscle cells in vitro. *J Vasc Res* 37: 345-354, 2000.

98. **Low RB, White SL, Low ES, Neuville P, Bochaton-Piallat ML, and Gabbiani G.** Age dependence of smooth muscle myosin expression by cultured rat aortic smooth muscle cells. *Differentiation* 65: 151-159, 1999.

99. **MacLeod DC, Strauss BH, de Jong M, Escaned J, Umans VA, van Suylen RJ, Verkerk A, de Feyter PJ, and Serruys PW.** Proliferation and extracellular matrix synthesis of smooth muscle cells cultured from human coronary atherosclerotic and restenotic lesions. *J Am Coll Cardiol* 23: 59-65, 1994.

100. **Mallat Z and Tedgui A.** Apoptosis in the vasculature: mechanisms and functional importance. *Br J Pharmacol* 130: 947-962, 2000.

101. **Mandegar M, Fung YC, Huang W, Remillard CV, Rubin LJ, and Yuan JX.** Cellular and molecular mechanisms of pulmonary vascular remodeling: role in the development of pulmonary hypertension. *Microvasc Res* 68: 75-103, 2004.

102. **McGrath JC, Deighan C, Briones AM, Shafaroudi MM, McBride M, Adler J, Arribas SM, Vila E, and Daly CJ.** New aspects of vascular remodelling: the involvement of all vascular cell types. *Exp Physiol* 90: 469-475, 2005.

103. **Mei Y, Yuan Z, Song B, Li D, Ma C, Hu C, Ching YP, and Li M.** Activating transcription factor 3 up-regulated by c-Jun NH(2)-terminal kinase/c-Jun contributes to apoptosis induced by potassium deprivation in cerebellar granule neurons. *Neuroscience* 151: 771-779, 2008.

104. **Michel JB, Thaunat O, Houard X, Meilhac O, Caligiuri G, and Nicoletti A.** Topological determinants and consequences of adventitial responses to arterial wall injury. *Arterioscler Thromb Vasc Biol* 27: 1259-1268, 2007.

105. **Misra S, Fu AA, Puggioni A, Karimi KM, Mandrekar JN, Glockner JF, Juncos LA, Anwer B, McGuire AM, and Mukhopadhyay D.** Increased shear stress with upregulation of VEGF-A and its receptors and MMP-2, MMP-9, and TIMP-1 in venous stenosis of hemodialysis grafts. *Am J Physiol Heart Circ Physiol* 294: H2219-2230, 2008.

106. **Mitra SK, Hanson DA, and Schlaepfer DD.** Focal adhesion kinase: in command and control of cell motility. *Nat Rev Mol Cell Biol* 6: 56-68, 2005.

107. **Montgomery AM, Reisfeld RA, and Cheresh DA.** Integrin alpha v beta 3 rescues melanoma cells from apoptosis in three-dimensional dermal collagen. *Proc Natl Acad Sci U S A* 91: 8856-8860, 1994.

108. **Moon JJ, Matsumoto M, Patel S, Lee L, Guan JL, and Li S.** Role of cell surface heparan sulfate proteoglycans in endothelial cell migration and mechanotransduction. *J Cell Physiol* 203: 166-176, 2005.

109. **Morgan MR, Humphries MJ, and Bass MD.** Synergistic control of cell adhesion by integrins and syndecans. *Nat Rev Mol Cell Biol* 8: 957-969, 2007.

110. **Mu H, Wang X, Lin PH, Yao Q, and Chen C.** Chlorotyrosine promotes human aortic smooth muscle cell migration through increasing superoxide anion production and ERK1/2 activation. *Atherosclerosis* 201: 67-75, 2008.

111. **Mu H, Wang X, Lin PH, Yao Q, and Chen C.** Chlorotyrosine promotes human aortic smooth muscle cell migration through increasing superoxide anion production and ERK1/2 activation. *Atherosclerosis*, 2008.

112. **Mu H, Wang X, Wang H, Lin P, Yao Q, and Chen C.** Lactosylceramide promotes cell migration and proliferation through activation of ERK1/2 in human aortic smooth muscle cells. *Am J Physiol Heart Circ Physiol* 297: H400-408, 2009.

113. **Muslin AJ.** MAPK signalling in cardiovascular health and disease: molecular mechanisms and therapeutic targets. *Clin Sci (Lond)* 115: 203-218, 2008.

114. **Nelson WJ and Nusse R.** Convergence of Wnt, beta-catenin, and cadherin pathways. *Science* 303: 1483-1487, 2004.

115. **Newby AC.** Dual role of matrix metalloproteinases (matrixins) in intimal thickening and atherosclerotic plaque rupture. *Physiol Rev* 85: 1-31, 2005.

116. **Newby AC.** Matrix metalloproteinases regulate migration, proliferation, and death of vascular smooth muscle cells by degrading matrix and non-matrix substrates. *Cardiovasc Res* 69: 614-624, 2006.

117. **Ng CP, Hinz B, and Swartz MA.** Interstitial fluid flow induces myofibroblast differentiation and collagen alignment in vitro. *J Cell Sci* 118: 4731-4739, 2005.

118. **Ng CP and Swartz MA.** Fibroblast alignment under interstitial fluid flow using a novel 3-D tissue culture model. *Am J Physiol Heart Circ Physiol* 284: H1771-1777, 2003.

119. **Ni J, Waldman A, and Khachigian LM.** c-Jun regulates shear- and injury-inducible Egr-1 expression, vein graft stenosis after autologous end-to-side

transplantation in rabbits, and intimal hyperplasia in human saphenous veins. *J Biol Chem* 285: 4038-4048, 2010.

120. **Nurcombe V and Cool SM.** Heparan sulfate control of proliferation and differentiation in the stem cell niche. *Crit Rev Eukaryot Gene Expr* 17: 159-171, 2007.

121. **Oishi K, Ogawa Y, Gamoh S, and Uchida MK.** Contractile responses of smooth muscle cells differentiated from rat neural stem cells. *J Physiol* 540: 139-152, 2002.

122. **Okina E, Manon-Jensen T, Whiteford JR, and Couchman JR.** Syndecan proteoglycan contributions to cytoskeletal organization and contractility. *Scand J Med Sci Sports* 19: 479-489, 2009.

123. **Onodera S, Nishihira J, Iwabuchi K, Koyama Y, Yoshida K, Tanaka S, and Minami A.** Macrophage migration inhibitory factor up-regulates matrix metalloproteinase-9 and -13 in rat osteoblasts. Relevance to intracellular signaling pathways. *J Biol Chem* 277: 7865-7874, 2002.

124. **Owens GK.** Regulation of differentiation of vascular smooth muscle cells. *Physiol Rev* 75: 487-517, 1995.

125. **Owens GK, Kumar MS, and Wamhoff BR.** Molecular regulation of vascular smooth muscle cell differentiation in development and disease. *Physiol Rev* 84: 767-801, 2004.

126. **Pahakis MY, Kosky JR, Dull RO, and Tarbell JM.** The role of endothelial glycocalyx components in mechanotransduction of fluid shear stress. *Biochem Biophys Res Commun* 355: 228-233, 2007.

127. **Palumbo R, Gaetano C, Melillo G, Toschi E, Remuzzi A, and Capogrossi MC.** Shear stress downregulation of platelet-derived growth factor receptor-beta and matrix metalloprotease-2 is associated with inhibition of smooth muscle cell invasion and migration. *Circulation* 102: 225-230, 2000.

128. **Park CH, Lee MJ, Ahn J, Kim S, Kim HH, Kim KH, Eun HC, and Chung JH.** Heat shock-induced matrix metalloproteinase (MMP)-1 and MMP-3 are mediated through ERK and JNK activation and via an autocrine interleukin-6 loop. *J Invest Dermatol* 123: 1012-1019, 2004.

129. **Park F, Mattson DL, Roberts LA, and Cowley AW, Jr.** Evidence for the presence of smooth muscle alpha-actin within pericytes of the renal medulla. *Am J Physiol* 273: R1742-1748, 1997.

130. **Parsons JT, Martin KH, Slack JK, Taylor JM, and Weed SA.** Focal adhesion kinase: a regulator of focal adhesion dynamics and cell movement. *Oncogene* 19: 5606-5613, 2000.

131. **Parsons JT, Slack-Davis J, Tilghman R, and Roberts WG.** Focal adhesion kinase: targeting adhesion signaling pathways for therapeutic intervention. *Clin Cancer Res* 14: 627-632, 2008.

132. **Patel S, Shi Y, Niculescu R, Chung EH, Martin JL, and Zalewski A.** Characteristics of coronary smooth muscle cells and adventitial fibroblasts. *Circulation* 101: 524-532, 2000.

133. **Pedersen JA, Boschetti F, and Swartz MA.** Effects of extracellular fiber architecture on cell membrane shear stress in a 3D fibrous matrix. *J Biomech* 40: 1484-1492, 2007.

134. **Perlman H, Maillard L, Krasinski K, and Walsh K.** Evidence for the rapid onset of apoptosis in medial smooth muscle cells after balloon injury. *Circulation* 95: 981-987, 1997.

135. **Prescott MF, Sawyer WK, Von Linden-Reed J, Jeune M, Chou M, Caplan SL, and Jeng AY.** Effect of matrix metalloproteinase inhibition on progression of atherosclerosis and aneurysm in LDL receptor-deficient mice overexpressing MMP-3, MMP-12, and MMP-13 and on restenosis in rats after balloon injury. *Ann N Y Acad Sci* 878: 179-190, 1999.

136. **Prockop DJ and Kivirikko KI.** Collagens: molecular biology, diseases, and potentials for therapy. *Annu Rev Biochem* 64: 403-434, 1995.

137. **Raffetto JD and Khalil RA.** Matrix metalloproteinases and their inhibitors in vascular remodeling and vascular disease. *Biochem Pharmacol* 75: 346-359, 2008.

138. **Ramanujan S, Pluen A, McKee TD, Brown EB, Boucher Y, and Jain RK.** Diffusion and convection in collagen gels: implications for transport in the tumor interstitium. *Biophys J* 83: 1650-1660, 2002.

139. **Rao GN, Alexander RW, and Runge MS.** Linoleic acid and its metabolites, hydroperoxyoctadecadienoic acids, stimulate c-Fos, c-Jun, and c-Myc mRNA expression, mitogen-activated protein kinase activation, and growth in rat aortic smooth muscle cells. *J Clin Invest* 96: 842-847, 1995.

140. **Rensen SS, Doevendans PA, and van Eys GJ.** Regulation and characteristics of vascular smooth muscle cell phenotypic diversity. *Neth Heart J* 15: 100-108, 2007.

141. **Rensen SS, Niessen PM, Long X, Doevendans PA, Miano JM, and van Eys GJ.** Contribution of serum response factor and myocardin to transcriptional regulation of smoothelins. *Cardiovasc Res* 70: 136-145, 2006.

142. **Reunanen N, Li SP, Ahonen M, Foschi M, Han J, and Kahari VM.** Activation of p38 alpha MAPK enhances collagenase-1 (matrix metalloproteinase (MMP)-1) and stromelysin-1 (MMP-3) expression by mRNA stabilization. *J Biol Chem* 277: 32360-32368, 2002.

143. **Rizzo V.** Enhanced interstitial flow as a contributing factor in neointima formation: (shear) stressing vascular wall cell types other than the endothelium. *Am J Physiol Heart Circ Physiol* 297: H1196-1197, 2009.

144. **Roelofs M, Faggian L, Pampinella F, Paulon T, Franch R, Chiavegato A, and Sartore S.** Transforming growth factor beta1 involvement in the conversion of fibroblasts to smooth muscle cells in the rabbit bladder serosa. *Histochem J* 30: 393-404, 1998.

145. **Rosenberger SF, Gupta A, and Bowden GT.** Inhibition of p38 MAP kinase increases okadaic acid mediated AP-1 expression and DNA binding but has no effect on TRE dependent transcription. *Oncogene* 18: 3626-3632, 1999.

146. **Roux PP and Blenis J.** ERK and p38 MAPK-activated protein kinases: a family of protein kinases with diverse biological functions. *Microbiol Mol Biol Rev* 68: 320-344, 2004.

147. **Roy-Chaudhury P, Sukhatme VP, and Cheung AK.** Hemodialysis vascular access dysfunction: a cellular and molecular viewpoint. *J Am Soc Nephrol* 17: 1112-1127, 2006.

148. **Roy J, Kazi M, Hedin U, and Thyberg J.** Phenotypic modulation of arterial smooth muscle cells is associated with prolonged activation of ERK1/2. *Differentiation* 67: 50-58, 2001.

149. **Rutkowski JM and Swartz MA.** A driving force for change: interstitial flow as a morphoregulator. *Trends Cell Biol* 17: 44-50, 2007.

150. **Saku T and Furthmayr H.** Characterization of the major heparan sulfate proteoglycan secreted by bovine aortic endothelial cells in culture. Homology to the large molecular weight molecule of basement membranes. *J Biol Chem* 264: 3514-3523, 1989.

151. **Saoncella S, Echtermeyer F, Denhez F, Nowlen JK, Mosher DF, Robinson SD, Hynes RO, and Goetinck PF.** Syndecan-4 signals cooperatively with integrins in a Rho-dependent manner in the assembly of focal adhesions and actin stress fibers. *Proc Natl Acad Sci U S A* 96: 2805-2810, 1999.

152. **Sartore S, Chiavegato A, Faggin E, Franch R, Puato M, Ausoni S, and Pauletto P.** Contribution of adventitial fibroblasts to neointima formation and vascular remodeling: from innocent bystander to active participant. *Circ Res* 89: 1111-1121, 2001.

153. **Sasisekharan R, Shriver Z, Venkataraman G, and Narayanasami U.** Roles of heparan-sulphate glycosaminoglycans in cancer. *Nat Rev Cancer* 2: 521-528, 2002.

154. **Schlaepfer DD, Hanks SK, Hunter T, and van der Geer P.** Integrin-mediated signal transduction linked to Ras pathway by GRB2 binding to focal adhesion kinase. *Nature* 372: 786-791, 1994.

155. **Schulze-Bauer CA, Regitnig P, and Holzapfel GA.** Mechanics of the human femoral adventitia including the high-pressure response. *Am J Physiol Heart Circ Physiol* 282: H2427-2440, 2002.

156. **Schwartz RS, Edwards WD, Huber KC, Antoniades LC, Bailey KR, Camrud AR, Jorgenson MA, and Holmes DR, Jr.** Coronary restenosis: prospects for solution and new perspectives from a porcine model. *Mayo Clin Proc* 68: 54-62, 1993.

157. **Schwartz RS and Henry TD.** Pathophysiology of coronary artery restenosis. *Rev Cardiovasc Med* 3 Suppl 5: S4-9, 2002.

158. **Scott NA, Cipolla GD, Ross CE, Dunn B, Martin FH, Simonet L, and Wilcox JN.** Identification of a potential role for the adventitia in vascular lesion formation after balloon overstretch injury of porcine coronary arteries. *Circulation* 93: 2178-2187, 1996.

159. **Sedding DG, Homann M, Seay U, Tillmanns H, Preissner KT, and Braun-Dullaeus RC.** Calpain counteracts mechanosensitive apoptosis of vascular smooth muscle cells in vitro and in vivo. *Faseb J* 22: 579-589, 2008.

160. **Sharifi AM and Schiffrin EL.** Apoptosis in vasculature of spontaneously hypertensive rats: effect of an angiotensin converting enzyme inhibitor and a calcium channel antagonist. *Am J Hypertens* 11: 1108-1116, 1998.

161. **Shaulian E and Karin M.** AP-1 in cell proliferation and survival. *Oncogene* 20: 2390-2400, 2001.

162. **Shemesh T, Geiger B, Bershadsky AD, and Kozlov MM.** Focal adhesions as mechanosensors: a physical mechanism. *Proc Natl Acad Sci U S A* 102: 12383-12388, 2005.

163. **Shi Y, O'Brien JE, Fard A, Mannion JD, Wang D, and Zalewski A.** Adventitial myofibroblasts contribute to neointimal formation in injured porcine coronary arteries. *Circulation* 94: 1655-1664, 1996.

164. **Shi Y, Patel S, Niculescu R, Chung W, Desrochers P, and Zalewski A.** Role of matrix metalloproteinases and their tissue inhibitors in the regulation of coronary cell migration. *Arterioscler Thromb Vasc Biol* 19: 1150-1155, 1999.

165. **Shi ZD, Abraham G, and Tarbell JM.** Shear stress modulation of smooth muscle cell marker genes in 2-D and 3-D depends on mechanotransduction by heparan sulfate proteoglycans and ERK1/2. *PLoS One* 5: e12196, 2010.

166. **Shi ZD, Ji XY, Berardi DE, Qazi H, and Tarbell JM.** Interstitial flow induces MMP-1 expression and vascular SMC migration in collagen I gels via an ERK1/2-dependent and c-Jun-mediated mechanism. *Am J Physiol Heart Circ Physiol* 298: H127-135, 2010.

167. **Shi ZD, Ji XY, Qazi H, and Tarbell JM.** Interstitial flow promotes vascular fibroblast, myofibroblast, and smooth muscle cell motility in 3-D collagen I via upregulation of MMP-1. *Am J Physiol Heart Circ Physiol* 297: H1225-1234, 2009.

168. **Shi ZD, Wang H, and Tarbell JM.** Heparan sulfate proteoglycans mediate interstitial flow mechanotransduction regulating MMP expression and cell motility via FAK and ERK in 3D. *PLoS One*, 2010.

169. **Shibata R, Kai H, Seki Y, Kato S, Morimatsu M, Kaibuchi K, and Imaizumi T.** Role of Rho-associated kinase in neointima formation after vascular injury. *Circulation* 103: 284-289, 2001.

170. **Shields JD, Fleury ME, Yong C, Tomei AA, Randolph GJ, and Swartz MA.** Autologous chemotaxis as a mechanism of tumor cell homing to lymphatics via interstitial flow and autocrine CCR7 signaling. *Cancer Cell* 11: 526-538, 2007.

171. **Shou Y, Jan KM, and Rumschitzki DS.** Transport in rat vessel walls. I. Hydraulic conductivities of the aorta, pulmonary artery, and inferior vena cava with intact and denuded endothelia. *Am J Physiol Heart Circ Physiol* 291: H2758-2771, 2006.

172. **Shum JK, Melendez JA, and Jeffrey JJ.** Serotonin-induced MMP-13 production is mediated via phospholipase C, protein kinase C, and ERK1/2 in rat uterine smooth muscle cells. *J Biol Chem* 277: 42830-42840, 2002.

173. **Silver FH, Horvath I, and Foran DJ.** Viscoelasticity of the vessel wall: the role of collagen and elastic fibers. *Crit Rev Biomed Eng* 29: 279-301, 2001.

174. **Siow RC, Mallawaarachchi CM, and Weissberg PL.** Migration of adventitial myofibroblasts following vascular balloon injury: insights from in vivo gene transfer to rat carotid arteries. *Cardiovasc Res* 59: 212-221, 2003.

175. **Slack-Davis JK, Martin KH, Tilghman RW, Iwanicki M, Ung EJ, Autry C, Luzzio MJ, Cooper B, Kath JC, Roberts WG, and Parsons JT.** Cellular characterization of a novel focal adhesion kinase inhibitor. *J Biol Chem* 282: 14845-14852, 2007.

176. **Snoek-van Beurden PA and Von den Hoff JW.** Zymographic techniques for the analysis of matrix metalloproteinases and their inhibitors. *Biotechniques* 38: 73-83, 2005.

177. **Sodek KL, Brown TJ, and Ringuette MJ.** Collagen I but not Matrigel matrices provide an MMP-dependent barrier to ovarian cancer cell penetration. *BMC Cancer* 8: 223, 2008.

178. **Stegemann JP, Hong H, and Nerem RM.** Mechanical, biochemical, and extracellular matrix effects on vascular smooth muscle cell phenotype. *J Appl Physiol* 98: 2321-2327, 2005.

179. **Stenmark KR, Davie N, Frid M, Gerasimovskaya E, and Das M.** Role of the adventitia in pulmonary vascular remodeling. *Physiology (Bethesda)* 21: 134-145, 2006.

180. **Sterpetti AV, Cucina A, D'Angelo LS, Cardillo B, and Cavallaro A.** Shear stress modulates the proliferation rate, protein synthesis, and mitogenic activity of arterial smooth muscle cells. *Surgery* 113: 691-699, 1993.

181. **Stringa E, Knauper V, Murphy G, and Gavrilovic J.** Collagen degradation and platelet-derived growth factor stimulate the migration of vascular smooth muscle cells. *J Cell Sci* 113 (Pt 11): 2055-2064, 2000.

182. **Swartz MA and Fleury ME.** Interstitial flow and its effects in soft tissues. *Annu Rev Biomed Eng* 9: 229-256, 2007.

183. **Tada S and Tarbell JM.** Fenestral pore size in the internal elastic lamina affects transmural flow distribution in the artery wall. *Ann Biomed Eng* 29: 456-466, 2001.

184. **Tada S and Tarbell JM.** Flow through internal elastic lamina affects shear stress on smooth muscle cells (3D simulations). *Am J Physiol Heart Circ Physiol* 282: H576-584, 2002.

185. **Tada S and Tarbell JM.** Interstitial flow through the internal elastic lamina affects shear stress on arterial smooth muscle cells. *Am J Physiol Heart Circ Physiol* 278: H1589-1597, 2000.

186. **Tarbell JM.** Mass transport in arteries and the localization of atherosclerosis. *Annu Rev Biomed Eng* 5: 79-118, 2003.

187. **Tarbell JM and Ebong EE.** The endothelial glycocalyx: a mechano-sensor and -transducer. *Sci Signal* 1: pt8, 2008.

188. **Tarbell JM and Pahakis MY.** Mechanotransduction and the glycocalyx. *J Intern Med* 259: 339-350, 2006.

189. **Tarbell JM, Weinbaum S, and Kamm RD.** Cellular fluid mechanics and mechanotransduction. *Ann Biomed Eng* 33: 1719-1723, 2005.

190. **Tedgui A and Lever MJ.** Filtration through damaged and undamaged rabbit thoracic aorta. *Am J Physiol* 247: H784-791, 1984.

191. **Thi MM, Tarbell JM, Weinbaum S, and Spray DC.** The role of the glycocalyx in reorganization of the actin cytoskeleton under fluid shear stress: a "bumper-car" model. *Proc Natl Acad Sci U S A* 101: 16483-16488, 2004.

192. **Thomas PE, Peters-Golden M, White ES, Thannickal VJ, and Moore BB.** PGE(2) inhibition of TGF-beta1-induced myofibroblast differentiation is Smad-independent but involves cell shape and adhesion-dependent signaling. *Am J Physiol Lung Cell Mol Physiol* 293: L417-428, 2007.

193. **Tomasek JJ, Gabbiani G, Hinz B, Chaponnier C, and Brown RA.** Myofibroblasts and mechano-regulation of connective tissue remodelling. *Nat Rev Mol Cell Biol* 3: 349-363, 2002.

194. **Tsai RY and McKay RD.** Cell contact regulates fate choice by cortical stem cells. *J Neurosci* 20: 3725-3735, 2000.

195. **Tsukioka K, Suzuki J, Fujimori M, Wada Y, Yamaura K, Ito K, Morishita R, Kaneda Y, Isobe M, and Amano J.** Expression of matrix metalloproteinases in cardiac allograft vasculopathy and its attenuation by anti MMP-2 ribozyme gene transfection. *Cardiovasc Res* 56: 472-478, 2002.

196. **Ueba H, Kawakami M, and Yaginuma T.** Shear stress as an inhibitor of vascular smooth muscle cell proliferation. Role of transforming growth factor-beta 1 and tissue-type plasminogen activator. *Arterioscler Thromb Vasc Biol* 17: 1512-1516, 1997.

197. **van Eys GJ, Niessen PM, and Rensen SS.** Smoothelin in vascular smooth muscle cells. *Trends Cardiovasc Med* 17: 26-30, 2007.

198. **Vera RH, Genove E, Alvarez L, Borros S, Kamm R, Lauffenburger D, and Semino CE.** Interstitial Fluid Flow Intensity Modulates Endothelial Sprouting in Restricted Src-Activated Cell Clusters During Capillary Morphogenesis. *Tissue Eng Part A*, 2008.

199. **Vincenti MP and Brinckerhoff CE.** Transcriptional regulation of collagenase (MMP-1, MMP-13) genes in arthritis: integration of complex signaling pathways for the recruitment of gene-specific transcription factors. *Arthritis Res* 4: 157-164, 2002.

200. **Vuoriluoto K, Jokinen J, Kallio K, Salmivirta M, Heino J, and Ivaska J.** Syndecan-1 supports integrin alpha2beta1-mediated adhesion to collagen. *Exp Cell Res* 314: 3369-3381, 2008.

201. **Wang DM and Tarbell JM.** Modeling interstitial flow in an artery wall allows estimation of wall shear stress on smooth muscle cells. *J Biomech Eng* 117: 358-363, 1995.

202. **Wang H, Yan S, Chai H, Riha GM, Li M, Yao Q, and Chen C.** Shear stress induces endothelial transdifferentiation from mouse smooth muscle cells. *Biochem Biophys Res Commun* 346: 860-865, 2006.

203. **Wang N, Butler JP, and Ingber DE.** Mechanotransduction across the cell surface and through the cytoskeleton. *Science* 260: 1124-1127, 1993.

204. **Wang S and Tarbell JM.** Effect of fluid flow on smooth muscle cells in a 3-dimensional collagen gel model. *Arterioscler Thromb Vasc Biol* 20: 2220-2225, 2000.

205. **Weinbaum S, Tarbell JM, and Damiano ER.** The structure and function of the endothelial glycocalyx layer. *Annu Rev Biomed Eng* 9: 121-167, 2007.

206. **Westermarck J, Li SP, Kallunki T, Han J, and Kahari VM.** p38 mitogen-activated protein kinase-dependent activation of protein phosphatases 1 and 2A inhibits MEK1 and MEK2 activity and collagenase 1 (MMP-1) gene expression. *Mol Cell Biol* 21: 2373-2383, 2001.

207. **Wilcox-Adelman SA, Denhez F, and Goetinck PF.** Syndecan-4 modulates focal adhesion kinase phosphorylation. *J Biol Chem* 277: 32970-32977, 2002.

208. **Williams C and Wick TM.** Endothelial cell-smooth muscle cell co-culture in a perfusion bioreactor system. *Ann Biomed Eng* 33: 920-928, 2005.

209. **Xu F, Ji J, Li L, Chen R, and Hu W.** Activation of adventitial fibroblasts contributes to the early development of atherosclerosis: a novel hypothesis that complements the "Response-to-Injury Hypothesis" and the "Inflammation Hypothesis". *Med Hypotheses* 69: 908-912, 2007.

210. **Yamamoto K and Yamamoto M.** Cell adhesion receptors for native and denatured type I collagens and fibronectin in rabbit arterial smooth muscle cells in culture. *Exp Cell Res* 214: 258-263, 1994.

211. **Yuan Z, Gong S, Luo J, Zheng Z, Song B, Ma S, Guo J, Hu C, Thiel G, Vinson C, Hu CD, Wang Y, and Li M.** Opposing roles for ATF2 and c-Fos in c-Jun-mediated neuronal apoptosis. *Mol Cell Biol* 29: 2431-2442, 2009.

212. **Zaman MH, Trapani LM, Sieminski AL, Mackellar D, Gong H, Kamm RD, Wells A, Lauffenburger DA, and Matsudaira P.** Migration of tumor cells in 3D matrices is governed by matrix stiffness along with cell-matrix adhesion and proteolysis. *Proc Natl Acad Sci U S A* 103: 10889-10894, 2006.

213. **Zamir E and Geiger B.** Molecular complexity and dynamics of cell-matrix adhesions. *J Cell Sci* 114: 3583-3590, 2001.

214. **Zempo N, Kenagy RD, Au YP, Bendeck M, Clowes MM, Reidy MA, and Clowes AW.** Matrix metalloproteinases of vascular wall cells are increased in balloon-injured rat carotid artery. *J Vasc Surg* 20: 209-217, 1994.

215. **Zempo N, Koyama N, Kenagy RD, Lea HJ, and Clowes AW.** Regulation of vascular smooth muscle cell migration and proliferation in vitro and in injured rat arteries by a synthetic matrix metalloproteinase inhibitor. *Arterioscler Thromb Vasc Biol* 16: 28-33, 1996.